TID-7632

MASTER

RADIOACTIVE FALLOUT FROM NUCLEAR WEAPONS TESTS

Proceedings of a Conference Held in Germantown, Maryland

November 15-17, 1961

BOOK 1

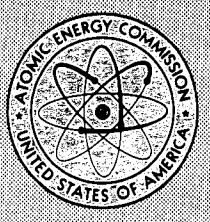

United States Atomic Energy Commission
Division of Technical Information

FRACTIONATION IN SURFACE BURSTS

Edward C. Freiling
U. S. Naval Radiological Defense Laboratory
San Francisco, California

Abstract

A description is presented of a combination of A. D. Anderson's Dynamic Fallout Model (NRDL-D Model) with C. F. Miller's thermodynamic model of fractionation which will be used to account for fractionation in fallout predictions. Weaknesses of the method are pointed out. Data required for testing the model (both from laboratory experiments and nuclear detonations), and for achieving more meaningful documentation of future nuclear bursts, are discussed.

Introduction

At NRDL* we are carrying out a project supported by the Atomic Energy Commission under the general supervision of the Fallout Studies Branch of the Division of Biology and Medicine entitled: "The Formation, Distribution and Characteristics of Nuclear Debris." The objective of this project is to develop a generalized fallout model capable of quantitatively predicting the formation and composition of nuclear bomb debris and its partition between stratospheric, tropospheric and local fallout. We are carrying out this project in two concurrent phases. The first phase is designed to produce short-range results and the second phase is oriented towards long-term progress. The present paper is concerned with the short-range phase and the following paper (page 47) on air

* U. S. Naval Radiological Defense Laboratory, San Francisco, California.

burst fractionation is concerned with the long-range phase. We are fortunate in having the opportunity to describe this work at such an early stage of development and the concomitant advantage of conferees' comments, which we earnestly solicit.

In the present paper I will describe our efforts to establish a computer program to calculate fallout patterns which account for the phenomena of fractionation. Fractionation is defined as any process which causes the radionuclide composition of a sample of nuclear debris to be unrepresentative of the debris taken as a whole, and the subject has been treated in detail elsewhere.(1) The manner of accounting for fractionation consists essentially of a union of the NRDL dynamic fallout model of Anderson(2-5) with the thermodynamic model of fractionation devised by Miller.*

This paper is divided into five parts. Part 1 describes the fractionation model, Part 2 describes the fallout model, Part 3 describes the adaptation of the fractionation model to the fallout model, Part 4 discusses means of testing the results, and Part 5 describes data relating to this part of the program which should be obtained in the event that future land surface bursts occur.

It is intended to devise the computer program in a compartmented fashion in order that the various parts can be revised as new developments in theory and experimental data become available. Revision is a continuing process and the description given here may well be partially obsolete by the time of publication.

Part I. The Miller Thermodynamic Model of Fractionation

The Miller thermodynamic model of fractionation can be outlined briefly as follows: First, there is described an idealized carrier material with thermodynamic and chemical properties similar to the soil which is to be drawn into the fireball, but idealized to the point where there is no chemical interaction between the carrier material and any of the radioactive products of the detonation. Secondly, the energy of the nuclear detonation is accounted for in as reasonable a manner as possible and the fraction of that energy which goes into vaporizing and melting the idealized carrier material is calculated. When the vaporized soil condenses, it and the melted soil are considered as one single phase in equilibrium with a vapor phase. The vapor phase consists of air and uncondensed radionuclides. Its volume is taken as the maximum volume of the fireball and its temperature as that of the idealized carrier material at its melting point. The time at which this temperature is

---

* Additional work on this model, described in USNRDL-TR-425, is being carried out by C. F. Miller.

reached is calculated from scaling laws, and the elemental distribution of the mass chains of the fission fragments and the other product nuclides at this time is determined from known and estimated fission yield and decay relationships. The distribution of each product element between the liquid and vapor phases is then calculated according to Raoult's Law. The idealized carrier than solidifies, freezing in the trapped radionuclides. This point marks the end of the first period of condensation. The second period of condensation treats the deposition of those product nuclides still in the vapor phase upon the frozen soil particles. Some suggestions were offered by Miller as to how such a deposition might be accounted for, but the actual calculations were never carried out. According to this model the fractionation is now seen to result from two sources. The first source is the separation of particles from the cloud before the second stage of condensation has occurred. These particles will contain normal quantities of refractory elements but will be depleted in volatile elements. With regard to those particles which remain in the cloud during the second stage of condensation, another type of fractionation occurs. Here those product elements which dissolved in the particles up to the time of solidification will have been distributed throughout the particles in proportion to the particle volume, whereas those elements which condensed after solidification will have distributed themselves among the particles in accordance with the available surface. In the remainder of this section the aforementioned processes will be described in greater detail and the defects of the model will be discussed in a later section. It should be stated that Miller was well aware of the inadequacies of this approach but for lack of time and suitable experimental data was unable to carry his calculations to a higher degree of refinement.

The properties chosen for the idealized carrier material are as close as practical to those of anorthoclase ($Na_2O.Al_2O_3.6SiO_2$). It is non-reactive towards the fission product elements and their oxides and dissolves the elements as stable oxides. Its melting point is 1400°C at which temperature its vapor pressure is negligible. The molecular weight is 524 and the entropy of fusion is 29 cal./mole degrees. The heat of fusion is 48,000 cal./mole, the dissociation energy is 3,370,000 cal./mole and the heat capacity is such that 200,000 cal./mole are required to raise the temperature of the soil from 298°K to its melting point.

The discussion of the partition of burst energy which follows is based upon the considerations outlined by Miller. It differs, however, to the extent to which new thermodynamic data and scaling relationships have been incorporated into the treatment since the initial appearance of his work. The calculations can be outlined as follows: First the manner in which the energy of the burst has been distributed at the time of the final temperature maximum is calculated. The energy is considered to be distributed between nuclear radiation, thermal radiation, blast and shock, and the internal energy of the fireball. The distribution is shown schematically in Fig. 1.

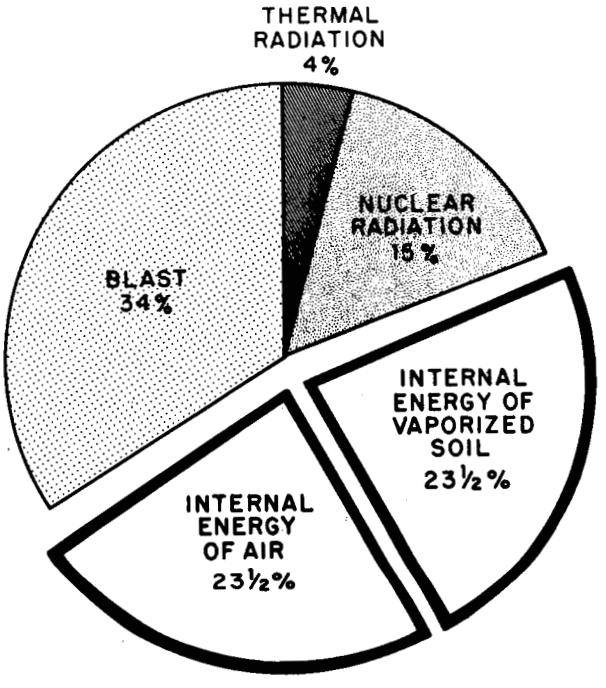

FIGURE 1. ESTIMATED ENERGY PARTITION AT THE TIME OF SECOND MAXIMUM IN MILLER'S MODEL.

In these calculations the energy equivalent of 1 KT of TNT has been taken as 10^{12} cal. The dissociation energy of air is 101,830 cal./mole. The heat capacity and pressure--volume--temperature relationship of gases have been assumed to be ideal.

Miller next defines "the model surface burst" as one in which one half of the internal energy in the fireball at the second maximum was utilized in dissociating and heating air molecules and the other half for the vaporization of soil molecules. Applying this principle leads to the result that, well within the error of estimate, equal number of moles of air and soil atoms are present in the fireball at the time of second maximum. Relating these to the total energy available by means of the perfect gas law and the estimated soil properties leads to 1.6×10^6 moles per KT of yield for each; or 840 tons of soil per KT of yield.

Hillendahl[6] gives a number of useful scaling relations for surface bursts. In his nomenclature:

W = total weapon yield (kilotons)
t = time (seconds)
ρ_0 = ambient air density (g/l)
$t^* = t/t_{fmax}$ = ratio of the time t to that of the final maximum in observed temperature

H = power (kilotons per second)
$\sigma A \psi^4$ = (Stefan's constant x total radiating area x fourth power of power temperature)
T = absolute temperature of the fireball

1 Kiloton = 10^{12} calories
R_1 = Radius of uniform brightness
R_2 = Main radiation front radius
R_3 = Absorption shell radius
R_4 = Main shock front radius
R_5 = Precursor shock front radius
(The radii are shown in Fig. 2 and are further discussed in the following paper, page 47 . They are taken in meters).

The scaling equations are

$$W = 0.65 \rho_o (2R_4)^5/t^2$$

$$t_{min} = 0.0030 W^{0.49}$$

R_4 min = R_2 min = 33 $W^{0.396}$ = the values of the radii at the minimum in observed temperature

$$H = 3.75 W^{0.51} t^{*-1.45} e^{-9e^{-2.73t^*}} e^{-93^{-12Wt^*}}$$

And from his figures one finds

$$T = 7000 W^{-0.07} t^{*-0.34}$$

while, at $t^* = 1$

$$R_1 = 48 W^{0.39}$$

$$R_2 = 66 W^{0.39}$$

$$R_3 = 75 W^{0.39}$$

$$R_4 = 90 W^{0.39}$$

From the time of second maximum to the time required to reach 1400°C. the internal energy of the cloud will decrease. Dissociated air and soil will release energy by cooling and reassociating. The energy released will be distributed among radiation, expansion, heating additional air, and heating and melting additional soil. The amount of energy radiated up to any time is obtained by integrating Hillendahl's power function. The work of expansion is calculated from the change in volume of the 1.6 x 10^6 moles per KT of air atoms due to cooling from 6000° to 1400°C. The difference between the maximum volume of the fireball calculated from Miller's scaling equation

$$R_m = 922 \times 10^3 W^{0.314}$$

and the volume of the original air at 1400°C. is used to calculate the additional amount of heated air. Some 3% of the original device energy turns out to become available for heating and melting soil. It is assumed that only half of this residual energy produces molten soil. The additional soil melted turns out to equal about half of the condensed soil. The total amount of molten soil is thus calculated to be 2150 tons for a 1.7 KT shot, in poor agreement with the 800 tons found in the Rainier shot (Nevada Test Site, 1957), where no radiation was lost, although much water was present. (cf. Part IV).

With the foregoing considerations the stage is set for the application of Raoult's Law by definition of the macroscopic state. This state consists of the calculated number of moles of molten soil in equilibrium with a vapor phase. The previous discussion took the temperature down to 1400°C., but the same principles could be used to reach definitions of the macroscopic state for intermediate temperatures. At higher temperatures, however, the vapor pressure and partial dissociation of the soil will become increasingly important.

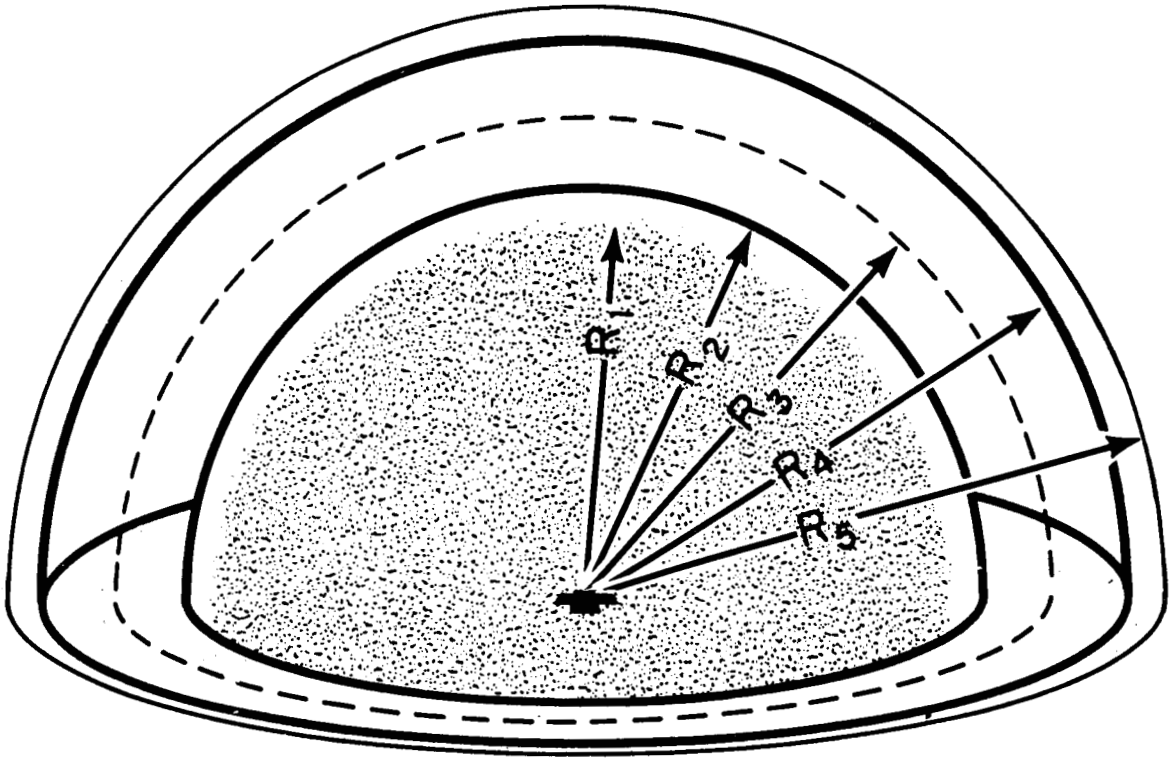

FIGURE 2. ILLUSTRATION OF FIREBALL RADII (FROM (6)).

According to Raoult's Law, the vapor pressure of each component of an ideal solution at thermodynamic equilibrium is equal to the vapor pressure of the pure substance multiplied by its mole fraction in the solution. Thus, if there are n_1 moles of component 1 and n_2 moles of component 2 in a two component solution the mole fraction of component 1 is

$$N_1 = \frac{n_1}{n_1 + n_2},$$

Its vapor pressure above the solution is

$$p_1 = N_1 p_1^{\square}$$

where $p_1^{\square}$ is the vapor pressure of the pure component. The law is illustrated graphically in Fig. 3. Here, the dashed lines illustrate ideal behavior while the solid lines indicate two cases of real behavior Positive deviations are attributed to mutual repulsion of the components, and negative deviations are attributed to mutual attraction.

In order to apply this to the system at hand, one further concept must be mentioned, namely, that of the partial pressure. In an ideal mixture of gases, the partial pressure of component is given by

$$p_1 = n_1^{\circ} RT/V$$

where n_1° is the number of moles in the vapor phase, R is the gas constant, T the absolute temperature and V the volume. Eliminating **pl** and noting that $n_1 \sim n_1/n_2$:

$$\frac{n_1^{\circ}}{n_1} = \frac{p_1^{\square} V}{n_2 RT}$$

On this basis it therefore becomes a straightforward, if complex, problem to calculate the amount of each radionuclide present, as was done by Hunter and Ballou, and then distribute each one between the vapor phase and the condensed phase. The fission product radionuclides are present in such small concentrations that interaction between them can be neglected. The values of p_i for some important elements are shown in Fig. 4

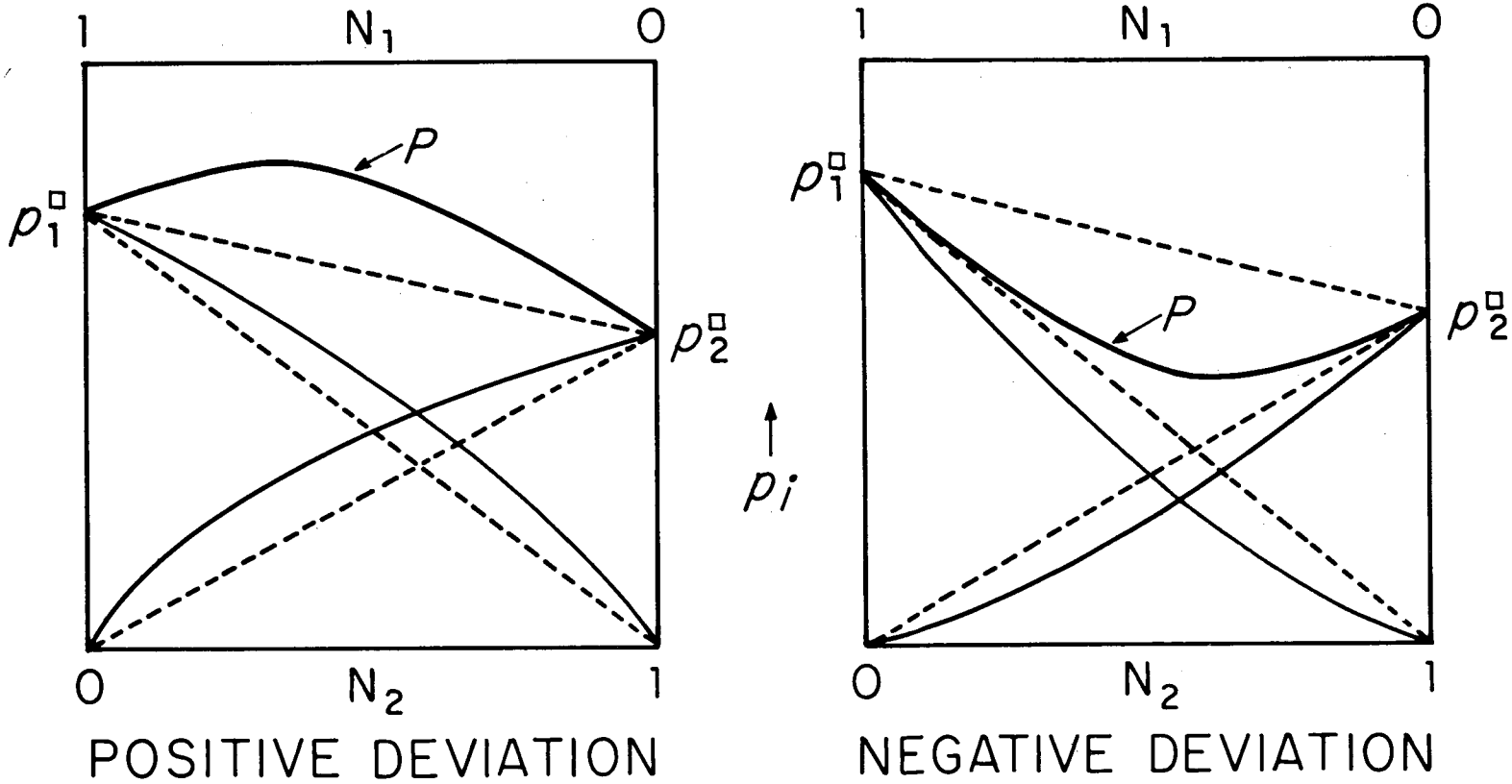

FIGURE 3. VAPOR PRESSURES OF NONIDEAL SOLUTIONS (DASHED LINES INDICATE IDEAL BEHAVIOR CALCULATED FROM RAOULT'S LAW)

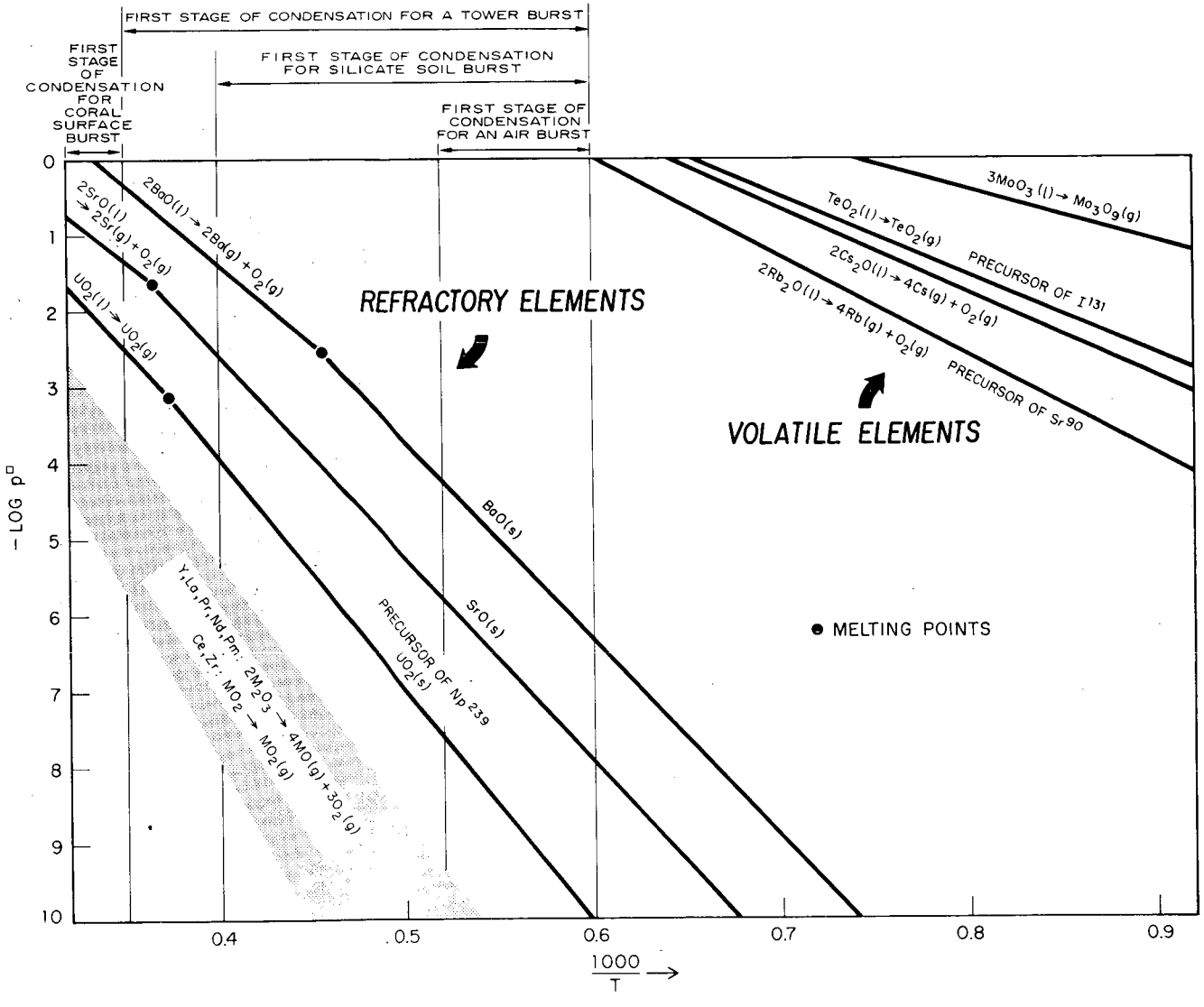

FIGURE 4. VAPOR PRESSURES OF IMPORTANT FISSION AND CAPTURE PRODUCT ELEMENTS DURING VARIOUS CONDENSATION PROCESSES.

Miller refers to the adsorption processes occurring after the particles solidify as the second stage of condensation. He suggests either using Langmuir adsorption isotherms or sublimation pressures to estimate the distributions at this stage, but doesn't apply them in his work. His results show an "ionization rate" of fractionated fission products equal to 0.4 that of unfractionated fission products at one hour, while his observed data show an "ionization rate" of 0.3 that of unfractionated fission products. From what has been said, it should be clear that there is not one fractionated composition, but many. The comparison stated is that of a single calculated composition with one of many possible observed compositions. Without radiochemical documentation the significance of the comparison remains obscure.

Part II. The NRDL Dynamic Model for Fallout from Land Surface Nuclear Bursts

The NRDL D-Model (Dynamic Model) was developed by Anderson and is described in detail in several reports.(2-5) This section will be primarily a summary of Anderson's description. Enough detail will be given to allow the reader to understand the application of Miller's fractionation model to fallout predictions for land surface bursts.

In the cooling fireball the temperature will eventually reach a point where soil particles entering the fireball are no longer vaporized and where vaporized soil present in the fireball begins to condense. This temperature is estimated as the boiling point for an abundant high boiling constituent of the soil. In the case of Nevada Test Site soil this constituent would be quartz which boils at about 2200°C. In the case of coral surface bursts this substance would be CaO which boils at about 2800°C. In the D-Model the time at which the fireball temperature reaches this value is taken as the time of the beginning of fallout. This time is about 0.6 sec. for a 1 KT burst, 6.4 sec. for a 100 KT burst, and 64.3 sec. for a 10 MT burst. The cloud at this time is approximated by a cylinder. The total residual activity is assumed to have a uniform distribution of particle sizes contained in a volume coincident with this cylinder. The activity-particle size distribution is divided into 100 classes. These classes range from a 40-60 μ diameter class up to a 8700-10,000 μ diameter class. Particles smaller than 40 μ are considered beyond the scope of local fallout. It is convenient therefore to think of the cloud at this time as consisting of 100 identical coincident right circular cylinders each corresponding to one of the particle size classes. In addition, each cylinder is divided up into N equisized discs. N may be as small as 7, as in the case of a 0.01 KT burst or as large as 231, as in the case of a 100 MT burst. The total number of discs therefore varies from 700 to 23,000. The situation is illustrated in Fig. 5.

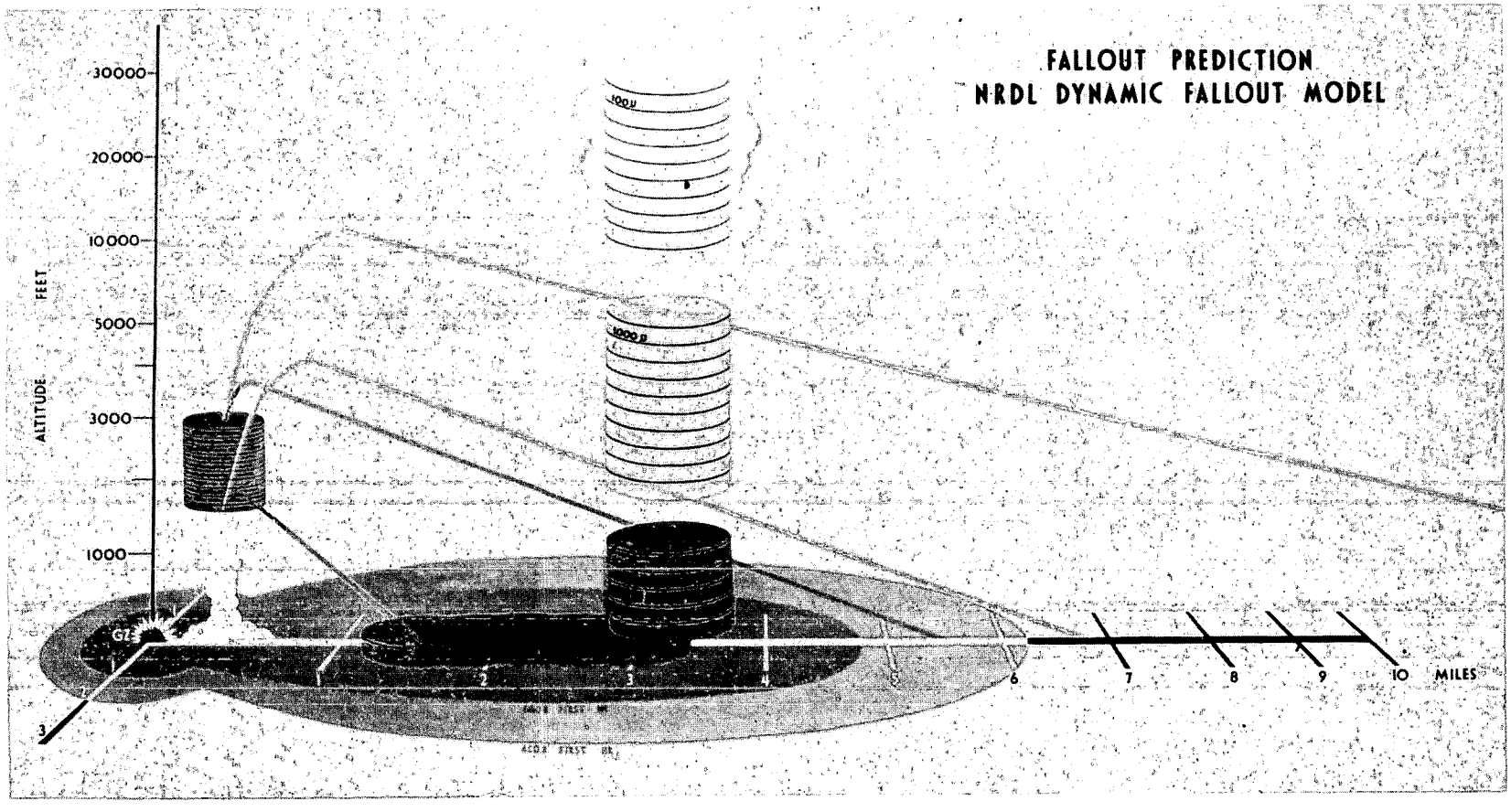
FALLOUT PREDICTION
NRDL DYNAMIC FALLOUT MODEL
ALTITUDE FEET
30000
20000
10000
5000
3000
1000
GZ
100 Y
1000 R
1
2
3
4
6
7
8
9
10 MILES

In contrast to those fallout models which begin when the cloud has reached its maximum height, the D-Model must account for the upward motion of the cloud in calculating the vertical velocity of the particles. Thus, the rate with respect to the ground at which a particle moves upward or downward is taken as equal to the difference between the velocity with which it is carried up by the rising cloud and the velocity due to gravitational fall. Vertical winds are not considered. Wind speed and direction during the time of rise and fall determine the particles horizontal displacement. The trajectory of each disc is now taken as the trajectory of a particle whose size is the midpoint of the size class of the disc and whose location is the center of the disc. Cylinders corresponding to different particle size classes are therefore seen to diverge gradually from one another. Cylinders representing large particles will not rise very high and will fall more rapidly. Cylinders representing small size particles will rise higher and level off more slowly. The time-altitude history is approximated by a finite difference equation dividing the time intervals from the start of fallout to the time the particle reaches the ground into N smaller intervals. The first interval is 1 sec. and each interval is 1 sec. longer than the preceding interval.

In treating the stem, the D-Model ignores the much higher velocities present there and treats the motion in the same manner as for the main part of the cloud.

Fig. 6 shows the cumulative percent of residual activity for particles of different size as determined from the Operation JANGLE underground shot. It is seen to be log-normal. For most siliceous soils the sparse data available indicate that for local fallout the fraction of radioactivity in a given size range is roughly independent of yield. However, the size-radioactivity distribution for coral is markedly different from that for siliceous soil.

If one of the discs representing a particular size class lands on the ground before one hour after burst and covers a point p on a rough plane, then the deposited dose rate R in r/hr. at 1 hr. and 3 feet above this location is given by $R = 120\ FA/NS$. Here 120 is a constant that takes into account final surface irregularities and other factors. The contribution of discs arriving after one hour to the calculated one hour dose rate is accounted for. F is the fraction of total residual radioactivity associated with the particle size class of the disc. A is the total residual radioactivity in curies remaining at one hour after burst, and is taken as 5×10^8 W curies for a weapon yield which is 100% due to fission. S is the area in square feet on the ground covered by the radioactivity contained in the disc. The edge effect is ignored. The total deposit dose rate at P is the sum of the individual dose rates contributed by the discs that cover this location. The effects of induced activities and fractionation are not taken into account by Anderson. S is assumed to be πr^2 where r is the radius of the disc. The method of finding the radius of the disc is based upon the

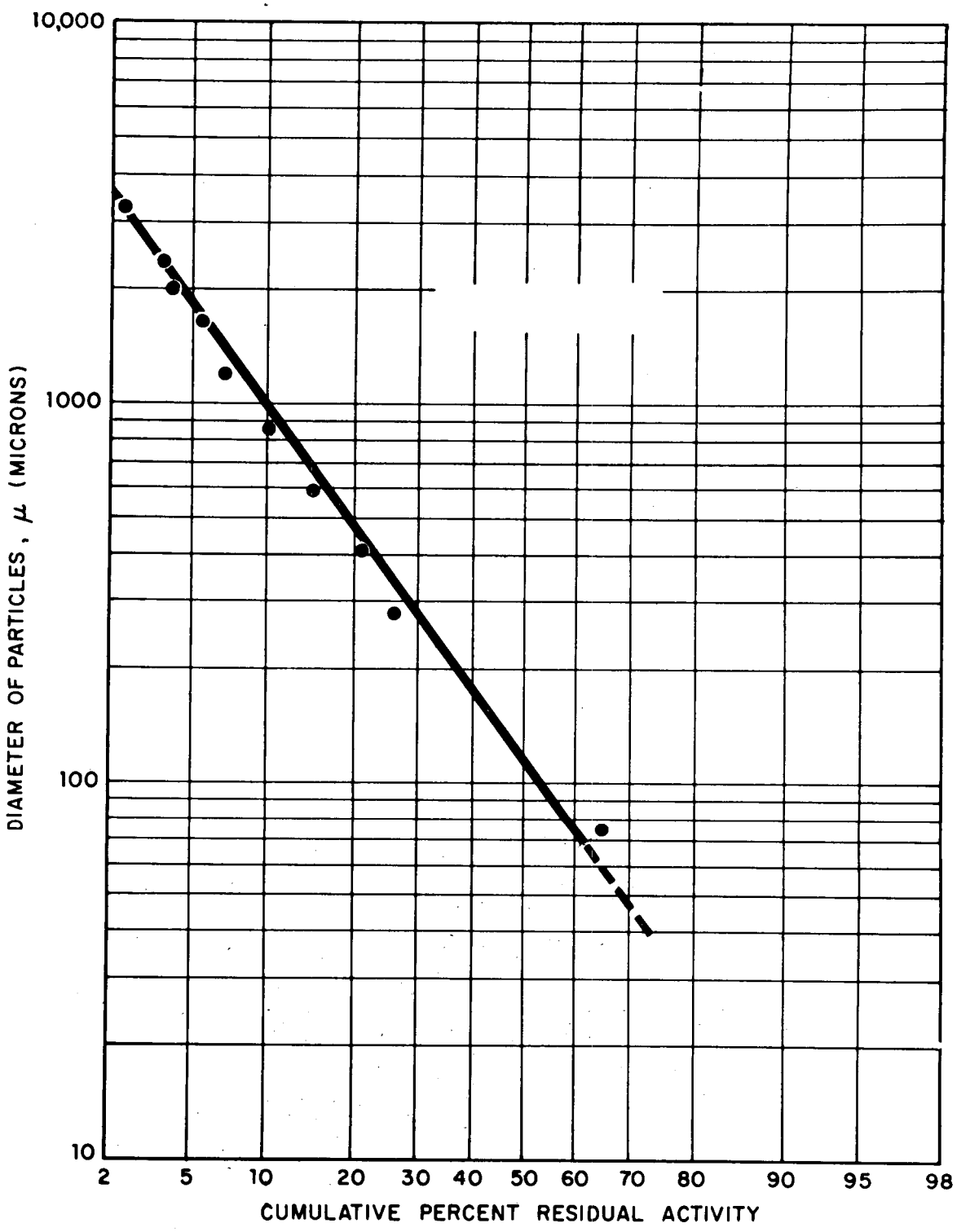

FIGURE 6. ACTIVITY-PARTICLE SIZE DISTRIBUTION FROM OPERATION JANGLE-U DATA (FROM (2)).

following three assumptions.

(1) The fallout is dispersed uniformly throughout the initial visible cloud at the time of start of fallout,

(2) As the cloud expands, the fallout expands laterally at the same rate as the cloud, and

(3) The lateral expansion of fallout stops after the cloud has stopped expanding.

The maximum disc diameter for all yields is taken as that given for 360 sec.

Because of the early time at which the D-Model begins to consider the fallout processes it can be readily seen that it is particularly suitable to being modified for the effects of fractionation according to the methods of Part I above. The details of this modification are described in the following section.

Part III. Modification of the NRDL Dynamic Model for Fractionation

The modification of the NRDL dynamic model for fractionation has been carried out by Lee, Kiley, and Johnson(7) according to a method outlined by Miller and is in the process of being programmed for an IBM 704 computer. The modification proceeds as follows. First, it is necessary to change from the activity-particle size input of Anderson to a mass-particle size input. To do this we use Miller's cratering equation

$$M = 5.03 \times 10^9 \, W^{0.92} \text{ grams}$$

for the mass thrown out, and assume 7.5% of this comes in contact with radioactivity. This 7.5% is assumed to have a log-normal mass distribution with 50% of the mass in particles of less than 100 μ diameter and 0.4% of the mass in particles larger than 10,000 μ . The fraction of a particle melted will be, for the present, considered independent of particle size.

There is next established a 69th concentric figure, a sphere, which is to represent the vapor phase of the cloud. At the end of the Anderson's first time interval (1 sec.) it is determined which discs have left the cloud. From the yields and half-lives of the primary fission products the quantities of the various product nuclides present at the midpoint of the time interval (0.5 secs.) are calculated. The temperature at this time is also determined. The temperature is used to calculate the vapor pressure of each fission product oxide at a partial pressure of oxygen of 0.2 atmospheres. This is used in conjunction with calculated cloud volume and number of moles of vaporized soil material to determine the distribution of each element between the vapor and condensed states.

The quantities condensed which leave the cloud can now be considered to be initial quantities for a Hunter-Ballou type calculation.[8] The uncondensed radionuclides are considered to be equally distributed throughout the fireball. Again, the Hunter-Ballou type calculation is employed using these uncondensed quantities as starting values in order to compute the quantities present at the midpoint of the next time interval. This process of gradual depletion of particles and radionuclides in the cloud is carried out until the temperature falls to 1400°C.

The second phase of condensation now begins. The portions of each radionuclide present in the condensed phase are now considered to be frozen in. The nuclides in the vapor phase are considered to be either one of two kinds: volatile or involatile. The choice depends upon whether or not their concentration in the cloud is greater than the vapor pressure of the pure substance at the given temperature. At the midpoint of the next time interval the temperature and vapor pressures are calculated as before. Those elemental forms which exceed their vapor pressures are distributed among the particles present according to the surface offered by the particles. Particles leaving the cloud therefore now scavenge radioactivity in proportion to their area rather than their volume and the quantity of each radionuclide remaining behind is equal to that required to saturate the cloud at the given temperature. The process is carried out until all discs have left the cloud.

It is now seen that the rate of arrival of any given radionuclide at any point can be calculated as well as the radionuclide distribution at any point at any time after burst. This radionuclide distribution can now be used as the starting point for the calculation of dose rate according to the decay schemes of the radionuclides involved.

Problems of throwout, stem treatment, and environment induced activities are still under consideration.

The calculations described are very complex and the amount of computer time required to make them has not yet been determined. It is not beyond the realm of possibility that the time required for a complete calculation would be prohibitive were it not for certain simplifications that might be made. First of all, there are those substances which are refractory to an equal or greater extent than the vaporized soil. Those mass chains which consist entirely of such elements will be completely condensed from the outset. At the other extreme are mass chains which will be present primarily as gaseous materials throughout the better part of the condensation process. It has been pointed out[1] that the relative abundances of one such refractorily-behaving radionuclide and one such volatilely-behaving radionuclide at any point in the fallout pattern would determine the relative abundances of the other radionuclides to an extent which was quite adequate for the purposes of estimating fractionation and furthermore was grounded more solidly in experimental observation than is the preceding treatment. In principle, therefore, an ability to predict the abundance of two such nuclides, coupled with a knowledge

of the fractionation systematics obtained through observation, would yield a method of accounting for fractionation in fallout which is at once more simple and more reliable than the detailed calculations described. We will return to this subject in subsequent sections.

Part IV. Means of Testing the Miller-Anderson Fractionated-Fallout Model

The model which we have described is a complex combination of mechanical, thermodynamical, physical-chemical and nuclear-physical considerations. The intricate structure rests shakily on a large number of simplifying assumptions and approximations. The questions we now ask are, "How much closer are we now to reality than we were before in our ability to predict fallout patterns?", "What can we do to improve this approach to reality?" and "How much of this do we want to do?" The first two questions will be discussed in these last two parts of this paper.

One thing we hope to do very soon is to apply the considerations described here to the treatment of data from Operation JANGLE shots. When we do we may achieve better agreement between predicted and observed values than have been obtained before or we may not. Improved agreement would naturally be more encouraging. But how could we be sure that this was not obtained by a fortuitous concellation of errors for the particular event studied? And how could we be sure that in some subsequent application these errors would not cancel and we would not be so fortunate? Observational data in the form of dose patterns and decay curves are themselves complex results of the radioactive properties of the radionuclides present in the fallout material. The calculation of these quantities from the radionuclide composition is a fairly straightforward problem. The reverse calculation is, however, virtually impossible, for while a certain radionuclide composition will result in only one dose and one decay curve, the particular dose or decay curve can be described by a number of radiochemical compositions. It is therefore seen that the radiochemical composition of the fallout at particular points is the basic knowledge that is wanted. It is this knowledge which we expect our fallout model to predict and it is observation of this composition which constitutes one of the most desirable types of data for determining the reliability of the predictions. The quality of radiochemical data available for Operation JANGLE shots is very poor by present day standards and so our uncertainty will be increased by having to rely upon the less desirable and more complex type of observation.

Land surface shots in the Eniwetok Proving Grounds are better sources of material for testing fractionated fallout predictions. Shots Zuni (1956) and Koa (1958) in particular, were the subjects of considerable useful documentation. However, the chemical and thermal properties of coral differ so greatly from those of Nevada Test Site soil and other surfaces to be expected within the continental limits of the United States that success in these areas would be no guarantee of success in the latter cases. Nevertheless, the application of our fallout model to these

bursts appears to be a worthwhile method of testing and one which we intend to do.

The assumptions involved in Miller's approach can be thought of as falling into two groups. First, there are the assumptions bearing upon the distribution of radionuclides between vapor and condensed phase in the first stage of condensation. These are, namely, thermodynamic equilibrium and applicability of Raoult's Law. The second group of assumptions are those which are required to estimate the amount of molten soil present in the fireball at the time of condensation. In view of the tenuous nature of both of these sets of assumptions and desirability of testing each set independently of the other should be evident. To test the applicability of Raoult's Law and thermodynamic equilibrium independently requires a reliable knowledge of: (1) the quantity of molten soil; (2) the existence of a single vapor-liquid phase separation; (3) the time of separation; (4) the temperature at this time; (4) the volume of the vapor phase at this time; and (6) the resulting distribution of fractionated nuclides. This combination of requirements appears to be nearly fulfilled in the case of the Rainier shot. The Rainier shot occurred at the Nevada Test Site on September 19, 1957 about 800 feet underground with a yield of 1.7 KT. It appears to have vaporized 1.5 tons of rhyolite and melted another 850 tons. This molten soil was in contact with the vapor phase for a period of about 30 seconds to 2 minutes after the time of burst. At this time there appears to have occurred a sudden drop in pressure due to the venting of the vapor phase into some external volumes. The temperature at this time was not uniform throughout the system but there is evidence that condensation had already occurred in the vapor phase. The temperature in the vapor phase was therefore less than 2200°C. and the temperature of the lowest or coolest molten portion was greater than 1400°C. The volume of the vapor phase at the time of separation is known from the measured dimensions of the cavity. Fractionation data of good reliability is available for a significant number of radionuclides at several representative locations. It is from these data that the estimate of the time of separation has been made. This time is long enough so that much of the uncertainty in independent yields and half-lives of short-lived fission product will not significantly influence the calculations. The quantity of moisture present in this burst was much greater than would be expected in a Nevada surface burst. The effect of this may be neglected as the first approximation. The most serious drawback appears to be the difference in subdivision of the molten material in this case compared to that in a surface burst. The assumption of thermodynamic equilibrium includes an assumption that the radionuclides in the condensed phase have had the opportunity of distributing themselves uniformly throughout the molten volume. The speed at which this is accomplished depends upon the diffusion coefficient of the substance in the molten material. The diffusion constants of substances in silicates can be 10 or 100 times lower than the diffusion constants of other high temperature materials such as, for example, molten salts. Glass manufacturers are potential sources of additional information.

If the material under consideration is in a fine state of subdivision this will be less important. In the Rainier shot the material was essentially undivided. In order to have a reasonable hope of success it therefore would appear that this should be accounted for in the calculations involved in the model before it is applied to Rainier data. Needless to say, such a refinement would materially improve the realism of the approach taken in the initial model also. Therefore this is something which appears to be worth doing as part of the model refinement process.

Two kinds of experimental measurements which we are planning to carry out in the laboratory will help to alleviate our ignorance in these matters. First, we will measure the rate at which various fission products diffuse through molten silicates and determine if the rates are fast enough to permit equilibrium. Secondly, we will determine the ideality of behavior of various fission product oxides over molten Nevada soil. Both these types of experiments will not only yield evidence of the validity of the assumptions involved but will also yield information by which the assumptions can be corrected and more valid treatments incorporated.

Part V. Fallout Data Required for Testing

In this section I want to outline the kinds of observation which would be more or less ideal for testing the type of model that we have described and obtaining additional data which we need. These thoughts are put forth with little regard for the economics involved. In some cases order of magnitude estimates of the costs can be given. The decision as to whether a foundation for fractionated fallout models of the firmness to be obtained by basing it on the data described is worth the price of investigation is beyond the scope of these studies.

The main areas of ignorance have been summarized by Knapp.[9] This summary, which I now quote, forms the basis of this part of my presentation.

> "What we need to know, and what we generally do not know to within a factor of 2 to 3, may be partially described in the following way.
>
> (1) The distribution of the radioactivity created in nuclear explosions between stratospheric, tropospheric, and local fallout. This distribution depends strongly on the location and conditions of burst, and on the yield of the weapon.
>
> (2) The size distribution, physical and chemical form and properties of the fallout particles, and the distribution of fission products and induced activities among them.

(3) The degree and manner in which radioactivity from various types and conditions of bursts is fractionated. Different relative concentrations of the various nuclides may occur in stratospheric, tropospheric, and local fallout than in the total debris, and even within the region of local fallout the relative concentrations may vary significantly with distance from the explosion. Radiological fractionation may also be considered as occurring between particles of different sizes, different chemical form, and perhaps in other ways such as degree of solubility. Such factors need identification, study as to cause, and evaluation as to relative importance."

I can think of no better means of obtaining the answers for the first two areas of ignorance than that used in Project 2.8 of Operation HARDTACK[10] which I will not describe.

The primary objective of this project was to estimate the partition of Sr^{90} and Cs^{137} between local and long-range fallout in nuclear detonations over land and water surfaces. A secondary objective was to determine the spatial distribution of radioactivity and particles in the cloud a few minutes after detonation. These objectives were to be achieved by radiochemical analysis of the following types of samples:

1. Aircraft samples of particles and radioactive gases present in the upper portion of the clouds.

2. Rocket samples of the particulate matter in the clouds to be collected along nearly vertical flight paths, at several distances from the cloud axis.

3. Fallout samples collected along height lines at an altitude of 1,000 feet by aircraft.

Portions of particulate samples were separated into coarse and fine fractions (greater or less than 25 μ, the selected division between local and worldwide fallout) with a Bahco centrifuge and fall rate distributions for the two fractions determined with a micromerograph. These samples were analyzed separately.

The observations were carried out on high yield coral, water, and coral plus water surface bursts. A fractionation correlation of the Sr^{89}, Sr^{90}, Ce^{144} data is shown in Figure 7. Unfortunately, Zr^{95} was not determined in these samples, and Ce^{144} was chosen as the refractorily-behaving standard. The similarity to previously correlated data, from which the correlation line was taken, is obvious. In the land surface burst, it appears that Sr^{89} and Sr^{90} fractionate from each other in the coarse particles, but not in the fine.

Unfortunately, the rocket sampling part of the program failed and the

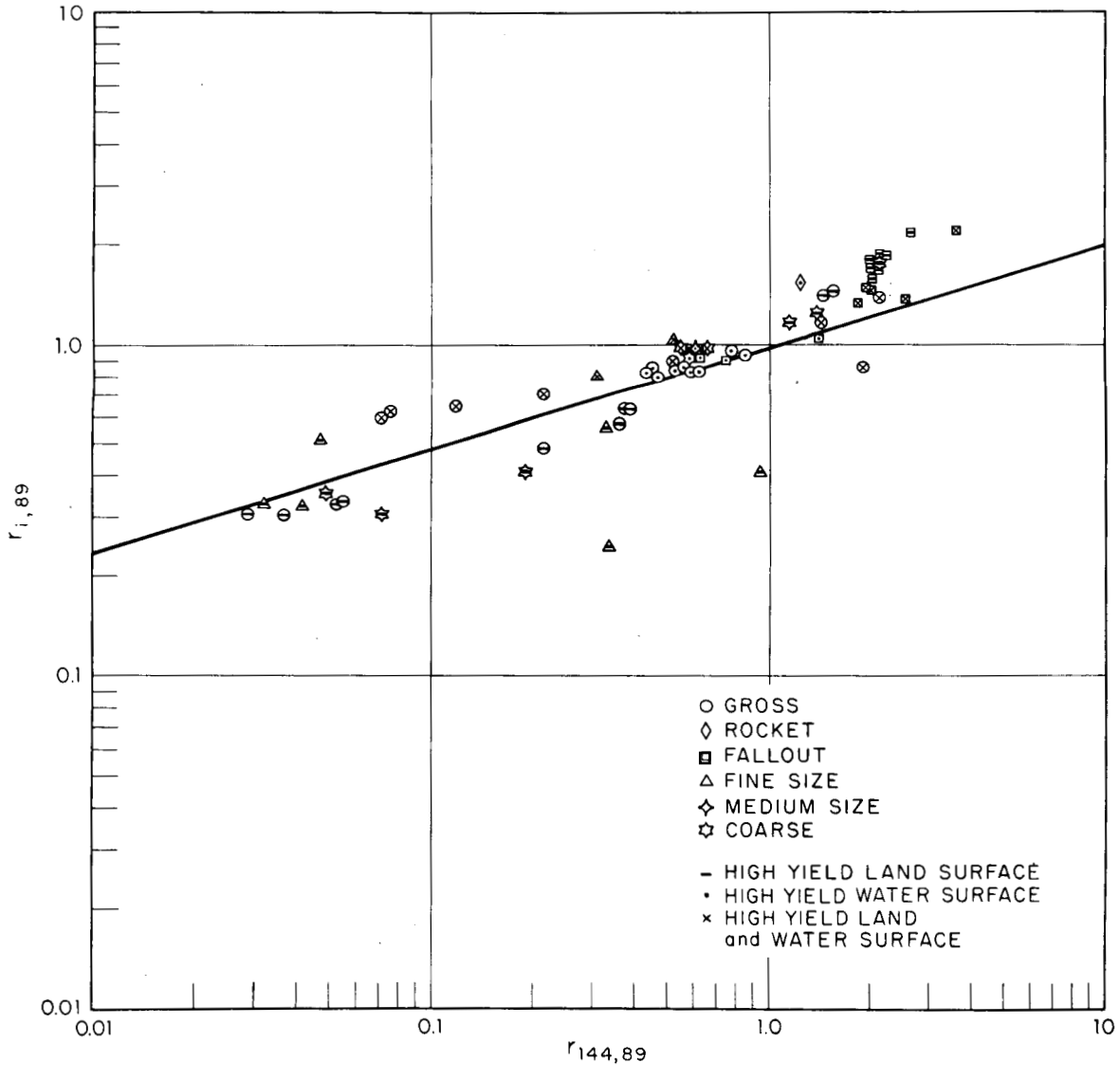

FIGURE 7. FRACTIONATION CORRELATION OF SR^{90}, SR^{89} and CE^{144} DATA FROM HARDTACK PROJECT 2.8 (THE LINE IS TAKEN FROM THE ANALOGOUS CORRELATION IN (1)).

project fell short of its goal. However, much valuable information and experience was obtained, and similar projects in the future would be highly desirable, with even more extensive and intensive documentation, particularly in the study of small particles.

Regarding the third area of ignorance mentioned by Knapp, what we require are fallout patterns which are basically different from the ones usually encountered. The familiar fallout pattern is a series of contours of dose rates at 1 hour after burst. This apparently represents the information most readily interpreted by military and civilian defense planners. It is far too unrevealing to allow adequate building and testing of a fractionated fallout model. What we need in any given burst is not one set of fallout contours, but two. The first set of contours would show the fraction of some refractorily-behaving radionuclides per unit area. For example, one might show the fraction of the total amount of Zr^{95} produced by the device which can be found per square foot at the locations indicated. The second set of contours might represent the same type of information for some volatilely-behaving radionuclides such as Sr^{89} or Cs^{137}. This would provide part of the required information but it would be more instructive to have for the second set of contours a chart of the ratio of Zr^{95} to Sr^{89}. We have called the logarithm of this ratio the "fractionation index." Fractionation index contours would clearly show how the degree of fractionation varied throughout the fallout pattern.

We would now be in possession of information concerning an extensive parameter to indicate the quantity of debris at a given location and an intensive parameter to indicate the departure from representativity at any location. We would still need data to be able to fill in the distribution of the other fission product radionuclides and important induced activities. If we were trying to predict the distribution of each nuclide with our model we would need these data in order to see if we had predicted the distribution properly. On the other hand, if we were only using our model to predict the Zr^{95} contours and the fractionation index contours, we would need these data to interpolate empirically the fractionation of the other radionuclides. Presumably, these data would require an exhaustive radiochemical analysis of a limited number of samples selected for their spread in fractionation index.

Such data could also be used to integrate the fractions of various radionuclides which deposited. By mass balance considerations, the amounts contributed to worldwide fallout could be calculated. Consistency with the data described above would offer valuable support to the results. Experience with field operations has led to the conclusion that whatever can go wrong, will go wrong, and planned over-documentation can turn out to be inadequate documentation.

One would of course want to obtain much other information at the same time such as dose rates, decay curves, gamma assays, and gamma spectra,

mass of fallout, of particle size data, individual particle analysis, etc., which are usually collected during a field test. If this kind of information were backed up by the kind of documentation I have described it is easy to visualize how the correlation of this knowledge with basic radiochemical information would permit a more meaningful interpretation and applicability to prediction than has ever been realized in the past.

References

1. Freiling, E. C. Radionuclide fractionation in bomb debris. Science 133: 1991(1961)

2. Anderson, A.D. The NRDL synamic model for fallout from land-surface nuclear bursts. U. S. Naval Radiological Defense Laboratory report USNRDL-TR-410, San Francisco, 5 April 1960.

3. Henry, G., and A. D. Anderson. Dose-time-distance curves for close-in fallout for low yield land-surface nuclear detonations. U. S. Naval Radiological Defense Laboratory report USNRDL-TR-390, San Francisco, 30 December 1959.

4. Anderson, A.D. Application of 'Theory for Close-In Fallout' to low-yield land surface and underground nuclear detonations. U. S. Naval Radiological Defense Laboratory report USNRDL-TR-289, San Francisco, 12 January 1959.

5. Anderson, A. D. A theory for close-in fallout. U. S. Naval Radiological Defense Laboratory report USNRDL-TR-249, San Francisco, 23 July 1958.

6. Hillendahl, R. W. Characteristics of the thermal radiation from nuclear detonations (U). U. S. Naval Radiological Defense Laboratory report USNRDL-TR-383, 3 Vols., San Francisco, 30 June 1959.

7. Lee, H., W. T. Kiley, and R. W. Johnson. Unpublished work.

8. Hunter, H. F., and N. E. Ballou. U. S. Naval Radiological Defense Laboratory report USNRDL ADC-65. 24 February 1949. Nucleonics 9 (5): C-1 (1951)

9. Knapp, H. Private communication. 1960.

10. Whitcher, S. L., L. R. Bunney, R. R. Soule, and R. da Roza. Operation HARDTACK, Project 2.8, Fallout measurements by aircraft and rocket sampling (U). U. S. Naval Radiological Defense Laboratory, U. S. AEC Weapons Test Report WT-1625, 29 September 1961. (SRD).

PARTICLE FORMATION AND FRACTIONATION IN AIR BURSTS

Edward C. Freiling
U. S. Naval Radiological Defense Laboratory
San Francisco, California

ABSTRACT

The relation of fallout formation processes in air bursts to processes occurring in other types of bursts are discussed. Results obtained to date on testing available particle formation theories and means of extending these theories to include fractionation are described. A brief summary of available results of fractionation correlations on air burst debris is given and data requirements from future detonations are presented.

Introduction

In this paper I will describe the long-range portion of the fallout model program at NRDL. The object of this portion of the program is two-fold: first, to refine the treatment of land surface bursts described in the previous paper; and second, to extend model-making capability to other types of bursts in line with the general objective of the program. The applicability of the study of air bursts to the latter objective is evident. The applicability to the first objective will be discussed in Part I below on the importance of air bursts. Part II will discuss gross phenomenonolgy and Part III will discuss the macroscopic features of the formation of air burst debris. Part IV will treat the interaction between the macroscopic debris and the product radionuclides and Part V will point out data required from future bursts.

In the remainder of this paper we will talk as much of plans as of

results. Nevertheless, even the preliminary state of accomplishment which we have reached has yielded information of interest and value.

Part I. Importance of Air Bursts

The knowledge obtained from the study of air bursts is applicable to the study of land surface, water surface, and tower bursts. The reason for this can be seen by considering the processes involved.

Fig. 1 outlines the processes which occur in a land surface burst. It is a complex picture of simultaneously occurring nuclear, physical and chemical reactions. The nuclear processes are shown at the top of the figure, namely, the formation of the primary induced and fission product activities followed by their decay into daughter activities or into stable nuclides. Below these are shown the physical-chemical processes, i.e., environment vaporization followed by nucleation in the cooling cloud, condensation, and scavenging by late-arriving particles. The chart is divided timewise on the horizontal scale into a blast phase, and a fallout phase. The chart is a gross simplification but it serves to orient the reader to the interplay of the various features involved in the overall picture of fallout formation.

With regard to the nuclear processes, although there is much missing data concerning independent fission yields and the half-lives of short-lived fission products, the means of estimating the missing parameters have been the subject of considerable study. The methods of estimating the unknown quantities are therefore relatively straightforward, if not completely satisfactory. Certainly we are on much firmer ground in this part of the picture than in the lower part. Before considering the interaction of the radionuclides with molten and solid particles in various stages of transition it is necessary to have some understanding of particle formation itself. Chronologically the first process to consider is that on nucleation. This if followed closely, and in part simultaneously, first by condensation and then by agglomeration. Nucleation is the first step in the transition from a vapor to a condensed phase, whereby clusters of condensing atoms or molecules finally attain a thermodynamically stable condition of existence. While nucleation is occurring in one part of the cloud, nuclei already formed in another part will be condensing vaporized material on their surface. As the number and size of the particles becomes sufficiently large the possibility of particles colliding and coalescing becomes greater, and at the same time, due to depletion of the carrier material in the vapor phase, the nucleation rate bcomes less.

The particles formed by these processes will be in the small size range, probably of the order of 20μ or less. When the temperature of the cloud has fallen to the point where incoming soil particles are no longer vaporized, these new particles will scavenge the previous ones. The

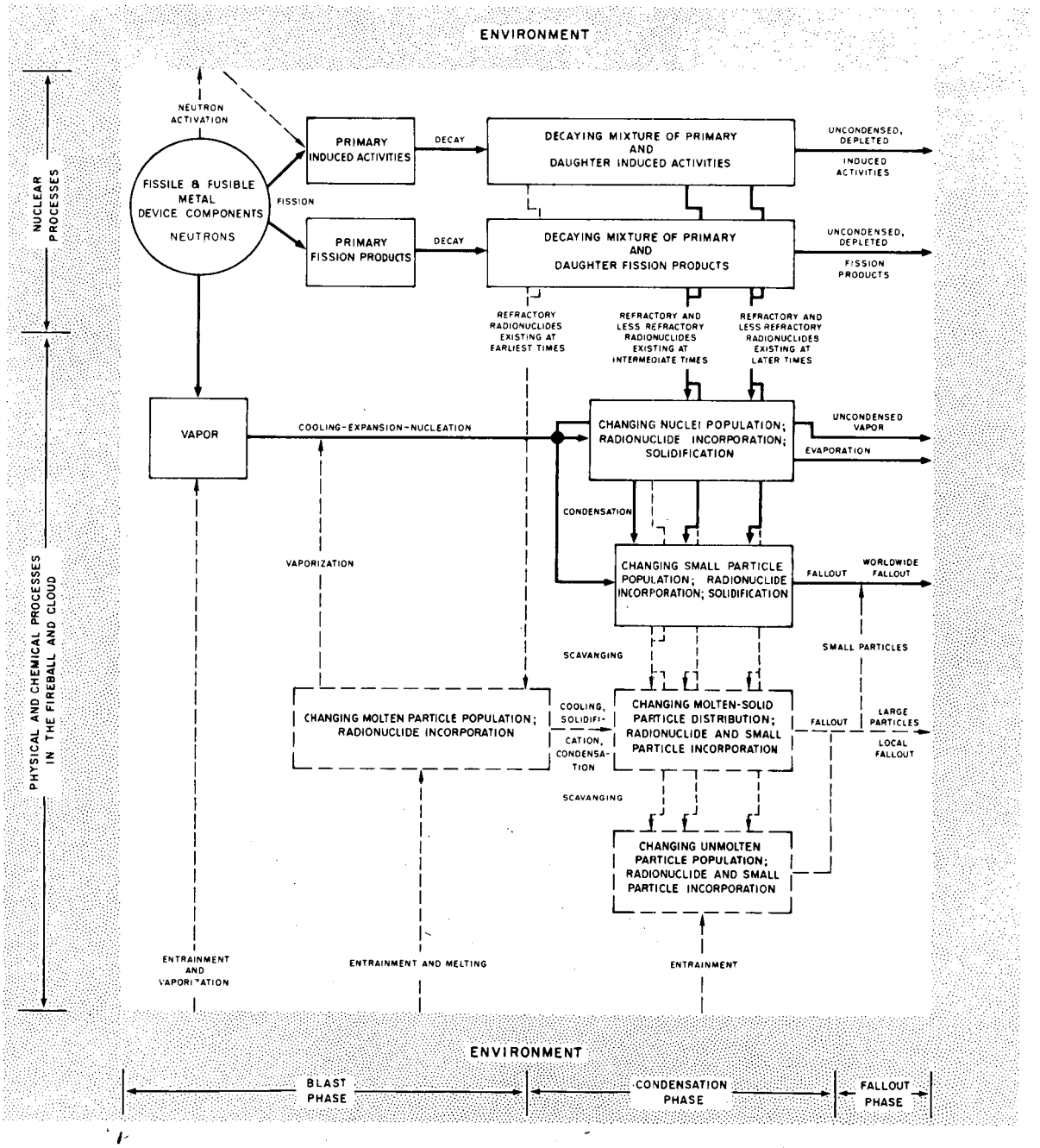

FIGURE 1. Fallout Formation Processes in Air and Surface Bursts.

number remaining unscavenged, together with the small incoming particles, will constitute the portion of the debris contributed to tropospheric and stratospheric fallout (cf. Parts (1) and (2) of the requirements outlined by Knapp and quoted in the previous paper, page 42).

Now it can be seen that subsequent interaction of these primary particles with engulfed but unvaporized soil material will obscure the effects of the primary processes that one sees by examination of the debris. In order to test a theoretical treatment of nucleation and condensation by the properties of such debris, one would have great difficulty not only in sorting out that portion of the observed data due to the processes of interest, but also in dealing with large uncertainties in the quantities of soil involved. On the other hand, in an air burst, such a theory could be tested with much greater hope of success for two reasons: first, the quantity of material vaporized is accurately known; and second, the processes are not complicated by scavenging.

There are other features of air bursts which make them important in themselves. First, whereas land surface bursts contribute only a fraction of their radioactivity to world-wide fallout, air bursts contribute virtually 100% of their activity to world-wide fallout. Secondly, air bursts are valuable sources of data for the prediction of fresh water surface burst phenomena such as might occur in the Great Lakes. Here the initial debris formation processes should be very similar to those occurring in an air burst, the presence of vaporized water being neglected as a first approximation. Subsequent interaction between the initial particles and the condensed water could be elucidated by laboratory studies of the interaction of air burst debris with water at high temperatures. The application of seawater surface burst data to the prediction of fresh water surface burst data is not as reliable as might be thought at first sight, due to the presence of large quantities of salts from the vaporized ocean water and the fact that most seawater surface bursts have been barge shots and have not covered a very wide yield range. The extent to which the presence of barge material and salts has altered the fundamental fallout particle formation processes is not known.

Finally, as will be seen from the subsequent part of this paper, there is a good possibility of reaching a fairly complete understanding of the subject of air bursts at an early date. Tower shots would then form a link between an air burst model and a land surface burst model because the initial particle formation processes in a tower shot would be dominated by the presence of iron, as are air bursts, but would have the additional complication of soil, as in the case of surface bursts. (See Fig. 4 of the preceding paper, page 33).

Part II. Phenomenonology

An air burst begins at a time called the zero time, t_o, with the release of a large amount of energy W in a small space called the fireball. The partition of energy between thermal and mechanical effects is different for "high altitude" bursts (defined as bursts at heights above 100,000 ft.) than for air bursts at moderate heights. We will limit our discussion to bursts at moderate heights. Then about 5% of the energy released is in the form of initial nuclear radiation (gamma rays and neutrons) and 10% in residual radiation (alpha, beta and gamma rays). The remainder is rather evenly dividied between mechanical energy (blast) and thermal energy (heat and light). The following description of subsequent phenomena is a blend of those found in "The Effects of Nuclear Weapons" and in Hillendahl's work.(1)

To quote The Effects of Nuclear Weapons: "Because of the very high pressure within the exploding bomb the residue, consisting of fission products and all other bomb materials, moves outward from the center of the explosion at a very high velocity... After a few microseconds, nearly all of the debris is contained in a relatively thin shell of high density called the 'hydrodynamic front': its initial temperature is about a million degrees and it is traveling at a speed of several hundred miles per second. ....The mass energy is transferred to the medium" and a blast front is formed. At first this is preceded by a radiation front (the surface of the fireball)," because the mean free path of the radiation in the hot gas is so long that the transfer of energy by radiation is more rapid than by mass motion." As the temperature drops, the transfer of energy by radiation becomes less rapid, the shock front begins to advance more rapidly and passes it at a time when the temperature has fallen to about 300,000°C. This phenomenon is called the "hydrodynamic separation." It occurs at about $10^{-4}\ W^{0.42}$ sec. at a radius of about $4W^{0.37}$ m. After this the fireball consists of two concentric regions. The inner one is called the isothermal sphere and is bounded by the radiation front. Its radius is R_2. The outer region consists of luminous, shock front heated air. It is bounded by the shock front, whose radious is R_4. (See Fig. 2 of previous paper, Page 30). The radius then grows accoring to the law

$$Wt^2 = 1.27 \times 10^{-8} \rho_o (2R_4)^5$$

where R_4 is in meters, t the time in milliseconds, and ρ_o the ambient air density in g/l. The luminous air produced by the shock front obscures the vision of the isothermal sphere until a time of $3.65 \times 10^{-3} W^{0.42}$ sec. called the "breakaway." At this time the apparent temperature is a minimum and the isothermal sphere again becomes visible. The temperature then rises again to a maximum value of $8900\ W^{-0.03}$ degrees K at a time of $0.045\ W^{0.42}$ sec. This time is called "the time of final maximum" and given the symbol t_f. The temperature drops to $3300\ W^{-0.03}$ degrees K at a time of 15 t_f. Its logarithmic dropping rate in this period is $(t/t_f)^{1/40}$. At this time (15 t_f) the

radius of the isothermal sphere has levelled off to a value somewhat exceeding 63 $W^{0.35}$ m. The radiated power equation is given by

$$H(W,t^*) = 6.68W^{0.58}\, t^{*-1.6}{}_e{}^{-9e^{-2.73t^*}}\, e^{-9e^{-1200t^*}}$$

according to which 0.55W eventually becomes radiated. Here $t^* = t/t_f$.

The cloud during this time has been rising. For a 1 MT burst the rise in feet is given approximately by $76{,}000\ (1 - e^{-0.42t(\text{sec.})})$ out to about 10 min.

Part III. Particle Formation

Three theories of particle formation have been found which apply to air bursts. These consider the basic processes previously mentioned in various detail and lead to particle size distributions in terms of two basic parameters: the total number of particles and a characteristic particle size. The shape or functional form of the distribution depends upon the relative importance given to the processes treated. The characteristic size depends upon various measurable or estimable parameters. Once these have been fixed, the total number of particles is determined by the mass of the device and the demand of mass balance. It is expected that the details of particle formation mechanisms will be most accurately revealed by the theory which best fits the observations, and therefore that theory would form the starting point for developing additional applications.

The first theory, due to Woodcock (2), will be quickly dispensed with. First, because it is described in a confidential report, and second, because it has not been found to fit the observed data. The treatment could concievably be more applicable to other burst conditions.

The second is due to Magee.(3) His treatment emphasizes the nucleation and condensation processes and arrives at the exponential distribution

$$n(r)\,dr = \frac{n_T}{\bar{r}} \exp\left(-\frac{r}{\bar{r}}\right) dr$$

where n_T is the total number of particles and $\bar{r}$ is the mean radius. In this theorty $\bar{r}$ is the ratio of β, the radial growth rate of a particle, to α, the logarithmic growth rate of the nucleation rate I.

The third treatment was devised by Stewart (4). It considers the process of nucleation, condensation and coagulation occurring simultaneously. Stewart arrives at the log normal distribution

$$n(r)\, d(\ln r) = \frac{n_T}{\sqrt{2\pi}} \exp\left[-\frac{1}{2}\left(\ln \frac{r}{\bar{r}}\right)^2\right] d(\ln r)$$

Here, again, n_T is the total number of particles. The modal radius is given by

$$\bar{r} = \frac{v_B N_o T_o}{Kn} \left(\frac{k}{2\pi mA}\right)^{\frac{1}{2}}$$

where

v_B = molecular volume in the liquid phase

N_o = initial number of atoms per unit volume

T_o = absolute temperature at the time of condensation

$K = 4\ kT/9\eta \approx 3 \times 10^{-9}$, T = absolute temperature, η = air viscosity

n = concentration of nuclei

k = Boltzmann's constant

m = molecular mass

A = 7500°K.

As mentioned above, the most fundamental property of the predicted distribution is their functional form, or what is equivalent, their shape. These predictions can be compared with observed data in various ways: by using either differential or integral curves and by comparing either slopes, areas or individual values. All of these means were considered. The method found to be most suitable, not only for determining the shape, but also for evaluating the parameters, is based upon converting these equations to linear form. Thus Magee's equation

$$n(r) = \frac{n_T}{\bar{r}} \exp\left(-\frac{r}{\bar{r}}\right)$$

becomes

$$\ln n(r) = \ln \frac{n_T}{\bar{r}} - \frac{r}{\bar{r}},$$

so that a plot of ln n(r) vs. r will have slope - $1/\bar{r}$ and intercept $\ln \frac{n_T}{\bar{r}}$, similarly, Stewart's equation

$$n(r) = \frac{n_T}{\sqrt{2\pi}} \exp\left[-\frac{1}{2} (\ln r/\underline{r})^2 \right]$$

becomes

$$\left[2 \ln n(r) + (\ln r)^2 \right] = \left[2 \ln \frac{n_T}{\sqrt{2\pi}} - (\ln \underline{r})^2 \right] + 2 \ln \underline{r} \ln r$$

so that a plot of $\left[2 \ln n(r) + (\ln r)^2 \right]$ vs. ln r will have a slope of 2 ln $\underline{r}$ and an intercept $\left[2 \ln \frac{n_T}{\sqrt{2\pi}} - (\ln \underline{r})^2 \right]$.

This technique has been applied to particle size data from a number of air bursts. It has resulted in discarding Woodcock's treatment in favor of the other two, but has not permitted a choice to be made between the treatments of Stewart and Magee. An example of its application in the latter two instances is shown in Figs. 2 and 3. The scatter at the large particle end of the curve is not statistically significant, due to the small number of particles involved. The value of 5μ is taken as the lower limit of reliability of the data. The values for the parameters obtained are: $n_T = 1.86 \times 10^6$, $\underline{r} = 0.0718\mu$; Magee, $n_T = 2195$, $\bar{r} = 1.83\mu$.

From these results one can calculate the following properties of the sample:

	Stewart	Magee
Total Surface	0.89 mm^2	0.185 mm^2
Total Volume	$2.65 \times 10^5 \mu^3$	$3.38 \times 10^5 \mu^3$
Total weight (assuming density 2.5)	652 smidgins	845 smidgins

From these data it is seen that particle size separations would have to be done in addition to chemical analysis in order to obtain the information required to eliminate one of these theories. If the surviving one were also able to predict the characteristic particle size with reasonable accuracy, one could proceed to apply the treatment with some degree of confidence that the processes involved were well understood and properly treated.

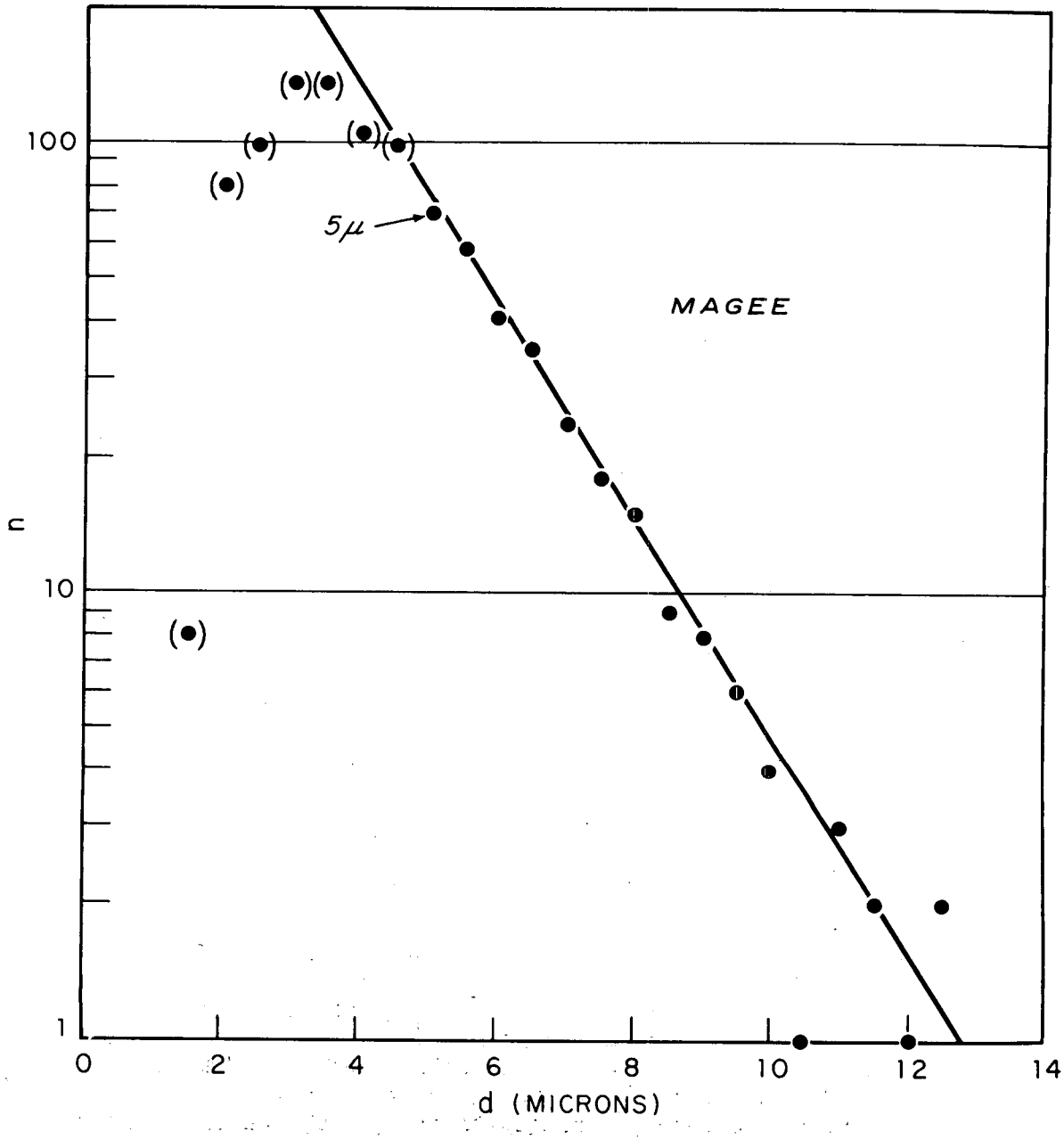

FIGURE 2. PARTICLE SIZE DATA FROM AIRBURST DEBRIS PLOTTED ACCORDING TO MAGEE'S THEORY. (DATA BELOW 5μ ARE BIASED).

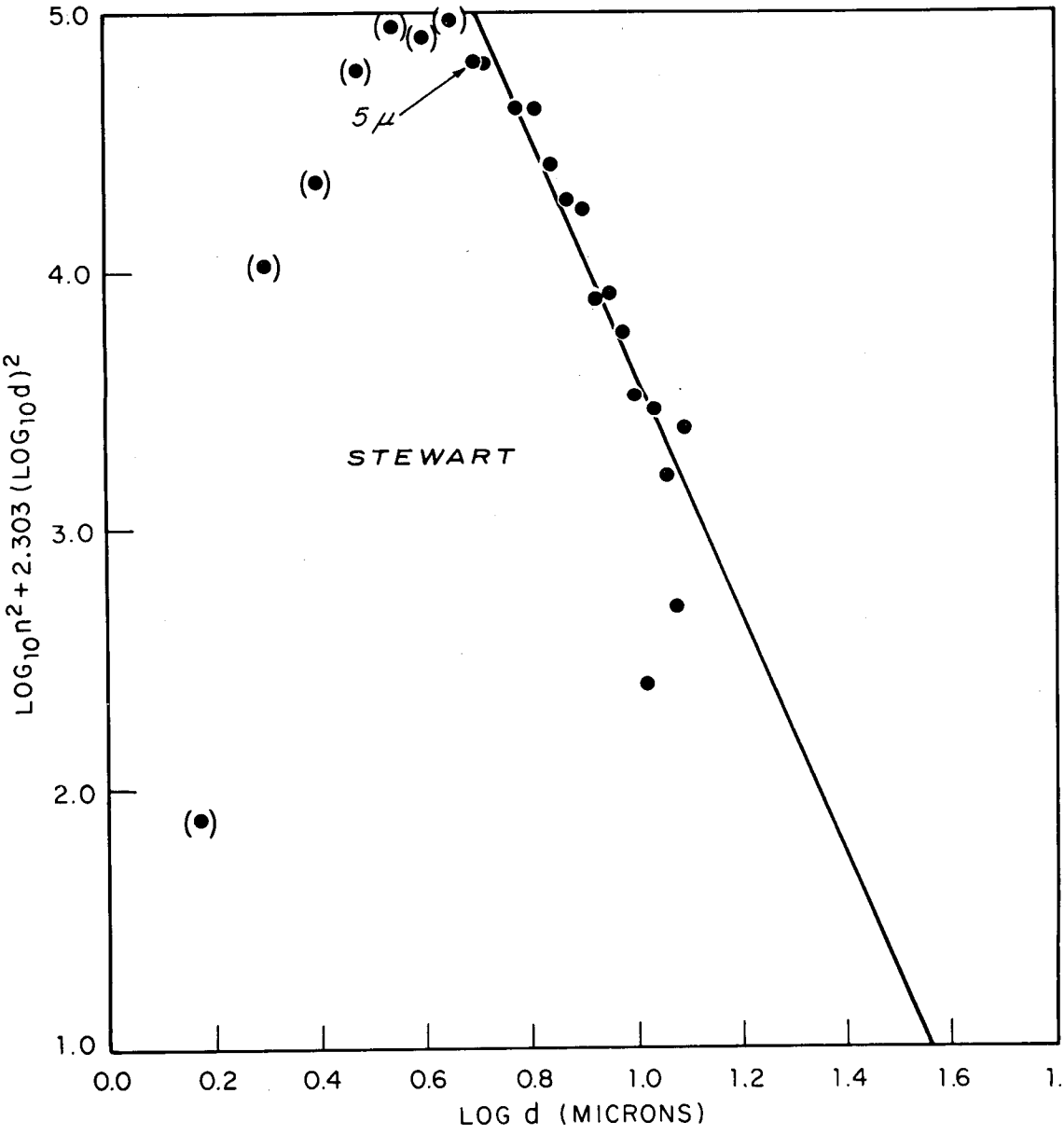

FIGURE 3. THE DATA USED IN FIGURE 2 ARE HERE PLOTTED ACCORDING TO STEWART'S THEORY.

Part IV. Radionuclide Incorporation

As indicated previously, the fractionation resulting from the interaction of radionuclides with the nascent particles can also be thought of in two regards: first, the fractionation index, or ratio of two extremely different behaving product radionuclides; and second, the interpolated behavior of the other products. The fractionation index is the result of such vastly different properties of the mass chains involved that there is hope that it can be treated by a very simple first approximation. This is, that the refractorily-behaving nuclide will be distributed among the particles according to their volume or the cube of their radius while the volatile radionuclide will be distributed according to the surface of the particles or the square of their radius. This is a result of the assumptions that (1) the particles are solidified before the volatilely-behaving radionuclide condenses and (2) that the particles remain in intimate contact with the vapor phase during the entire condensation period. From the distribution data for the debris sample in the previous section one calculates that the fractionation index for a given particle size would be log (0.18 r) according to Magee but log (1.1 r) according to Stewart. The former relationships would require 100 μ particles to account for the degree of fractionation observed, if the mechanism described above is realistic. The behavior of some of the intermediately fractionating radionuclides may also be handled fairly well on such a simple basis, while others will require a more refined treatment. This is visualized as involving considerations of collisions between nascent particles and vaporized fission products which lead to incorporations of the products in the carrier material with certain efficiencies (accommodation coefficients) and probabilities of escape. Additional refinements, if necessary, might include consideration of diffusion in the particle, correlations of accommodation coefficient with compound formation, and the extension of condensation theory to account for depletion of source material and for the inhomogeneous development of the fireball.

An important part of the work on the development of an air burst model is the accumulation and correlation of data with which to test it. Data have been gathered from the radiochemical analyses of fractionated samples from a large number of air bursts. The yields of these bursts range over a factor of several hundred. As in the case of high yield surface burst correlations, the logarithm of the ratio of the fraction of total Sr^{89} present in given sample to the fraction of total Zr^{95} was taken as the fractionation index. The values of this ratio range over a factor of about 100. Logarithms of various other ratios of radionuclide fractions were plotted against this index. By machine computation these plots have been fitted with straight lines, the intercepts adjusted to zero, and slopes of cumulative plots calculated. Analysis of the results is still in progress, but some qualitative statements can be made:

1. Many, but not all, of the ratios chosen indicate a gratifying constancy of behavior over the range of conditions involved.

2. The relative volatility of behavior observed bears both similarities to and differences from that exhibited in high yield surface bursts, reflecting the identity of the nuclides and the difference in carrier materials involved.

3. The order of increasingly refractory behavior is as follows: Cs^{137}, Sr^{89}, Sr^{90}, Cs^{136}, Cd^{115}, U and Ag radionuclides, Ba^{140}, Y^{91}, Ce^{141}, Mo^{99}, Pu and rare earth radionuclides, Zr radionuclides.

Part V. Data Required from Future Air Bursts

A representative sample of debris in significant size is the sine qua non for meaningful particle and fractionation data from future air bursts. This demand has been difficult to satisfy in the case of past land surface bursts, but the smaller particles present and recent developments in sampling apparatus make it quite reasonable in the case of air bursts. Furthermore, these samples can be collected in different size fractions. If such a sample were available, chemical analysis or activation analysis would reveal the amount of material in each particle size fraction, and from this the particle size frequency distribution could be calculated. Radiochemical analysis of the particle size fractions would test the hypothesis of volume distribution for refractorily-behaving radionuclides and surface distribution for gaseous-behaving radionuclides. Such an experiment appears feasible and would result in virtually complete documentation for the particle formation process. Information still lacking would be distribution of radionuclides within the small particles as the function of radius. For macroscopic substances this is on the borderline of present capabilities but for radionuclies it is quite beyond what we are able to do at the moment.

Valuable data could be obtained from less intensive tests. The minimum amount of information which would be useful would consist of (1) sufficient particle data to establish n_T and $\underline{r}$ or $\bar{r}$ for the respective theory, and (2) the measurement of some critical extensive property of the debris collected, such as the total mass iron content, number of fissions, etc., which could be used to distinguish between the merits of the distributions proposed.

Experiments such as these, carried out on airbursts, balloon bursts, and the smaller particle size fractions from tower shots where the fireball did not touch the ground, tower shots loaded with soil where the fireball did not touch the ground, and residual clouds from land surface bursts, would forge links for the theoretical chain which

would bind fallout formation processes under these diverse burst conditions into a unified structure.

References

1. Hillendahl, R. W. Characteristics of the thermal radiation from nuclear detonations (U). U. S. Naval Radiological Defense Laboratory Report USNRDL-TR-383, 3 Vols., San Francisco, 30 June 1959.

2. Woodcock, E. R. U. S. AEC Foreign Weapons Effects Report FWE-11, November 1953. (CRD)

3. Magee, J. L. Mechanisms of fractionation. U. S. AEC Report M-7140. 16 November 1953.

4. Stewart, K. The condensation of a vapor to an assembly of droplets or particles (with particular reference to atomic explosion debris). Trans. Faraday Soc. 52:161(1956).

A COMPARISON OF FALLOUT MODEL PREDICTIONS WITH A CONSIDERATION OF WIND EFFECTS

Gilbert J. Ferber and Jerome L. Heffter
U.S. Weather Bureau
Washington, D. C.

Over the past decade, a great many fallout prediction models have been developed by many different organizations for a variety of uses. Most of us in the fallout "model-making" business are aware that we deal with many uncertainties which are reflected in the discrepancies between the various model predictions. However, we have not always been able to clearly define and explain these uncertainties to the users of our product. One reason for this is that the extent of the discrepancies and the reasons for them have not always been clear to us. Obviously, this is an unsatisfactory state of affairs and efforts are being made to clarify the situation. The task is not a simple one and it is more likely to lead to a better understanding of the problem than to an improvement in fallout predictions.

It may well be that the limitations imposed on us by the available fallout data make it unlikely that demonstrably better model can be devised. If this is so, perhaps our efforts should be directed, not toward the development of still more models, but rather toward a quantitative statement of the uncertainties and a study of their significance in nuclear attack casualty assessment problems.

Our knowledge of fallout is based primarily on the data collected during nuclear tests at the Nevada Test Site and the Eniwetok Proving Ground. Nuclear bursts in Nevada have been confined to yields below 75 KT. Most of these shots were detonated on towers ranging in height from 100 to 700 ft. or from balloons at heights from about 400 to 1,500 ft. Adequate fallout prediction methods have been developed for these yields and burst conditions. There have also been a few surface bursts in Nevada with yields of about 1 KT or less. Tests at the Eniwetok Proving Ground have included thermonuclear devices with yields ranging up to about 15 MT.

Most detonations took place on barges in the Eniwetok and Bikini lagoons or on the coral reefs. A few were fired on atoll islands.

In a true land surface burst over a large city, the nature of the fallout particles may be quite different from those produced in a detonation on a coral atoll or atop a steel tower. Hence, conclusions drawn from nuclear test data must be applied with caution to the rather different burst conditions likely to be encountered in a nuclear attack situation. There are also many difficulties in the analysis and interpretation of the fallout data. This is particularly true for tests at Eniwetok since the fallout descends over vast stretches of the Pacific Ocean.

Therefore, it is not surprising that the many fallout models which have been developed for nuclear attack damage assessment applications show considerable differences in the predicted fallout pattern.

Fig. 1 illustrates some fallout predictions derived from several models currently in use. The predictions are for a 1 MT, all fission, land surface burst with a constant 25 mph wind speed from the ground to the top of the cloud. The vertical wind shear*, which determines the angular spread of the fallout sector, is taken to be 0.2 knots per 1,000 ft. The contours show the hypothetical H+1 dose-rates at 3 ft. above an infinite plane. Dose rates above average terrain would be about 70% of the infinite plane dose rates.

The WSEG-RM-10 prediction is taken from the Weapons System Evaluation Group, Research Memorandum No. 10 by Pugh and Galiano.(1) This model has been used by the National Resources Evaluation Center for nuclear attack casualty assessment.

The pattern labeled WSEG-NAS is a revision of the WSEG model in accordance with the as yet unofficial and unpublished recommendations of the National Academy of Science Working Group on Fallout Models for Attack Damage Assessment. The working group was formed at the request of the Office of Civil and Defense Mobilization (now Office of Emergency Planning) to recommend a model for their use. This model represents a reasonable compromise but is certainly not intended to be the final word in fallout prediction.

The next pattern represents the Weather Bureau model(2) which was developed primarily for fallout prediction in connection with nuclear tests. The model has been revised slightly for application to surface bursts in the megaton range and has also been used in attack damage assessment exercises.

---

* The vertical wind shear as used in this paper, is actually the component of the vertical wind shear, measured perpendicular to the mean wind vector. The mean wind is defined as the vector average of all the winds from the ground to some chosen level in the mushroom top of the nuclear cloud.

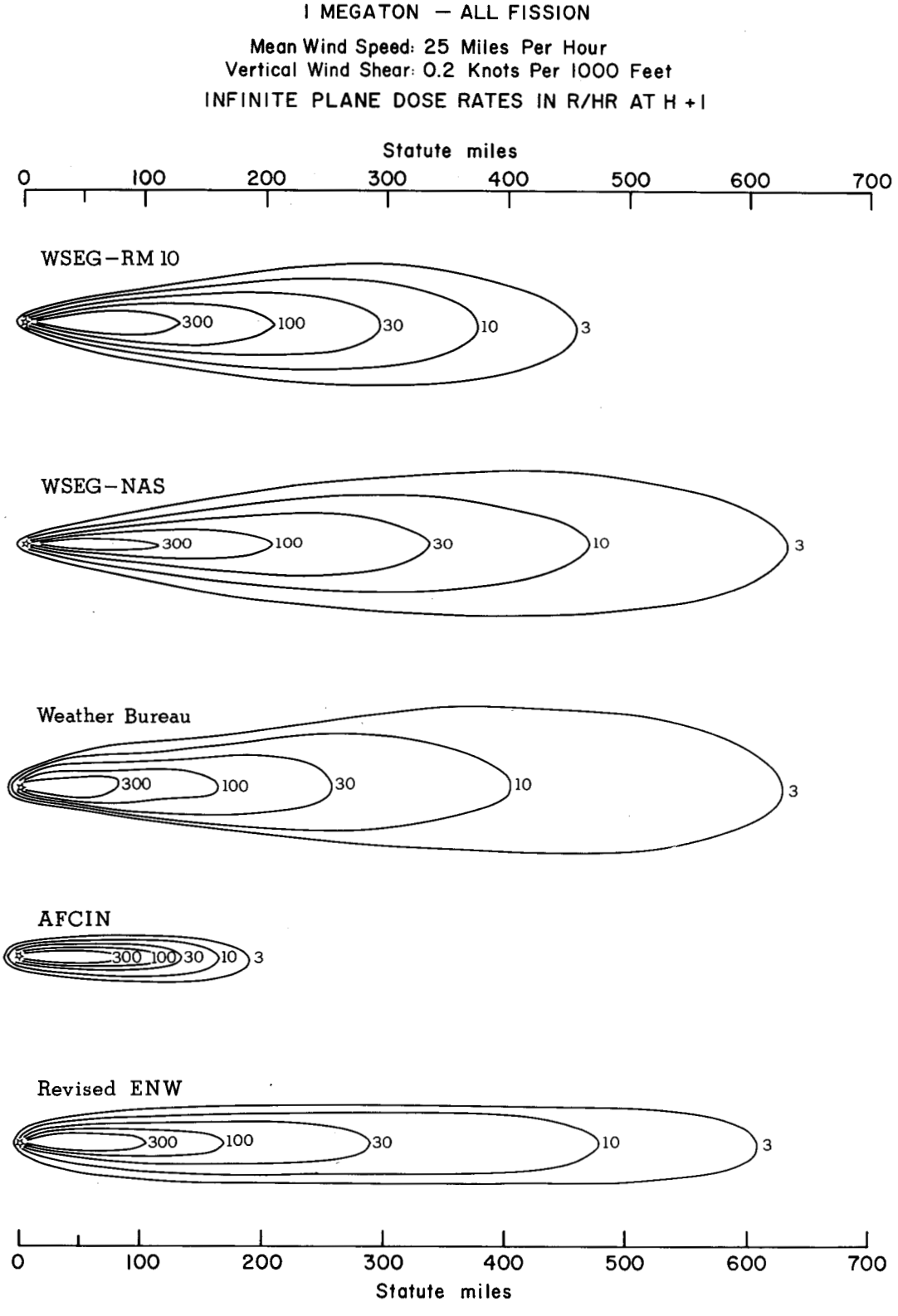

FIGURE 1. FALLOUT PATTERN COMPARISONS - 1 MT.

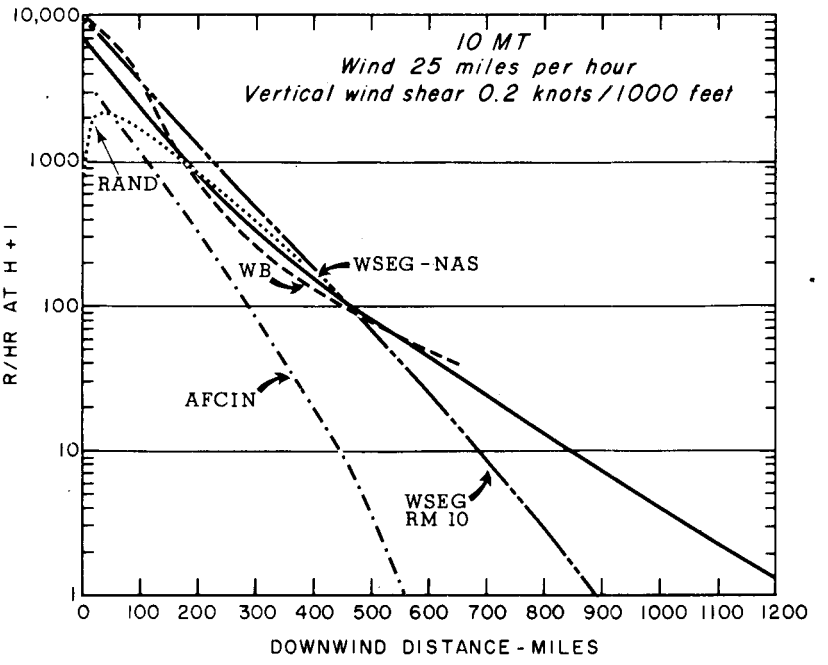

FIGURE 2. DOSE RATE - DISTANCE CURVES - 1 MT.

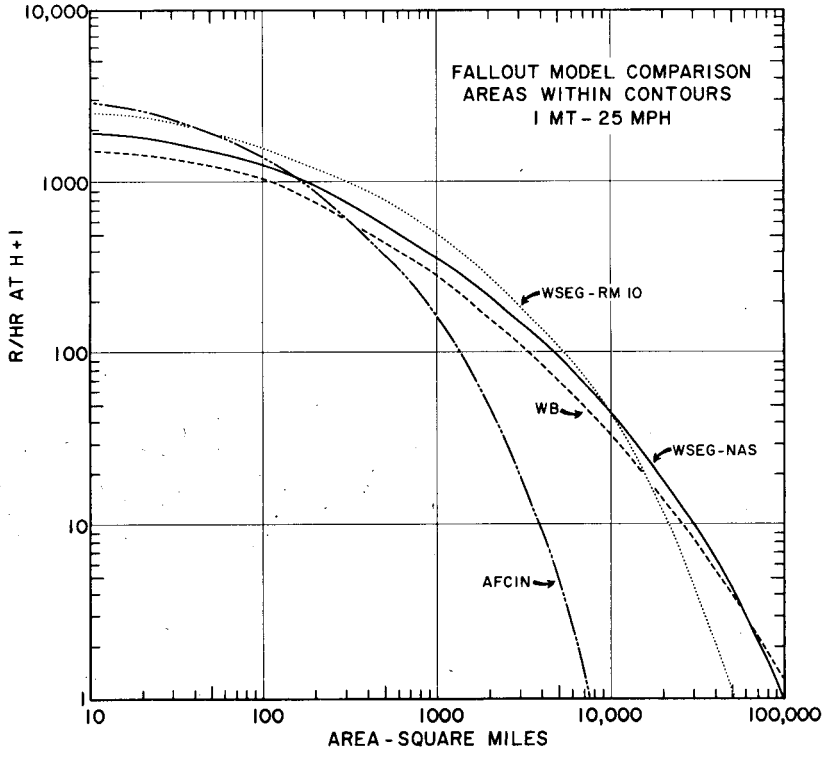

FIGURE 3. DOSE RATE - AREA CURVES - 1 MT.

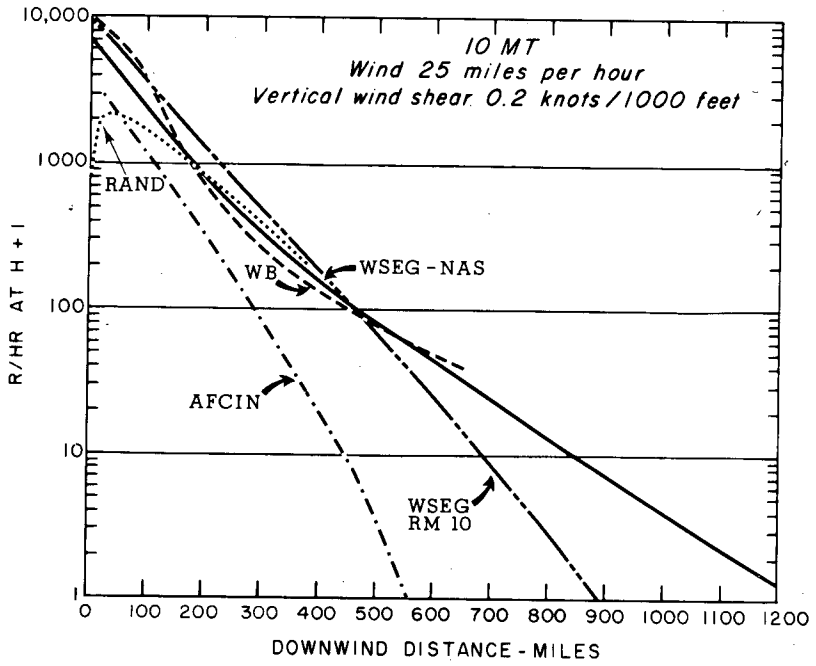

FIGURE 4. DOSE RATE - DISTANCE CURVES - 10 MT.

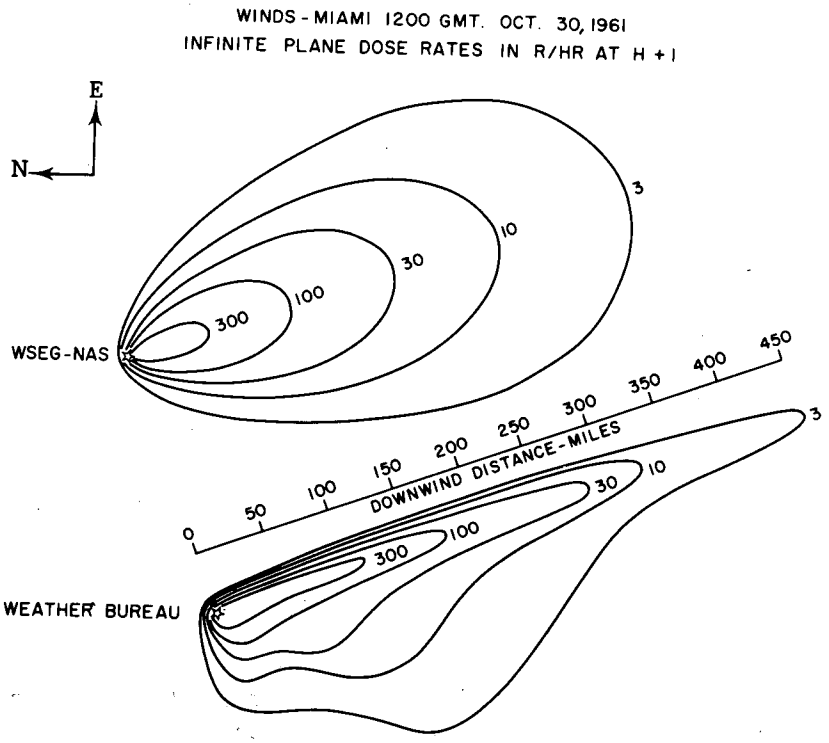

FIGURE 5. COMPARISON OF IDEALIZED PATTERN AND DETAILED COMPUTATION - 1 MT.

The AFCIN model[3] was developed by the Air Force Intelligence Center primarily for the assessment of the effects of a nuclear counterblow on enemy territory. The last pattern is one which will appear in the new edition of The Effects of Nuclear Weapons.[4] It is based on the Weather Bureau model with simplified scaling laws which enable the user to adjust for weapon size or wind speed.

At first glance, the most striking feature is the disparity between the AFCIN prediction and all the others. One may wonder about the outcome of a war game in which the AFCIN model is used to determine the fallout situation over enemy territory while our own fallout problem is evaluated with one of the other models. Actually this picture is somewhat misleading in that the greatest differences among the models appear in the lower dose-rate contours, well below the casualty-producing range.

In Fig. 2, we have plotted the hypothetical H+1 dose rate as a function of the distance from ground zero for some of the patterns shown in Fig. 1. Note that the extent of the 1 r/hr. contour varies from 200 to 800 mi. with different models but the uncertainty in the prediction decreases for the higher dose rates. Also notice that the AFCIN model predicts higher dose rates than the other models in the first 50 mi. A portion of the curve predicted by the Rand Corporation model[5] is also shown. The Rand model is interesting in that it predicts a lower peak dose and the peak occurs at some distance from the burst point.

In Fig. 3 we are still looking at the same predictions. Here we have plotted curves of H+1 dose rate versus area covered, for several of the models. The areas under the curves represent the total activity in the fallout patterns within the 1 r/hr. contour. The total activity is 2,500 r/hr. mi.^{2}/KT in the WSEG-RM-10 pattern, 2,400 r/hr. mi.^{2}/KT in the WSEG-NAS pattern, about 2,000 r/hr. mi.^{2}/KT in the Weather Bureau pattern and about 800 r/hr. mi.^{2}/KT in the AFCIN pattern. Thus, there is approximately a factor of 3 difference in total activity within the 1 r/hr. contour as predicted by AFCIN and WSEG-NAS. The activity total in the WSEG-NAS model is that recommended by the Academy of Science Working Group on Fallout Models as a best estimate. However, the number is still open to question and there is no clear proof that the AFCIN total is incorrect.

Note that the models differ not only in the total amount of activity which appears within the 1 r/hr. contour but also in the distribution of the activity. The AFCIN model puts even more activity in the very high dose-rate contours than do the other models. Thus multiplying the total activity by a factor of 3 would not bring AFCIN into line with WSEG-NAS, if the assumed activity distributions remain unchanged.

Fig. 4 shows the predicted dose rate versus downwind distance for a 10 MT, all fission, surface burst with the same wind conditions as before. For this yield, the extent of the predicted 1 r/hr. contour varies from 550 to over 1,200 mi. downwind. The 1,000 r/hr. predictions vary from 100 to about 230 mi. It is also interesting to look at the various dose-rate

predictions at a given distance. At 100 mi., for example, the predicted H+1 dose rates vary from 1,000 r/hr. to 3,500 r/hr. At 300 mi. the range is from 80 to 500 r/hr.; and at 500 mi., from 3 to 80 r/hr.

Notice that the AFCIN curve now falls entirely below the other curves, except for the Rand prediction in the first 50 mi. Thus, we see that the relationship between model predictions is not constant, but varies with the size of the detonation. It is this sort of thing which makes it impossible to reconcile the various models without delving into the details that went into their development.

So far, we have compared idealized, cigar-shaped patterns under uniform wind conditions. In Fig. 5, we have used an actual wind sounding with about 90° of angular shear to compare the WSEG-NAS idealized pattern with resulting from a detailed computation with the Weather Bureau model. The WSEG patterns are superior to most idealized patterns in that they incorporate vertical wind shear as a variable in addition to wind speed. Due to the large angular shear and somewhat lower wind speed, the patterns are shorter and wider than those in Fig. 1. However, the idealized pattern is symetrical about an axis which lies along the direction of the mean wind from the ground to the lower portion of the mushroom head of the nuclear cloud. The detailed computation, which takes into account the winds at all levels, results in an asymetrical pattern. The "hot-line" is in the same direction but there is no fallout to the east of this line and a considerable bulge to the west. It is evident that the idealized pattern, based on a single mean wind, does not always present an accurate picture of the fallout area.

In Fig. 6 we turn for a moment to fallout prediction for the critical area immediately upwind of the ground zero. Since the mushroom cloud from a 10 MT detonation has a radius of about 27 mi. (at 10 minutes after burst), fallout might be expected to occur at a considerable distance upwind of the ground zero. The upwind fallout estimate from the "Capabilities of Atomic Weapons", Technical Manual 23-200[6], which is shown here, is typical of the earlier estimates of upwind fallout based on Pacific test data. The curve is labelled "Old TM 23-200" since a revision of this manual is in preparation. With a 25 mph mean wind the 10 r/hr. line was predicted to extend about 26 miles upwind. More recent studies, here represented by the Weather Bureau[7] and WSEG-NAS predictions, indicate that the upwind fallout problem will probably be less severe than was formerly believed. The reason for this is that the Pacific tests were conducted under conditions of very light mean winds, generally less than 10 mph. The mean winds in the United States are much stronger, generally over 25 mph and, in winter often exceeding 60 mph. Fallout particles from the upwind portion of the nuclear cloud would be carried back toward ground zero by these winds, thus decreasing the upwind extent of the fallout pattern. The Weather Bureau and WSEG models predict that the 100 r/hr. contour will extend 4 to 7 mi. upwind rather than 11 mi. The 10 r/hr. line is predicted at 7 to 10 mi. rather than 26 mi. and virtually no fallout is expected beyond about 12 mi. upwind. This is for a

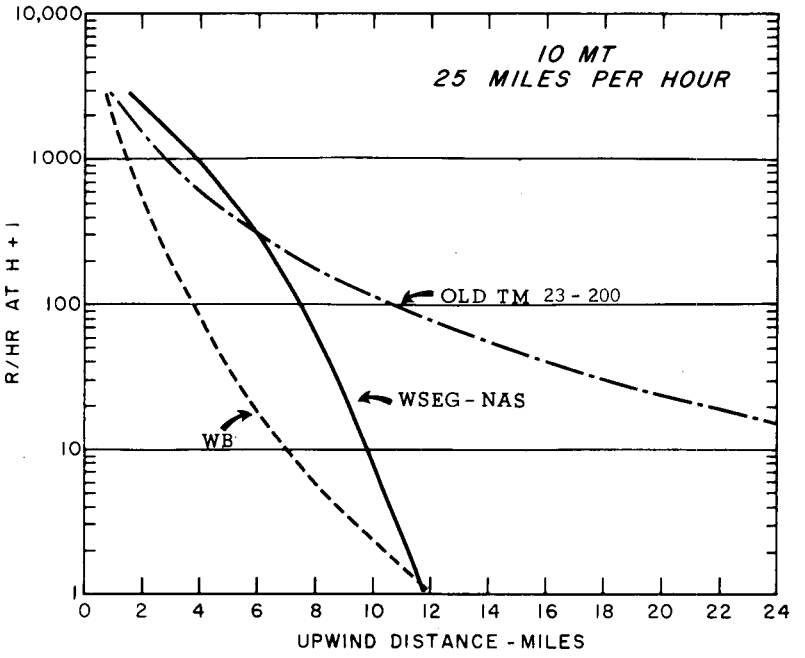

FIGURE 6. UPWIND FALLOUT PREDICTIONS.

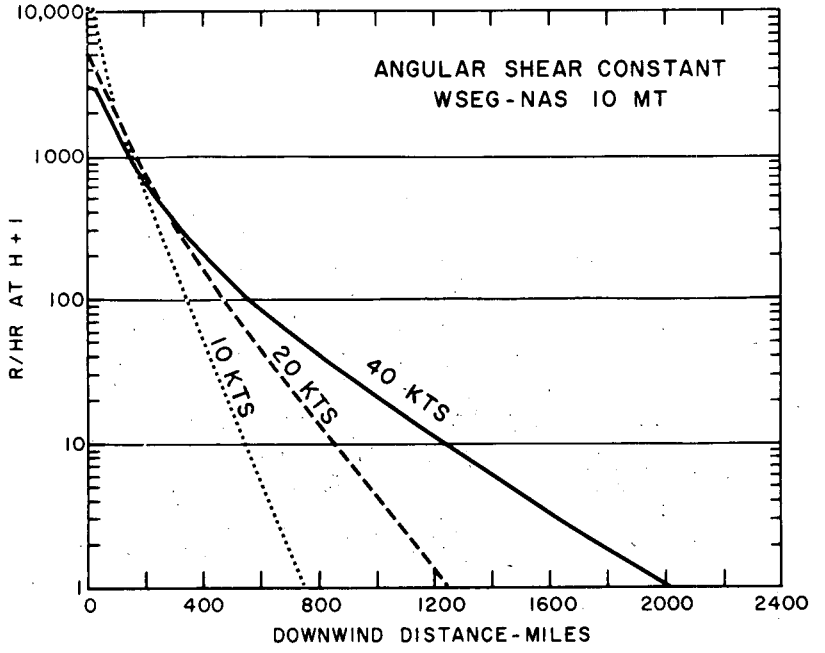

FIGURE 7. EFFECT OF WIND SPEED.

25 mph mean wind from the ground to about 40,000 ft. With higher winds there would be even less upwind fallout. The predictions for the very high dose rates have not changed significantly but these are rather academic since they are within the area of nearly total destruction from blast and fire.

Next we will take a look at the effects of wind speed on the downwind fallout pattern. In Fig. 7 curves of H+1 dose rate versus downwind distance are shown for the WSEG-NAS 10 MT patterns for 10, 20 and 40 knot mean winds with the same angular wind shear in all cases. Note that increasing the wind speed lowers the dose rates close to ground zero and increases the dose rates at greater distances. The dose rate at a given distance may vary by more than a factor of 10 due to wind speed alone. At 600 mi., for example, the dose rate varies from 5 r/hr. with a 10 knot wind to 45 r/hr. at 20 knots and 90 r/hr. at 40 knots.

The effect of wind speed can be described by a very simple scaling law. If the angular spread is kept constant, doubling the wind speed will result in $\frac{1}{4}$ the dose rate at twice the distance. Thus, with a 10 knot wind we have 4 r/hr. at about 625 mi. With a 20 knot wind we have $\frac{1}{4}$ the dose rate, or 1 r/hr. at twice the distance, or 1,250 mi.

Fig. 8 shows the effect of varying the vertical wind shear which governs the angular spread of the fallout sector. Again we have curves of dose rate versus downwind distance for a 10 MT burst with 20 knot mean winds. In going from 0.1 to 0.2 knots/1,000 ft. we are doubling the angular spread, and doubling again in going from 0.2 to 0.4 knots/1,000 ft. In general the dose rate at any distance is inversely proportional to the angular spread. At 380 mi., for example, the dose rate is 400 r/hr. at H+1 with a shear of 0.1 knots/1,000 ft. Doubling the shear, we obtain $\frac{1}{2}$ the dose rate, 200 r/hr.; doubling again, we obtain 100 r/hr. Very close to ground zero the change is much smaller since the diameter of the nuclear cloud is large compared to the spread due to directional wind shear. In general, the angular wind shear decreases with increasing wind speed, so that strong winds will tend to deposit the fallout in long narrow patterns, with high dose rates extending out to great distances.

We will now focus on predictions in the critical area where the radiation dose is in the lethal range. In Fig. 9 we have drawn contours of the cumulative 4-day dose to a completely unsheltered population. The patterns are for a 10 MT fission yield with a 25 mph mean wind. A factor of 0.7 was used for terrain shielding but no other shielding or biological repair factor was included in the calculation of the 4-day dose.

It is estimated[4] that no fatalities will occur with an exposure of less than 200 r, 450 r will result in about 50% fatalities and exposure to about 700 r or more over a period of a few days will result in close to 100% fatality.

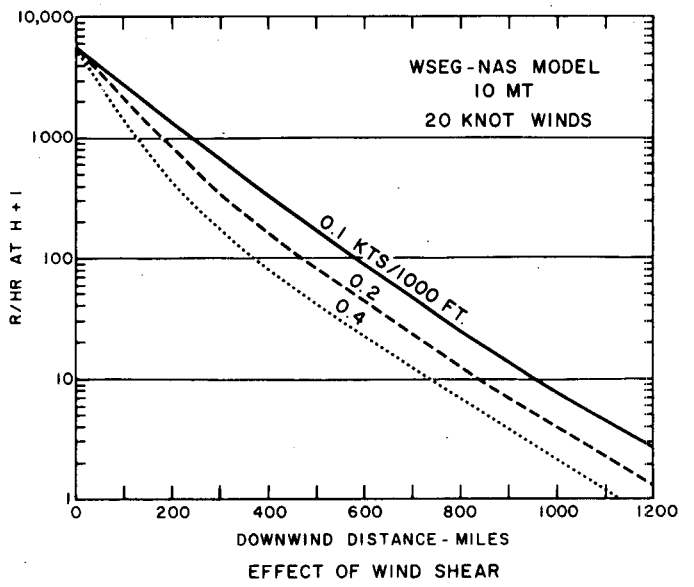

FIGURE 8. EFFECT OF WIND SHEAR.

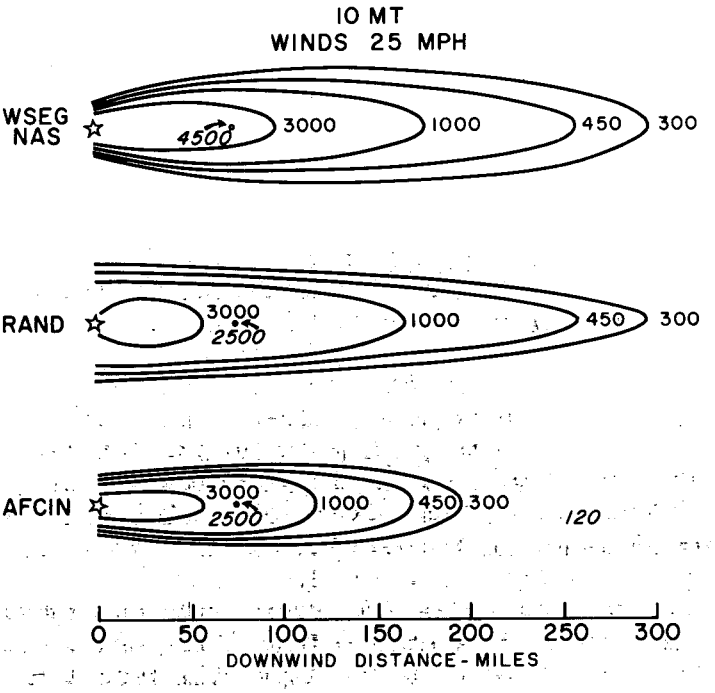

FIGURE 9. COMPARISON OF 4-DAY (ROENTGENS) PATTERNS - 10 MT.

Both the WSEG-NAS and Rand models predict 100% fatalities for an unsheltered population in an area about 40 miles wide extending about 200 mi. downwind. In the AFCIN prediction, this area extends only 150 mi. downwind. At a distance of 260 mi., where WSEG-NAS and Rand predict 450 r or 50% fatality, AFCIN predicts 120 r, or no fatalities.

Now if we assume a sheltered population, with an arbitrary shielding factor of 10, an outside dose of 4,500 r is required to produce 50% fatalities. A shielding factor of 10, or better, is provided by the basement of a frame house. The WSEG model predicts 4,500 r at 75 mi. while Rand and AFCIN are now in agreement with only 2,500 r at this distance. The area in which WSEG and AFCIN would predict 100% fatalities (7,000 r or greater), even with a shielding factor of 10, is about 10 to 20 mi. wide and, at most 60 mi. long. However, according to the Rand model, an outside dose of greater than 7,000 r may not occur anywhere in the fallout pattern for this yield and wind speed.

Fig. 10 shows the effect of wind speed on casualty estimates based on the WSEG-NAS prediction for a 10 MT fission yield. The hatched areas indicate, for wind speeds of 10, 20, 40, and 60 knots, the percentage of deaths due to fallout which is expected along the axis of the fallout pattern as a function of distance from ground zero. In computing the doses for the various wind speeds it was assumed that the angular wind shear is inversely proportional to the wind speed. The widths of the hatched areas reflect the uncertainty in the relationship between dose and biological effect.

First, consider the case where the population has no shielding whatsoever. With 10 knot winds, we may expect 100% fatalities out to about 140 mi. with no fatalities beyond about 200 mi. With a 60 knot wind, 100% fatality is expected out to about 400 mi. with no deaths due to fallout beyond 700 mi. Wind speed is evidently a critical factor here. However, when we apply a shielding factor of 10 to the same dose predictions, the results are very different. The area of 100% fatality extends about 50 mi. regardless of the winds. With a 10 knot wind, no deaths are expected beyond 90 mi. and even with a 60 knot wind there should be no fatalities beyond 220 mi. The effect of shielding is quite striking.

Summary

If we are interested in the entire fallout pattern produced by a single nuclear burst, we find that the various models can give very different results. Also, wind conditions can drastically effect the dose-distance relationship as well as the orientation and shape of the pattern. If our interest is confined to doses in the lethal range, and especially if a shielding factor is added, we find that the discrepancies among the various model predictions are smaller and the effect of wind speed on these high doses is also much smaller. Nevertheless, these differences are still quite important in the critical range from about 200 to 700 r where relatively small changes in dose result in large changes in the fatality estimates.

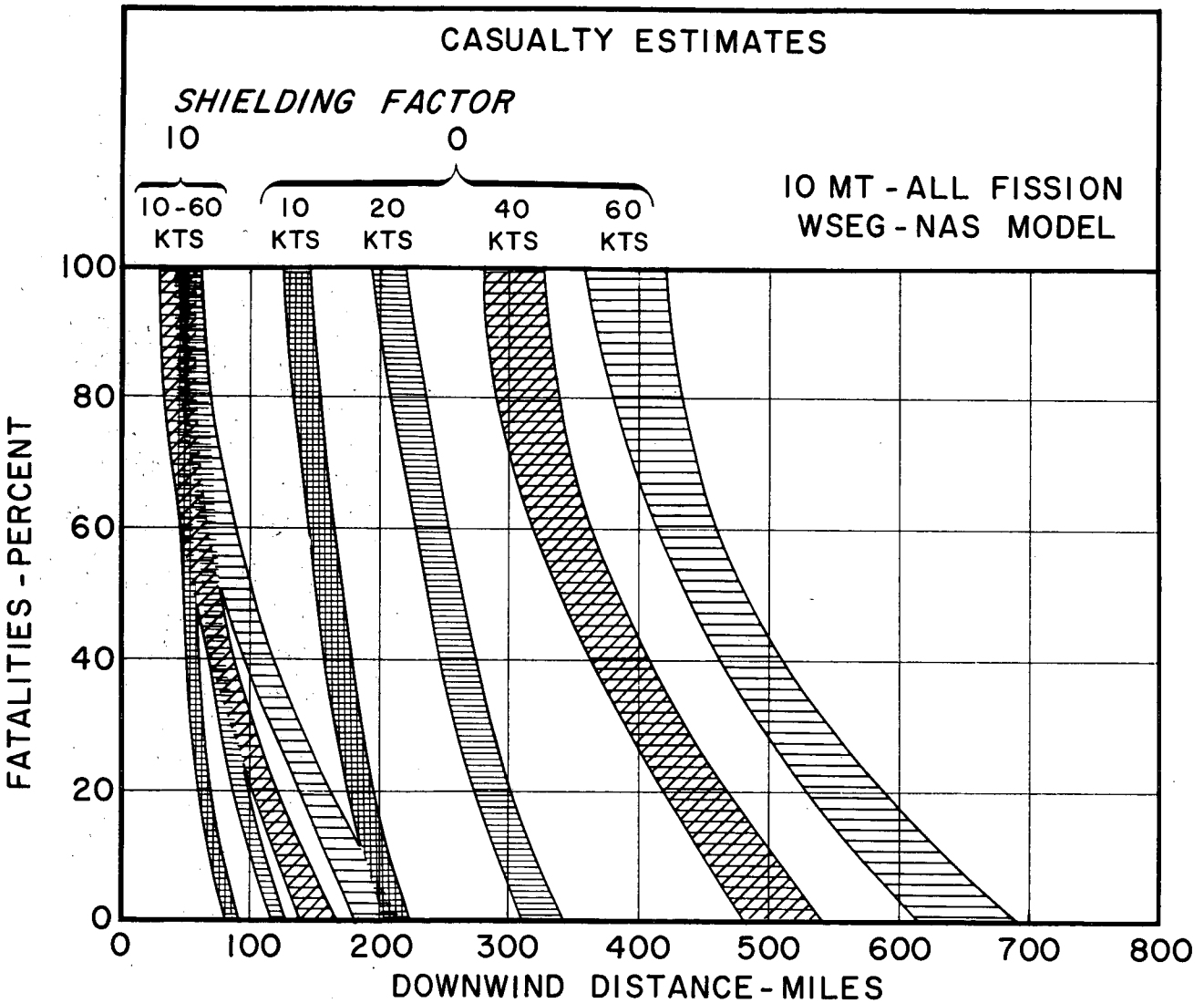

FIGURE 10. EFFECT OF WIND SPPED AND SHIELDING ON CASUALTY ESTIMATES - 10 MT.

Finally, when we consider nuclear attack damage assessment on a national scale, with the additive effects of hundreds of nuclear bursts, the significance of the fallout model uncertainties and wind conditions for the over-all casualty estimate is not at all clear. With the over-lapping of fallout patterns from many bursts, the lower dose-rate contours, for which predictions are least consistent may become important. It might prove quite interesting and enlightening to run a damage assessment problem several times for a selected attack situation, using a different fallout model each time. Then the uncertainty due to the fallout model may be evaluated and compared, for example, with the uncertainty in the shielding assumptions. In this way, the accuracy and precision required of fallout models for attack damage assessment can be determined in a realistic manner.

Similarly, the effect of wind forecast errors can be evaluated by running problems with both forecast and actual winds. The results of past damage assessment exercises seem to suggest that wind conditions do not greatly affect the total number of casualties. However, the winds will determine where the fallout casualties will occur.

We must learn to live with the fact that large uncertainties are inherent in all fallout model predictions. Further, there is little reason to hope for significant improvements in the absence of a series of nuclear tests designed primarily for the scientific study of fallout phenomena. Hence, error analyses and the development of statistical techniques to handle the uncertainties are at least as important as continued efforts to improve the fallout models for nuclear attack damage assessment.

References

1. Pugh, G.E., and R.J. Galiano. An Analytic Model of Close-In Deposition of Fallout for Use in Operational-Type Studies. U.S. Department of Defense, Weapons Systems Evaluation Group, Washington, October 1959.

2. Nagler, K.M., L. Machta and F. Pooler, Jr. A Method of Fallout Prediction for Tower Bursts at the Nevada Test Site. U.S. Weather Bureau, U.S.AEC report TID-5489, Washington, June 1955.

3. Nuclear Weapons Employment Handbook. U.S. Air Force Manual 200-8. Washington, 1 September 1961. (Confidential)

4. Glasstone, S., The Effects of Nuclear Weapons. U.S. Department of Defense - U.S.AEC. U.S. Government Printing Office, Washington, June 1957. (Revised edition in preparation, 1962).

5. Batten, E.S., D.L. Inglehart and R.R. Rapp. Derivation of Two Simple Methods for the Computing of Radioactive Fallout. The Rand Corporation, Santa Monica, California, Report RM-2560, February 1960.

6. Capabilities of Atomic Weapons. Department of the Army TM 23-200, Defense Atomic Support Agency, Washington, November 1957. (Revised edition in preparation.)

7. Ferber, J. Prediction of Upwind Fallout. U.S. Weather Bureau, Washington, June 1960.

THE EARLY TRANSPORT OF NUCLEAR DEBRIS

Phillip W. Allen, Frank D. Cluff and Isaac van der Hoven
Research Station
U. S. Weather Bureau
Las Vegas, Nevada

Introduction

The announced purpose of this conference was to provide a review of new information and developments in fallout research, and to discuss future needs of the program. I will discuss a few relatively minor improvements in our ability to predict close-in fallout, and some of the needs of the purely meteorological end of fallout prediction. My concept of these needs comes from my observation and study of the activities of United States weather and fallout prediction units since Operation SANDSTONE in the Pacific in 1948, and more particularly from the work of the Weather Bureau Research Station at the Nevada Test Site since 1956. This station has served as the Weather Prediction Unit for all continental United States nuclear tests since Operation PLUMBBOB in 1957 and is continuing in this capacity for the tests of nuclear rocket and ramjet engines, which produce very low levels of atmospheric contamination. If, in my remarks, I use the term nuclear debris it is because the word "fallout" implies particles, and this is only part of the problem. The gaseous components of nuclear debris also present an environmental problem, particularly in reactor tests.

Variability

Outside of that posed by the mere existence of debris or fallout, the

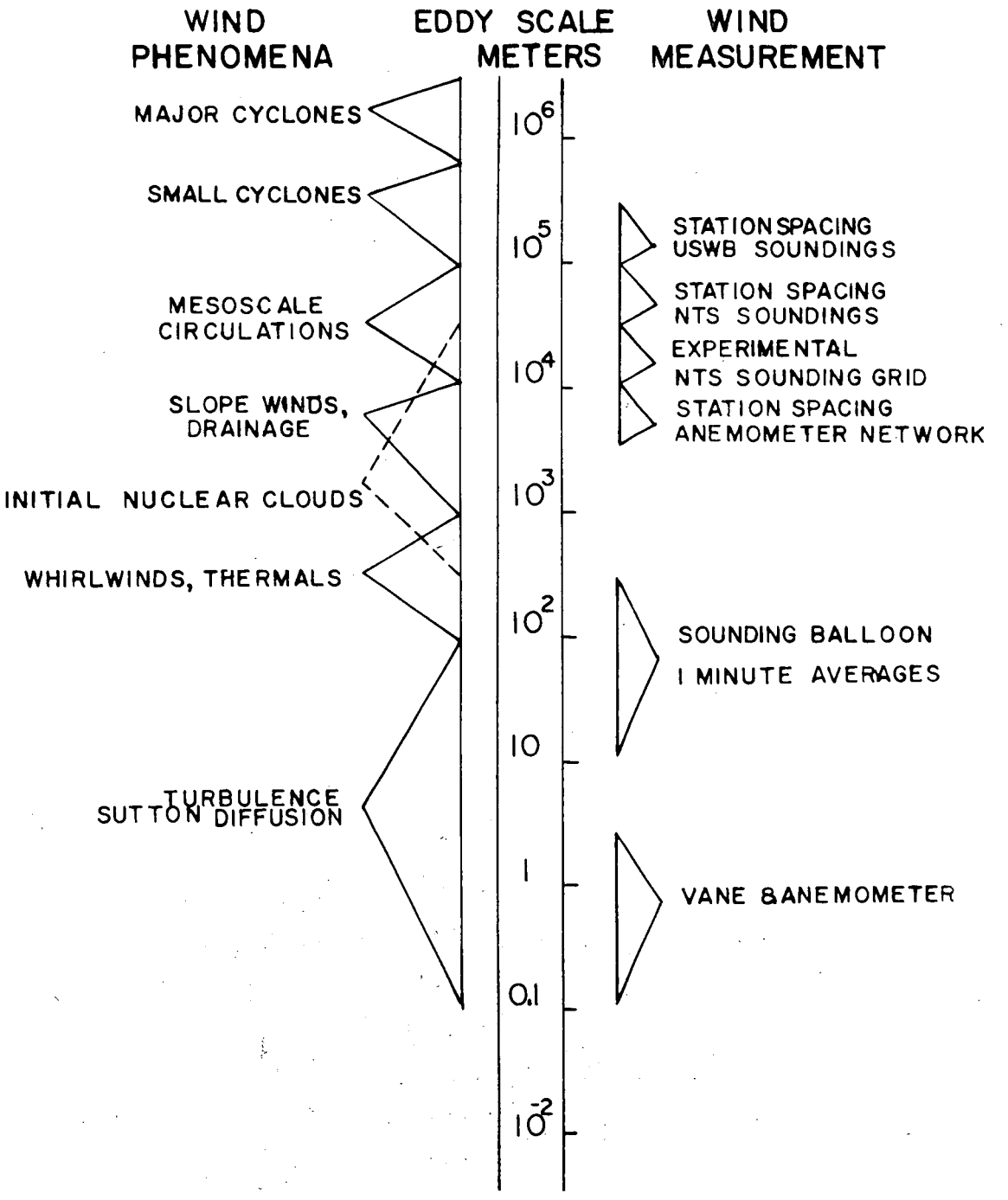

FIGURE 1. SCHEMATIC DIAGRAM OF THE SPECTRUM OF ATMOSPHERIC MOTIONS AND METHODS OF MEASUREMENT.

one problem that is the most difficult to solve, the one which gives operations people greatest concern, and which results in the otherwise needless cost of many thousands of dollars for some nuclear events, is wind variability. This characteristic of air motion has defied prediction, and in most meteorological considerations has been taken as one of the facts of life, something we just live with and accept. However, in this field where the transport of radioactive debris is involved, perhaps closer investigation is worthwhile.

A schematic of the spectrum of atmospheric motions is shown in Fig. 1. The sizes of eddies or the lengths of wave motions range all the way from Brownian motion on the small end to hemispheric on the large end. All scales exist every day, but the frequency of occurrence of a given scale may change from day to day or from place to place depending on the existence or suppression of the appropriate driving mechanism. Not all scales of eddies are driven in exactly the same way but most of them are influenced by the distribution of pressure and heat in the atmosphere, and this changes with season, cloudiness, surface slope, etc.

The size range of nuclear clouds, at time of stabilization following explosions, falls roughly midway in this spectrum, being larger than whirlwinds but smaller than such mesoscale circulations as thunderstorm high pressure cells. They cover about the same horizontal areas as drainage winds in a mountainous area but have must greater vertical extent.

On the other side of Fig. 1 are shown the scales of measurement of winds. At the low end the average wind vane and anemometer respond to circulations of the order of a meter or more across. A rising sounding balloon, on which positions are plotted every minute, will indicate motions of the order of tens or hundreds of meters across, and has the advantage of measuring at high altitude. No single instrument or device does a very complete job of recording motions larger than this, although rocketsondes with chaff clouds and smoke puffs are used effectively at very high altitudes, and constant level balloons are useful at individual altitudes.

To describe completely the motion of an eddy in any scale it is necessary to sample frequently or continuously at several points in the eddy. The spacing of the Weather Bureau's upper air sounding stations is between 10^5 and 10^6 meters (60 to 300 miles). This is adequate to define cyclones and anticyclones, upper level ridges and troughs of pressure systems that carry major changes of weather. However, mesoscale circulations are frequently not detected or if detected are poorly defined by this network.

For this reason, with the testing of nuclear weapons it became necessary to have upper air soundings closer together. The usual Nevada Test Site (NTS) sounding network for large atmospheric tests has had a station spacing of about 50 miles. In recent years with nuclear rocket engine

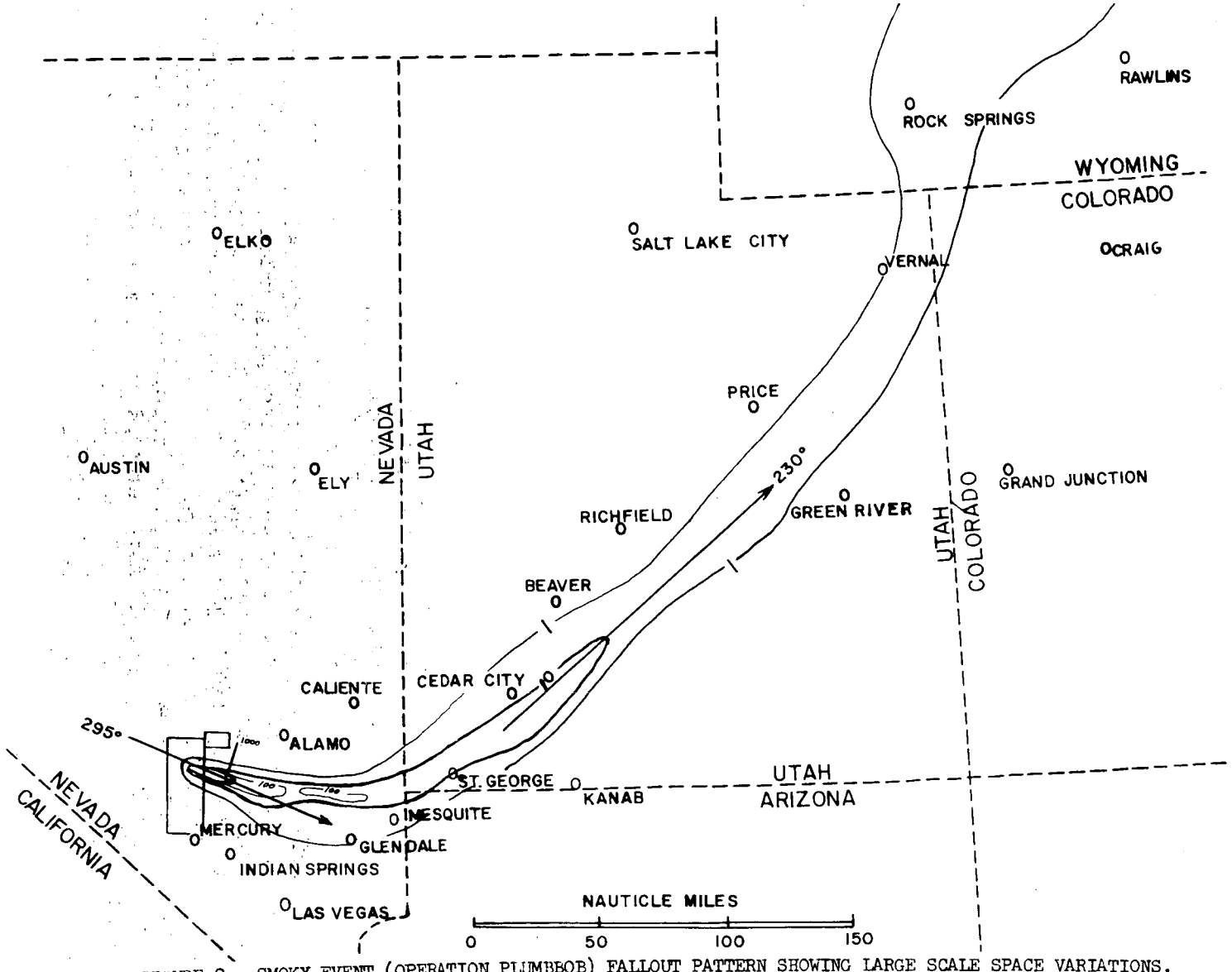

FIGURE 2. SMOKY EVENT (OPERATION PLUMBBOB) FALLOUT PATTERN SHOWING LARGE SCALE SPACE VARIATIONS.

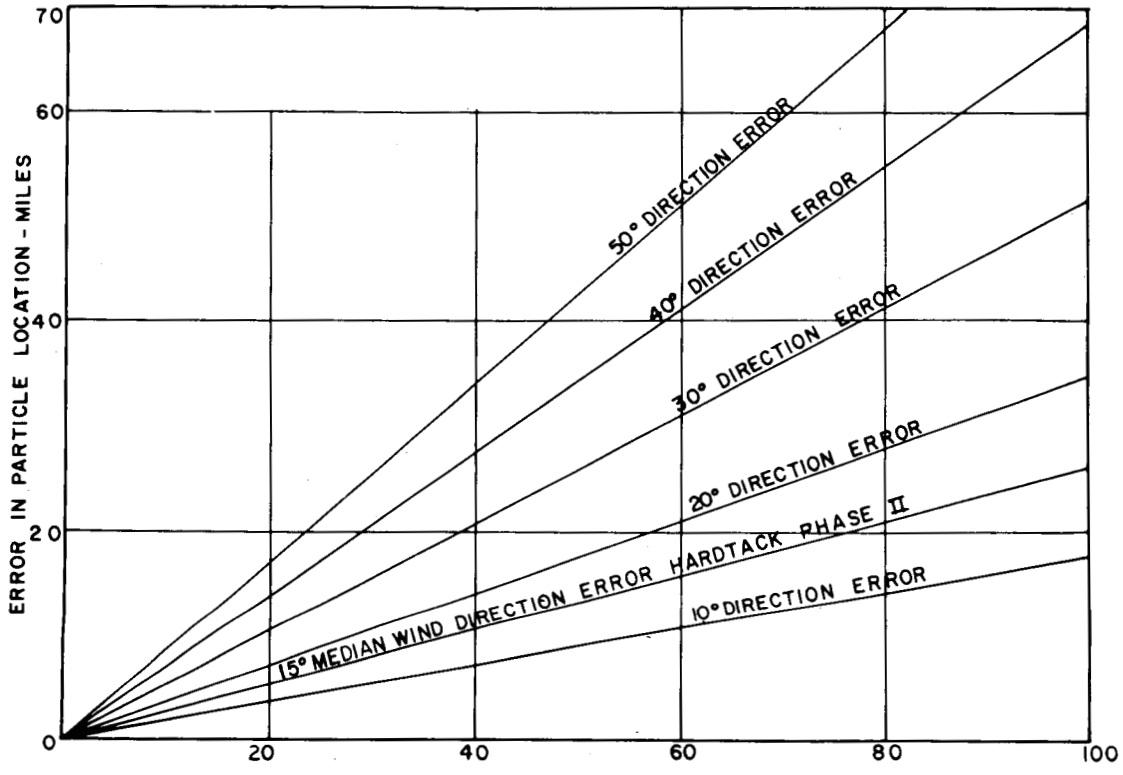

FIGURE 3. DISTANCE FROM GROUND ZERO-MILES.

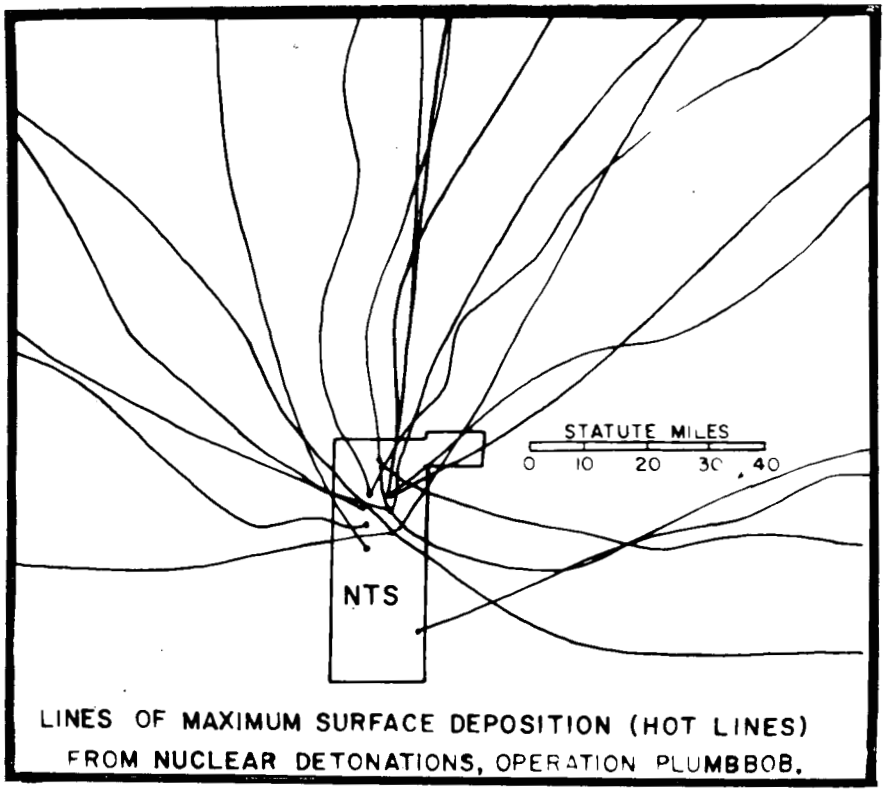

FIGURE 4.

tests it has become necessary to reduce the spacing to something like 15 miles between stations. With three or four such stations it is possible to detect most waves or perturbations of a size that would carry a small radioactive cloud astray. Anemometers on towers are located in an even denser grid to detect smaller surface eddies and slope-induced winds. Much of the meteorological study in progress at the NTS during recent years has been directed toward a full understanding of slope winds and mesoscale circulations peculiar to the area of southern Nevada. Other work has the objective of handling predictions statistically, in which the probability of occurrence of a given wind is made available. These studies have resulted in a definite improvement in the weather service provided for the Nevada Test Organization.

Why are we so concerned about these relatively small scale wind perturbations? For two reasons, one being that small perturbations make individual wind soundings non-representative, thereby possibly influencing the forecaster to make a wrong decision, and the other because the presence of a perturbation at zero time may well result in a nuclear cloud being carried in an unpredicted and undesirable direction.

The fallout pattern from the Smoky event in Operation PLUMBBOB, shown in Fig. 2, illustrates how the best fallout prediction in the world can be of little value unless the wind directions and wind changes are predicted correctly. Long narrow patterns like this would fall on very little of the predicted area if the wind direction forecast were off by as much as 10°.

Fig. 3 shows how far from a predicted location fallout particles will strike the ground for each 10° interval of wind direction error. The prediction group for Operation HARDTACK II has a median error of 15° in 6-hour predicted wind directions between 15,000 and 25,000 ft. At a distance from the Site of 40 miles this represents an error of 10 miles in cloud location. Several direction errors were as high as 30° or 40°. Fortunately, none of these errors involved significant radiation fields with respect to people. This safety feature was not accidental because in these cases it was known in advance that the directions might vary greatly, and speeds were low enough that heavy fallout would not reach inhabited areas. These factors were considered in decisions to proceed with the tests.

Fig. 4 shows the "hot-lines" or center-lines of maximum fallout for the Operation PLUMBBOB events. This illustrates the effects of perturbations and local circulations on fallout patterns. The wave lengths of these perturbations are from roughly twenty miles to values larger than the area shown, over 150 miles across. Smaller perturbations undoubtedly escaped detection in the analysis.

We have no very good information on the life expectancy or period of persistence of individual mesoscale waves but several have been observed to persist for periods of half an hour or more whereas only a few

of the larger ones have been traced through a 6-hour period in Nevada. It is completely impossible, with networks, sounding procedures, and data handling facilities now in use, to detect, measure and predict or extrapolate perturbations of this scale. We can detect them and sometimes can indicate roughly their maximum effect on a cloud trajectory. Sounding balloons take from several minutes to an hour to rise through the layers in question and several more minutes are required to process the data. By the time this has occurred and the forecaster can evaluate the meaning of the data and compute future motion the wave will have moved through the area or will have disappeared. A good example of this occurred with the test of the reactor Kiwi A in 1959 (Fig. 5) when a perturbation of at least an hour duration caused the motion of the cloud of the exhaust to depart from the predicted 190° wind direction by 15° on one side then return to 10° on the other side. The activity level for this event was very low and this departure is only of interest as an illustration of what can happen.

Many of the eddy motions in the atmosphere must now be considered to be random in the sense that their cause, source, history and dimensions are obscure. The speed and accuracy of the NTS radar wind plotter and surface weather network have contributed much to operational fallout safety. However, we believe that it will eventually be within our capability to handle intelligently, operationally, and on a dynamic rather than statistical basis, smaller scales of motion than we now do, and we suggest that more of our limited meteorological talent might well be applied in this direction.

Future Needs

The obvious goal in all air polluting activities should be, and is, to eliminate sources of pollution. However, the simple fact remains that the number of sources of radioactive and toxic pollutants is growing steadily. Instead of wishing them to hurry up and go away, meteorologists should be preparing to live with some of them for a long time.

The ultimate goal in meteorological support of projects involving toxic air pollution, whether from A-bomb fallout, nuclear engine exhaust gases, toxic chemical rocket exhausts, or industrial waste, should be, in my opinion, to develop a high speed weather data handling and computing system for mesoscale application, to go along with the development of a large-scale forecasting system of the National Meteorological Center's Numerical Unit. This mesoscale unit should include:

1. A close network of stations around each source, reporting upper air data frequently or even continuously. Network grid spacing horizontally and vertically should be designed to detect wind pressure and temperature changes which result in changes of wind and

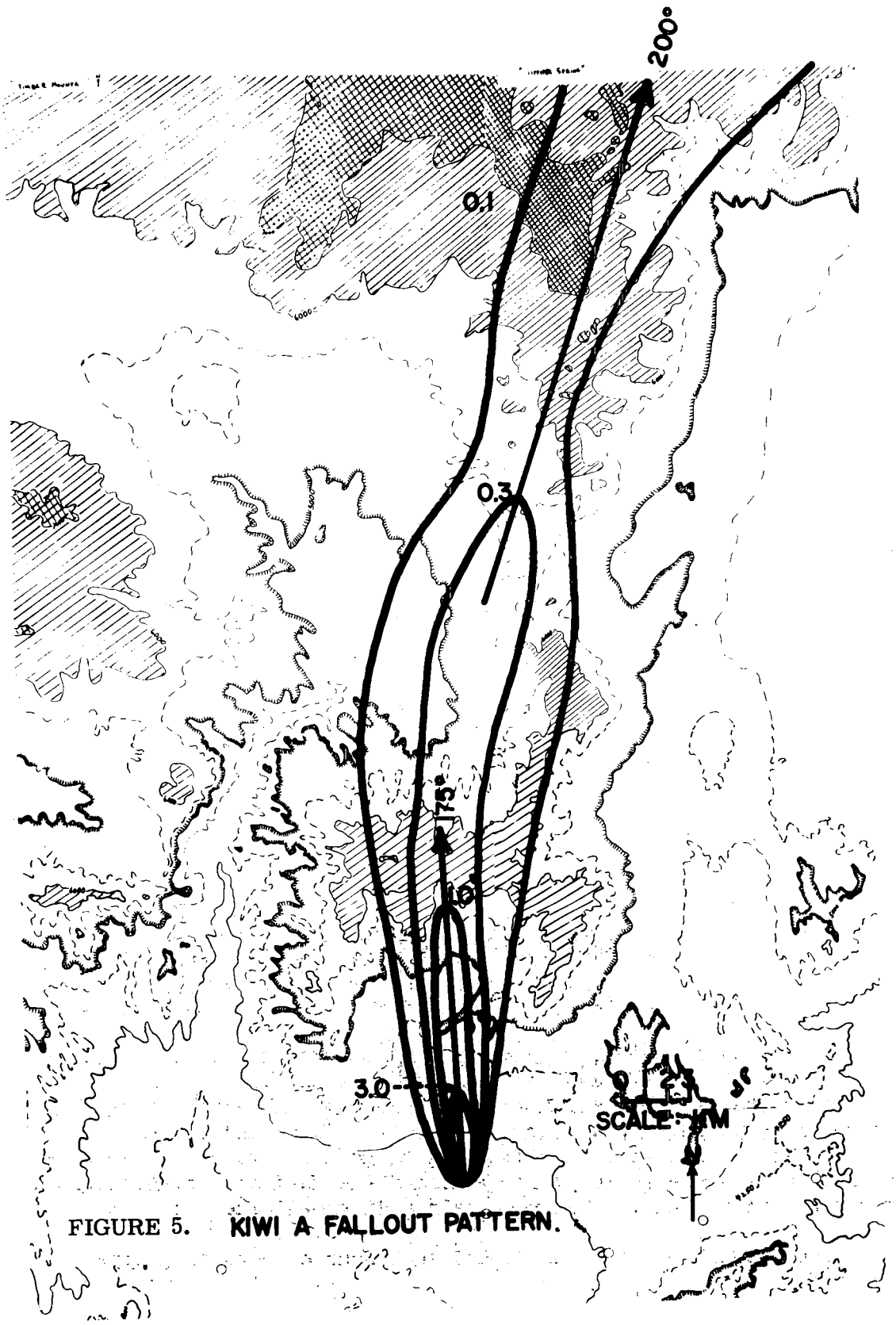

FIGURE 5. KIWI A FALLOUT PATTERN.

stability, just to determine the appropriate grid spacing requires knowledge not now available. Some development is already being made of means for continuously reporting upper air data.

2. Instantaneous telemetering of information to central analysis and computing facilities. This is now physically possible, but very expensive.

3. Computing stream functions and temperature field over the grid, then extrapolating these perhaps as much as 6 hours into the future. The real obstacle to this system is the development on mathematical models of mesoscale processes, and this is where additional research should be concentrated.

4. Distribution of forecasts to users. Such a high speed system would be of little value operationally unless its results were available and useful immediately. Specific applications should include forecast interpretation to the extent that acceptable forecasts would be so labeled and those presenting weather unacceptable for the particular operation would be clearly marked to eliminate loss of time for forecast interpretation on the part of the operations people.

Whether the large amount of effort necessary to realize such a complete mesoscale prediction system would be worth the cost in value to weapons test fallout prediction alone is difficult to determine. It would require investing effort in research units that are better equipped for this kind of work than our small test support group in Nevada. We are in the position that many close-in fallout patterns have been laid down without obvious change in the environment of the Nevada Test Site, and without excessive exposure of the off-site population to fallout radiation. This has been accomplished simply by waiting until atmospheric patterns of motion occurred in which it was possible to assure fallout safety. But these delays are costly and it might be possible to reduce them somewhat with more effective and confident use of marginal weather situations. The primary justification for this system in Atomic Energy Commission operations would probably be in its contribution to safety through establishing rapid and accurate indications of wind both currently and for a short time into the future.

AN INTERPRETATION OF GLOBAL FALLOUT

L. Machta, R. J. List and K. Telegadas
U. S. Weather Bureau*
Washington, D. C.

Introduction

This paper will cover the following subjects: An inventory of Sr^{90} prior to the U.S.S.R. 1961 nuclear tests; the goegraphical and temporal distribution of stratospheric fallout during the period 1959 to 1961 when very little of the fission product radioactivity was of tropospheric origin and finally a prediction of the Sr^{90} fallout from the U.S.S.R. 1961 tests.

The Inventory of Sr^{90} Prior to September 1961

There are two parts to the determination of the Sr^{90} inventory. First, the residual atmospheric content must be measured by filtration of the air at many places and altitudes in the atmosphere and second, the deposited Sr^{90} must be obtained by one of several techniques. We shall deal first with the atmospheric content.

In May 1960 the High Altitude Sampling Program of the Defense Atomic Support Agency was succeeded by a semi-annual program of monitoring in time and altitude at 4 latitudes. These are shown in Fig. 1 which displays the Sr^{90} concentrations in the atmosphere in November 1960. The data on this figure emphasize the broad governmental contributions largely instigated and supported by the Fallout Studies Branch of the U. S. Atomic Energy Commission (AEC) in measuring atmospheric radioactivity. Ground level observations are obtained on a monthly composite of daily filter collections made by the weather services along the 80th meridian (West) and analyzed by the U. S. Naval Research Laboratory.

* Research conducted under the auspices of the Fallout Studies Branch, Division of Biology and Medicine, U. S. Atomic Energy Commission.

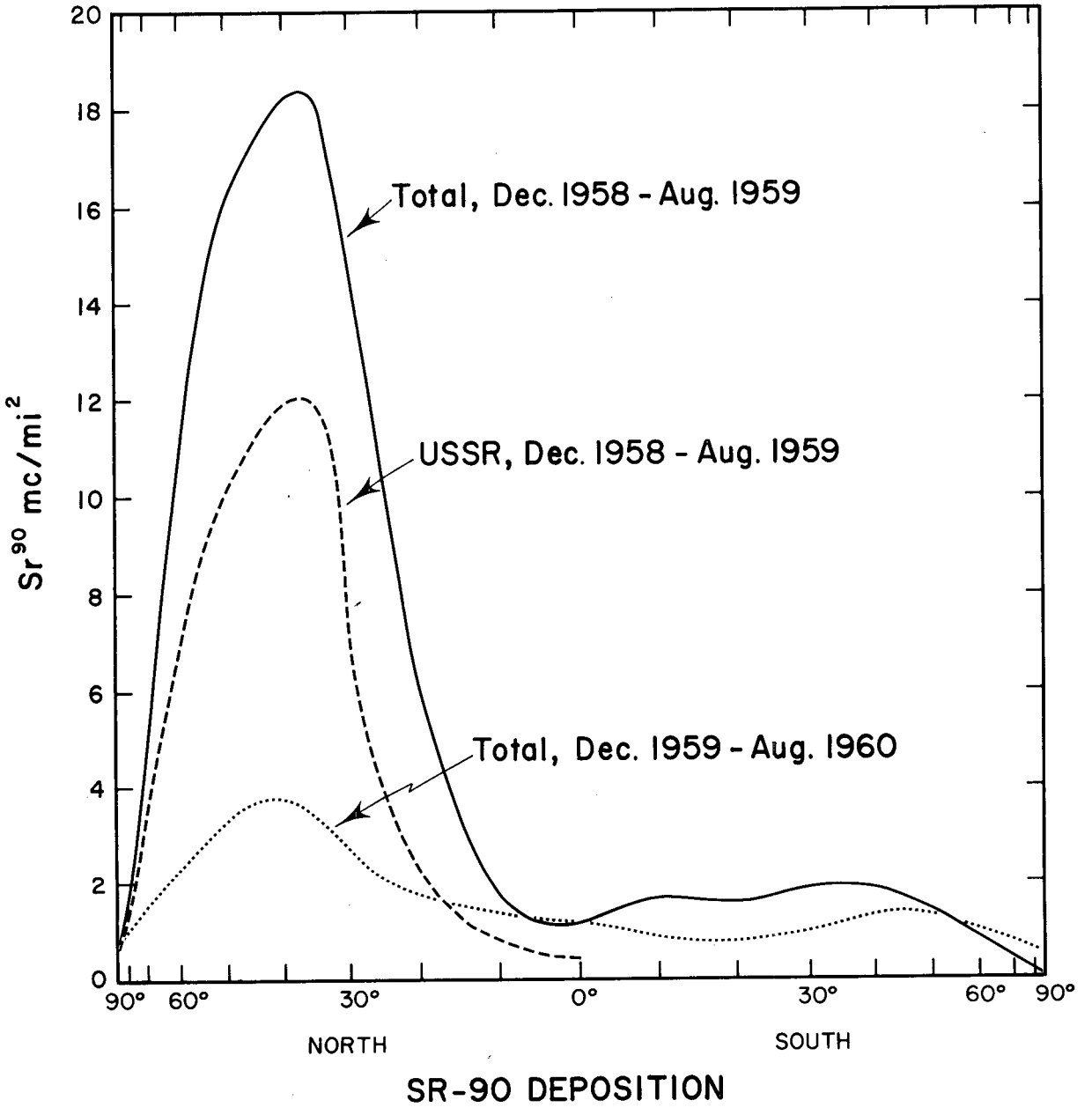

Figure 4. Global Distribution of Deposited Sr^{90} During the "Spring" of 1959 and 1960 Showing Also the Fallout from the U. S. S. R. October 1958 Tests in the "Spring" of 1959.

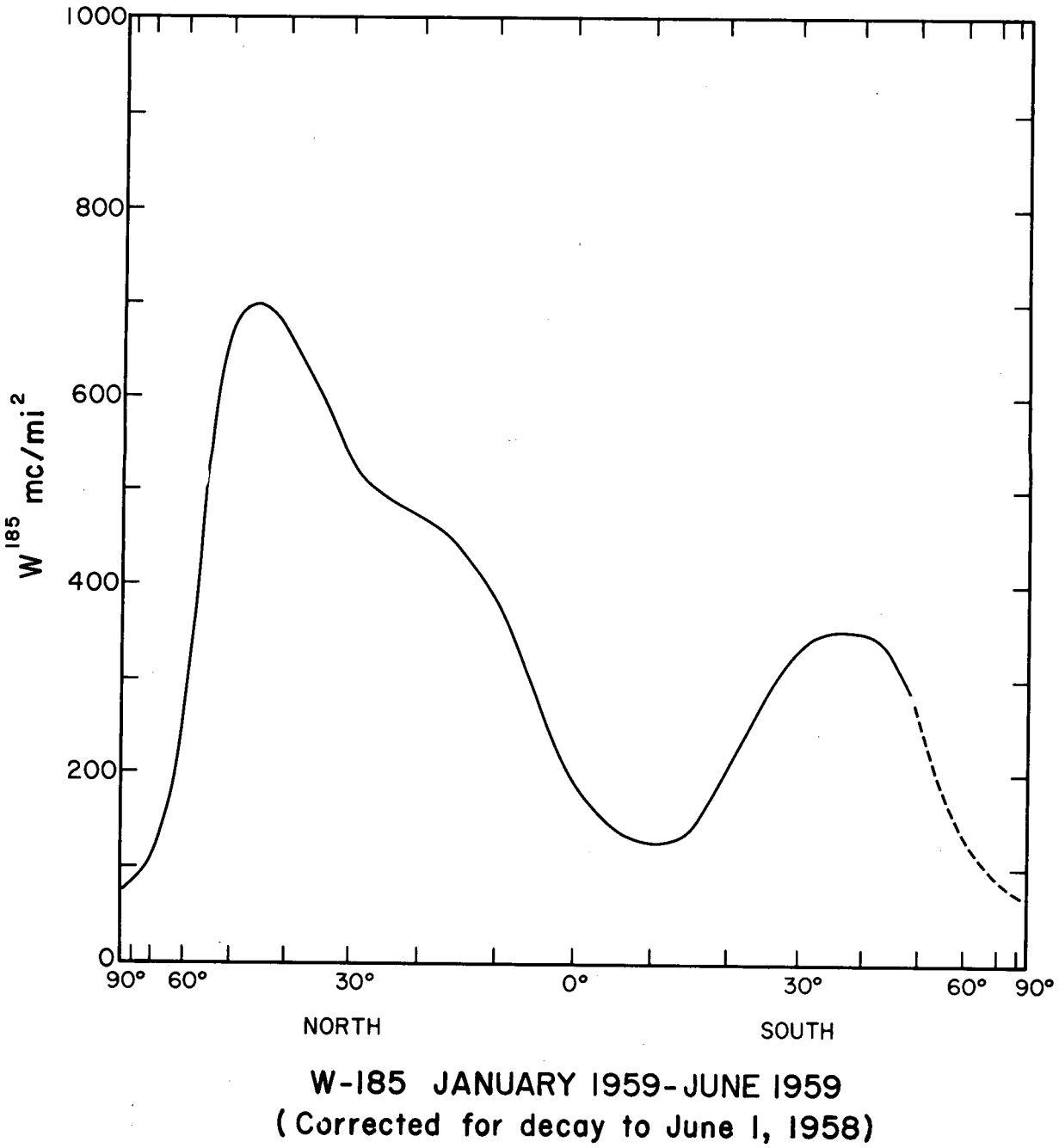

Figure 5. Global Distribution of W^{185} During the First Half of 1959.

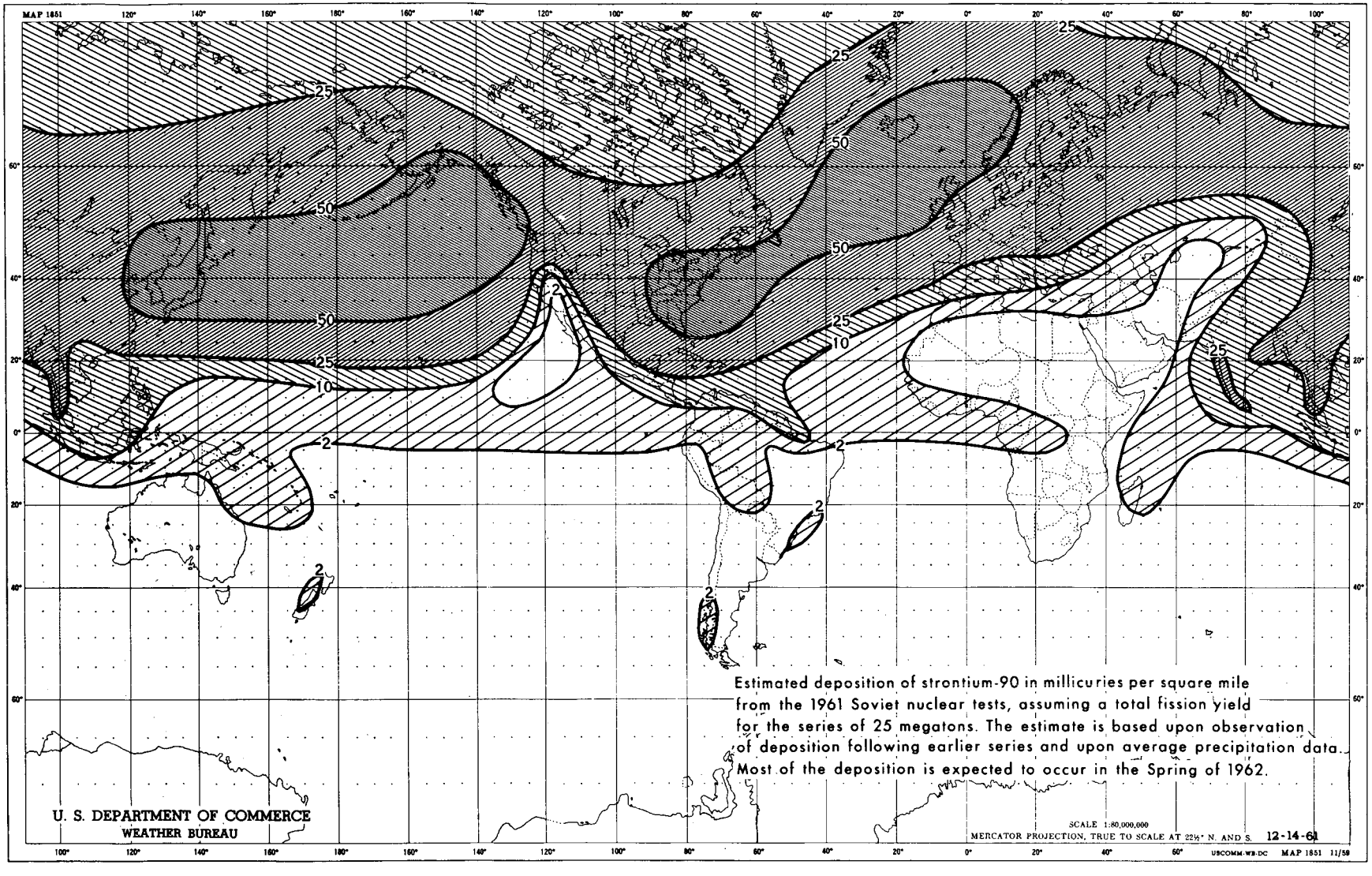

Figure 9. A Prediction of Fallout from the Autumn 1959 U. S. S. R. Test Series.

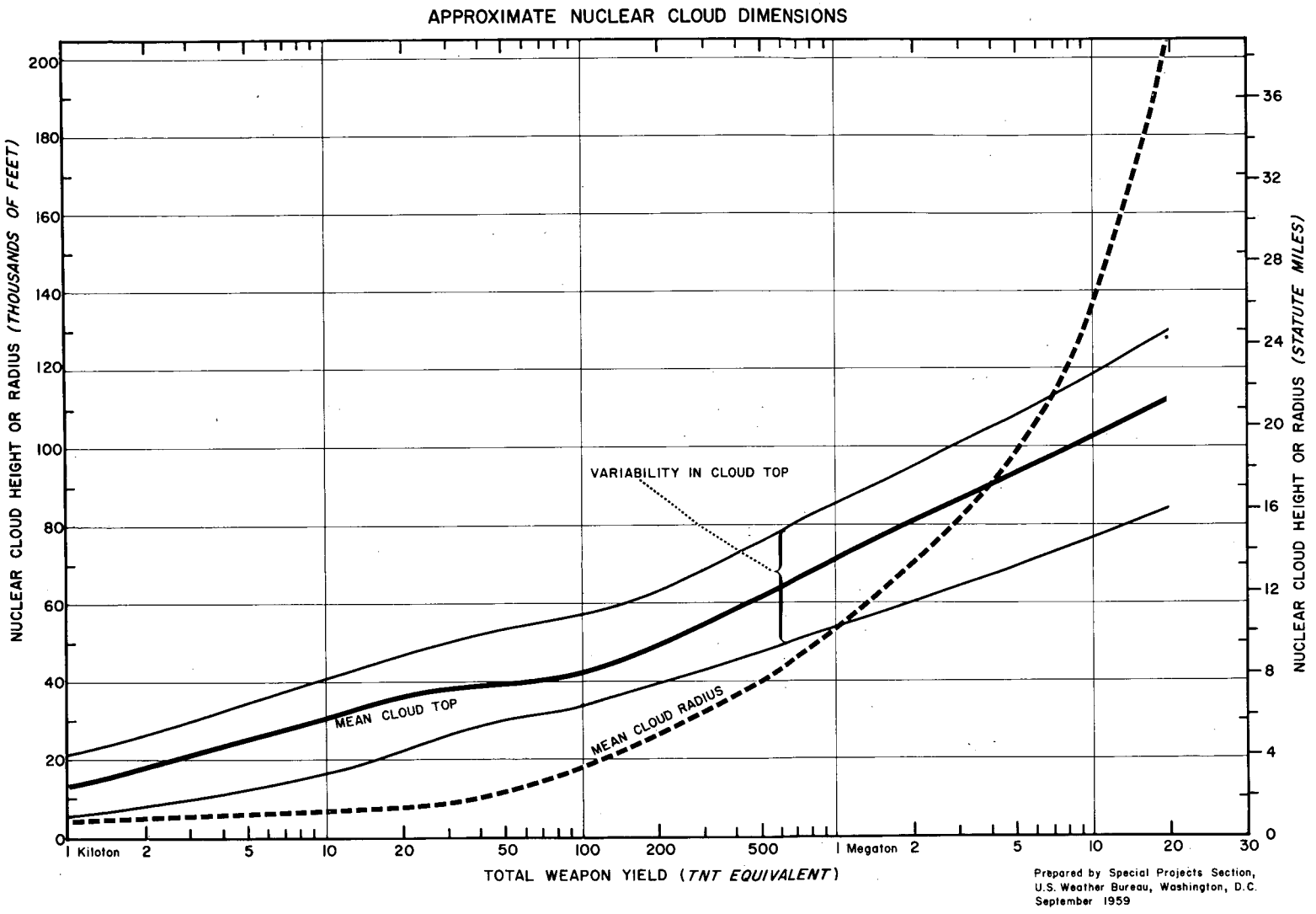

Figure 10. An Estimate of the Top and Lateral Dimension of Stablized Nuclear Clouds as a function of the Yield of the Nuclear Detonation.

GEOCHEMICAL STUDIES ON THE STRATOSPHERIC FALLOUT

P.K. Kuroda, H.L. Hodges, M.P. Menon, Tin Mo, Joe Nix, L.M. Fry and H.E. Moore*
Department of Chemistry
University of Arkansas
Fayettville, Arkansas

Introduction

This report gives a brief summary of the work being carried out in this laboratory on the radioactive fallout since the fall of 1958. The topics under investigation include: (a) nuclear fission in the early history of the earth, (b) spring peak of Sr^{90} fallout, (c) fallout from nuclear detonations of February and April 1960, (d) stratospheric residence time of Sr^{90}, and (e) stratospheric fallout of Ce^{144}.

Nuclear Fission in the Early History of the Earth

It has been pointed out by Kuroda(1), in 1958, that the Sr^{90} is produced in nature by the spontaneous fission of uranium and thorium and that the total amount of Sr^{90} produced by the spontaneous fission of U^{238} alone in the earth's crust is comparable to the amount of artificially produced Sr^{90} in the stratosphere.

After the mass spectrum of meteoritic xenon became known in 1960(2), Kuroda(3) pointed out that the differences between meteoritic and terrestrial xenon seemed to indicate an excess of the heavy isotopes of xenon (Xe^{131}, Xe^{132}, Xe^{134} and Xe^{136}) in the earth's atmosphere, and reported that the difference is much greater than that expected from the U^{238} spontaneous fission alone, but can be explained as due to the spontaneous fission of some of the extinct transuranium

*On leave from the Department of Chemistry, Arkansas State College, State College, Arkansas, during the summers of 1960 and 1961.

elements and/or the induced fission of U^{235} in the early history of the earth. It has been suggested that spontaneous fission of extinct Pu^{244} (7.6×10^7 years) might have produced the excess $Xe^{131-136}$ in the earth's atmosphere.

Kuroda(4) attempted to calculate the time interval between the cessation of the nucleosynthesis and formation of the earth, assuming that the extinct Pu^{244} was mainly responsible for the production of excess xenon isotopes in the earth's atmosphere and obtained a value of 5.2×10^7 years for the time interval.

Kuroda(5) has recently revised the calculation, and showed that the calculated time interval between the cessation of nucleosynthesis and formation of the earth based on the Pu^{244} model to be most likely approximately 10^8 years.

Another important source of contribution to the atmospheric inventory of xenon is the neutron-induced fission of U^{235} in nature. A number of reports have been published on this subject (6)(7)(8), but the exact contribution from this source can not be evaluated at the present time.

According to Kuroda(3), at least 10% of the total amount of Xe^{136} in the earth's atmosphere is "fissiogenic". It is interesting to note that the contribution from the recent artificial nuclear explosions is estimated to be less than only 10^{-6} of the contributions from the natural fission processes.

Spring Peak of Sr^{90} Fallout

To explain the vertical distributions of water vapor and ozone in the atmosphere, Brewer(9), in 1949, and Dobson(10), in 1956, proposed a model of global movement of the air masses. According to this model, there is a cold pool of air in the stratosphere over the winter pole during the late winter months, and it carries ozone-rich air to the lower levels in early spring. It was further suggested by Dobson that, if there is such a slow sinking of air in the middle latitudes from the stratosphere to the troposphere, it must be balanced elsewhere by a reserve current from the troposphere to the stratosphere. This upward flow of air is expected to occur in tropical regions.

Experimental results obtained in this laboratory seemed to support the Brewer-Dobson model of global circulation of air masses quite well. A pronounced peak of fallout rate occurred at Fayetteville, Arkansas, during the spring months of 1959(11). We concluded that

the spring peak was primarily due to an increase in the rate of material transfer from the stratosphere to the troposphere, caused by the sinking of every cold air masses which formed above the winter pole during the late winter months, and we predicted, in 1959, that there would be another peak in the Sr^{90} fallout rate during the spring months of 1960, regardless of whether or not there was a thermonuclear bomb explosion during the fall months of 1959.

The 1960 spring peak, clearly shown in Fig. 2, demonstrated that the seasonal and global movements of stratospheric air masses, such as described by Brewer and Dobson, play an extremely important role in causing the spring peaks of the Sr^{90} fallout.

Our data seem to be explained quite well by the assumption that whereas the transfer from the stratosphere occurred at a maximum rate in the spring months and at a minimum rate in the fall months, the overall rate of the Sr^{90} transfer from the stratosphere during the period 1959-1960 was roughly equivalent to an "apparent" stratospheric mean storage time of approximately 1 year or even less.

Fallout from Nuclear Detonations of February and April 1960

A sharp increase in the Sr^{89}/Sr^{90} ratio in rain was observed at Fayetteville, Arkansas, after the French nuclear detonations of February and April 1960, as shown in Fig. 1(12).

We have interpreted the strontium isotope ratio data and concluded that (a) the Sr^{90} inventory of the Northern Hemisphere has increased due to the French nuclear explosions by approximately 0.1 to 0.2% and (b) this is due to the fact that there is an upward flow of air in the tropical region and hence a material transfer from the troposphere to the stratosphere is expected to occur, according to the global circulation model of air masses, proposed by Brewer(9) and by Dobson(10).

It has been generally accepted that relatively low yield nuclear bombs such as those detonated at Reggan in the Sahara Desert on February 13 and on April 1, 1960, inject their debris solely into the troposphere, whereas debris from high yield thermonuclear bombs enter the stratosphere and cause the worldwide stratospheric fallout.

Although the French nuclear detonations caused seemingly small transient increases in fallout and the fresh debris most likely added no more than a few tenths percent to the total worldwide fallout of long-lived fission products, the radionuclide injection into the atmosphere by the French nuclear detonations was of unique scientific interest in that the nuclear explosions occurred in the

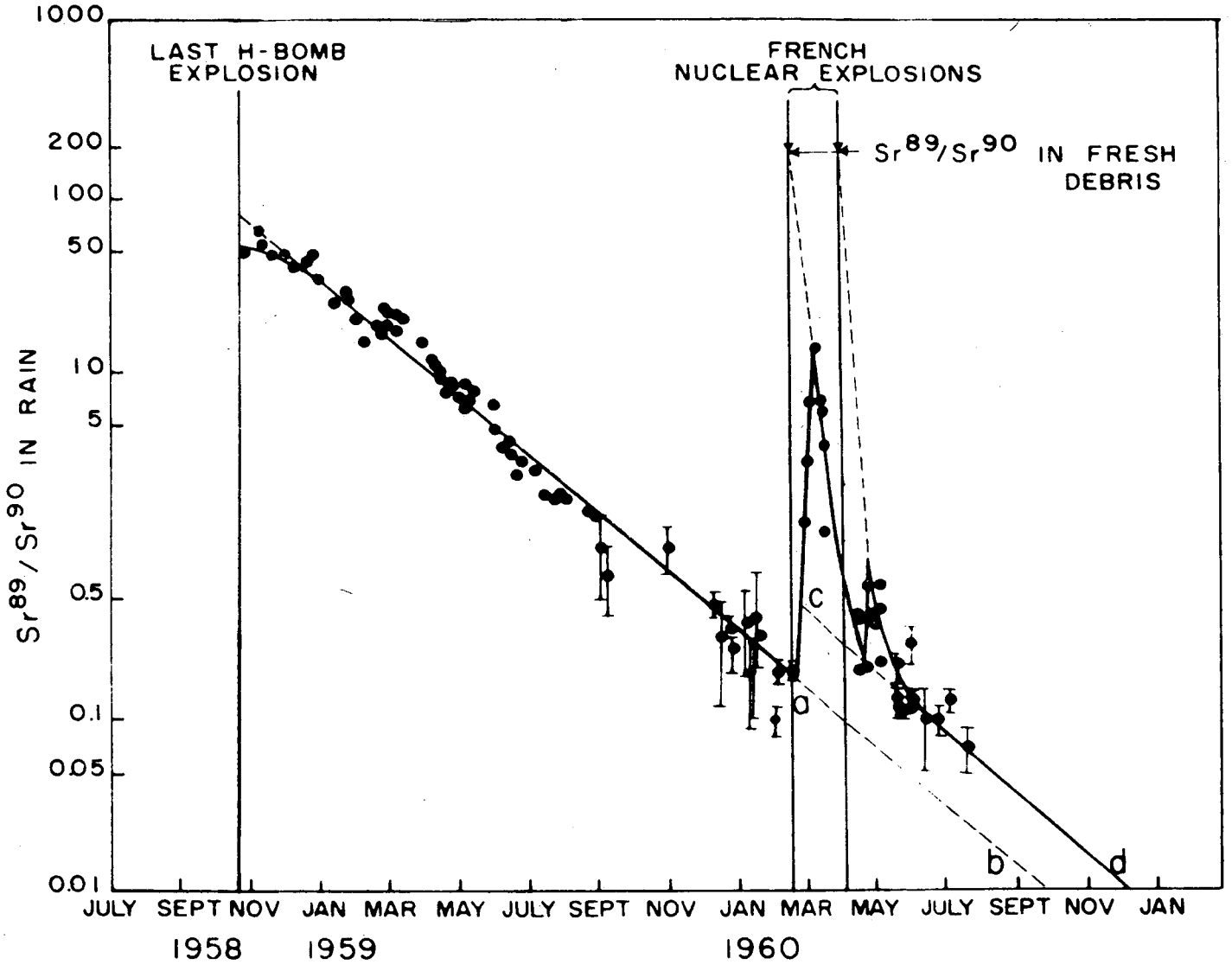

Figure 1. Variation of the Sr^{89}/Sr^{90} ratio in individual samples of rain and snow collected at Fayetteville, Arkansas, since November 1958

tropical region after a longer nuclear test suspension period.

Stratospheric Residence Time of Sr^{90}

Widely different values have been reported in the past for the stratospheric residence time of Sr^{90}. Libby (13) first pointed out the long hold-up of Sr^{90} in the stratosphere and estimated the mean stratospheric residence time to be 5 to 10 years. Machta and List (14) estimated the mean removal rate to be about 20% per year, but later pointed out the possibility that the actual rate might be much greater.

Kulp et al. (15) proposed a value of 3 years for the residence time, and Storebø (16) reported that the residence time in the stratosphere should not be much more than 1 year, while Feely (17), in 1960, estimated the residence half-time to be less than 1 year, equivalent to a mean residence time of less than 18 months.

A number of investigators (18)(19), on the other hand, have recently pointed out that the concept of a well-mixed stratosphere and a mean stratospheric residence time appear largely inapplicable to the interpretation of stratospheric fallout. Martell and Drevinsky (18)(19) proposed three stratospheric residence times instead of one: (a) a few months or more for Soviet test debris in the polar stratosphere; (b) 1 to 3 years for debris in the lower equatorial stratosphere; (c) 5 to 10 years for the debris at higher levels near the equator. Libby (20 has also expressed a similar view).

All these estimates were made on the basis of the experimental data obtained during the period when the nuclear test explosions were frequently conducted at various localities of the world. The magnitude and the types of weapons exploded were usually unannounced, and a certain amount of guess work was involved in the calculations as to the amounts of Sr^{90} injected by these bombs at different times.

We have attempted to calculate the stratospheric mean residence time from the Sr^{90} concentration data in rain obtained in this laboratory during the nearly three year test "suspension" period.

Monthly average Sr^{90} concentrations in rain ($\bar{C}$) were calculated from the equation,

$$\bar{C} = F/R \quad \ldots\ldots\ldots\ldots\ldots (1)$$

where F is the total amount of Sr^{90} (in $\mu\mu c/m^2$) transported by rain

TABLE 1

Monthly Average Sr^{90} Concentrations in Rain at Fayetteville, Arkansas ($\mu\mu c/l$)

Month	$\bar{C}$	Month	$\bar{C}$
November 1958	2.90	April 1960	3.23
December 1958	6.97	May 1960	1.92
January 1959	11.4	June 1960	3.35
February 1959	10.7	July 1960	0.75
March 1959	13.8	August 1960	1.13
April 1959	24.1	September 1960	0.84
May 1959	18.7	October 1960	0.51
June 1959	5.63	November 1960	0.30
July 1959	4.82	December 1960	0.44
August 1959	2.02	January 1961	1.43
September 1959	0.80	February 1961	2.11
October 1959	3.35	March 1961	2.44
November 1959	0.3	April 1961	3.51
December 1959	2.36	May 1961	1.86
January 1960	1.04	June 1961	1.71
February 1960	3.79	July 1961	0.86
March 1960	2.98	August 1961	0.65

during a period of a month and $\sum R$ is the total rainfall (in mm) during the same period. The values of $\bar{C}$ are shown in Table 1.

The data show that there is a marked seasonal variation of the Sr^{90} concentration in rain which follows a cyclic pattern with a maximum in the spring and a minimum in the fall.

The values of monthly average concentration of Sr^{90} in rain are not too accurate since the amounts and frequencies of rainfalls vary from month to month. For example, the value of $\bar{C}$ for the month of November 1959 is based on the measurement of a single rainfall. An exceptionally dry month may often be followed by an unusually wet month. For this reason, it has been decided to calculate the bi-monthly average concentrations by simple taking the arithemtic average of the values of $\bar{C}$ for two consecutive months.

The values of bi-monthly average Sr^{90} concentrations for the first year ($\bar{C}_1$), second year ($\bar{C}_2$) and third year($\bar{C}_3$) are shown in Table 2.

These values are plotted in Fig. 2. Values observed by Kuroda (1) in 1958 at Lemont, Illinois, are shown for comparison.

The percentage increase of the stratospheric Sr^{90} inventory in the Northern Hemisphere due to the French nuclear detonations of February and April 1960 was calculated to be approximately 0.1 to 0.2 % (12). Thus, we may neglect the contributions from a number of small French nuclear detonations, which occurred during the nuclear test "suspension" period, in the following calculation.

Contributions from the tropospheric fallout of the French tests and the fall 1958 Soviet tests appear to have been less than a few percent and hence should not affect the following calculation considerably.

Let us now compare the by-monthly Sr^{90} concentration during a two-month period with that during the same two-month period of the following year.

The average Sr^{90} concentrations in rain will certainly depend upon various factors, such as the types, total amounts and frequencies of rainfalls. However, let us by way of experiment write that

$$\bar{C}_{n+1} / \bar{C}_n = S_{n+1}/S_n \quad \ldots\ldots\ldots\ldots\ldots\ldots \quad (2),$$

TABLE 2

Bi-Monthly Average Sr^{90} Concentrations in Rain at Fayetteville, Arkansas
($\mu\mu c/l$)

Period	$\bar{C}_1$	Period	$\bar{C}_2$	Period	$\bar{C}_3$
November and December 1958	4.95	November and December 1959	1.33	November and December 1960	0.37
January and February 1959	11.1	January and February 1960	2.42	January and February 1961	1.77
March and April 1959	19.0	March and April 1960	3.11	March and April 1961	2.98
May and June 1959	12.2	May and June 1960	2.64	May and June 1961	1.79
July and August 1959	3.42	July and August 1960	0.94	July and August 1961	0.75
September and October 1959	2.08	September and October 1960	0.58		

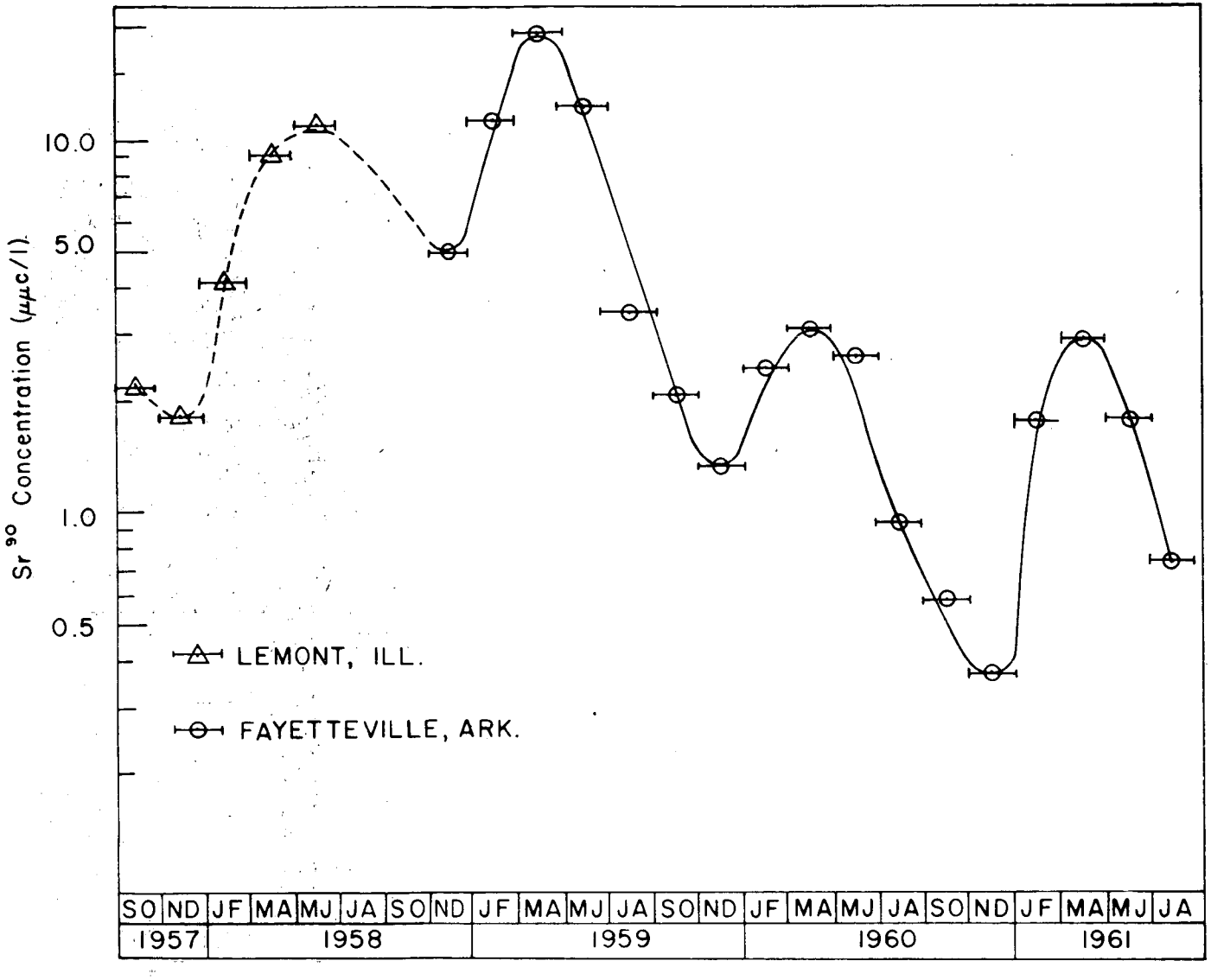

Figure 2. Bi-monthly Average Sr^{90} Concentrations in Rain

where S_n is the Sr^{90} inventory in the stratosphere during a two-month period in the nth year, S_{n+1} is that in the corresponding period in the (n+1)th year, and n=1 or 2.

The value of S_{n+1} will ordinarily be smaller than the value of S_n, because Sr^{90} in the stratosphere will be removed by the fallout and by the radioactive decay. Hence, we may write that

$$S_{n+1} = S_n \cdot e^{-(\bar{a} + \lambda_{90})} \quad \ldots\ldots\ldots\ldots (3)$$

where λ_{90} is the decay constant of Sr^{90} and $\bar{a}$ is a value which depends upon the annual average rate of stratospheric fallout.

It has to be noted that nothing has been said here about whether or not the stratosphere contains radioactivity which is uniformly mixed. In other words, we are by no means trying to give here what might ordinarily be described as an explanation for the mechanism of radioactive fallout.

The value of $\bar{a}$ may or may not be a constant depending upon the mechanism of radioactive fallout and also the "homogeneity" of the distribution of Sr^{90} in the stratosphere. It is entirely possible that even a negative value of $\bar{a}$ might be obtained if the stratosphere is not well mixed. Our next step is then to calculate the values of $\bar{a}$ from the values of $\bar{C}_1$, $\bar{C}_2$ and $\bar{C}_3$.

From equations (2) and (3), we have

$$\bar{C}_{n+1} = \bar{C}_n \cdot e^{-(\bar{a} + \lambda_{90})} \quad \ldots\ldots\ldots\ldots (4).$$

The values of $\bar{a}$ are calculated from the data given in Table 2 and are shown in Table 3.

It is interesting to note that the value of $\bar{a}$ remained fairly constant for almost two years, and then a sudden change to a new set of values took place after January 1961. The constancy of the value of $\bar{a}$ was as good as could be expected, however, during the first two-year period considering the many uncertainties involved in the treatment of the experimental data. For this reason, we have recently proposed (21) to define $(1/\bar{a})$ as the mean residence time and $\ln(2/\bar{a})$ as the residence half-time of Sr^{90} in the stratosphere. A value of 0.7 ± 0.1 years was obtained from the data available at that time for the mean residence time of Sr^{90}.

TABLE 3

Mean Residence Time and Residence Half-time of Sr^{90} in the Stratosphere (years)

Period	$\bar{a}$	Mean residence time, $1/\bar{a}$	Residence half-time
November and December 1958-1959	1.28	0.78	0.54
January and February 1959-1960	1.49	0.67	0.46
March and April 1959-1960	1.78	0.56	0.39
May and June 1959-1960	1.49	0.67	0.46
July and August 1959-1960	1.26	0.79	0.55
September and October 1959-1960	1.25	0.80	0.55
November and December 1959-1960	1.30	0.78	0.53
January and February 1960-1961	0.29	3.4	2.4
March and April 1960-1961	0.02	~50	~35
May and June 1960-1961	0.37	2.8	1.9
July and August 1960-1961	0.22	4.6	3.2

Excluding the March-April 1960-1961 value for $1/\bar{a}$, we now have an additional set of values roughly corresponding to 3.6 ± 0.9 years, which is quite in line with the values often mentioned by early investigators.

Perhaps a few words may have to be added here concerning the anomalous value from the March and April 1960-1961 data. We note in Table 3 that the value of $1/\bar{a}$ calculated from the March and April 1959-1960 data is also somewhat out of line and definitely lower than the average value of $1/\bar{a}$ for the first two-year period.

Suppose the value of $\bar{C} = 3.11$ μμc/l for March and April 1960 was too low for some reason. If it should have been 4 μμc/l, instead, then we have the following new values which can be beautifully incorporated in Table 3 as substitutes.

	$\bar{a}$	$1/\bar{a}$(year)
March and April 1959-1960	1.53	0.65
March and April 1960-1961	0.27	3.7

Such an error in obtaining the value of $\bar{C}$ can arise from various sources. To make sure that it is not due to analytical errors, we are now repeating the measurements of Sr^{90} in some of the March and April 1960 and 1961 rain samples. It is interesting to calculate an "overall apparent" mean residence time during the nuclear test suspension period by simply considering the ratio $\bar{C}_{n+2}$ and $\bar{C}_n$, i.e.,

$$\bar{C}_{n+2} = \bar{C}_n \cdot e^{-(\bar{a} + \lambda 90)(n + 2-n)} \quad \ldots . \quad (5).$$

The values of $\bar{a}$ are calculated from $\bar{C}_1$ and $\bar{C}_3$, and are shown in Table 4.

The constancy of the values of $\bar{a}$ thus obtained is again as good as could be expected. A value of 1.1 ± 0.3 years is thus obtained for the over-all apparent mean residence time. This value is similar to the estimates made earlier by Kuroda, Hodges and Moore (12), Storobø (16) and Feely (17).

TABLE 4

Over-all Apparent Mean Residence Time and Residence Half-time of Sr^{90} in the Stratosphere during the Nuclear Test Suspension Period 1958-1961 (years)

Period	$\bar{a}$	Mean residence time, $1/\bar{a}$	Residence half-time
November and December 1958-1960	1.27	0.79	0.55
January and February 1959-1961	0.89	1.12	0.78
March and April 1959-1961	0.90	1.11	0.77
May and June 1959-1961	0.93	1.08	0.75
July and August 1959-1961	0.73	1.37	0.95

Stratospheric Fallout of Ce^{144}

In connection with the observations on the Sr^{90} spring peaks, it was felt worthwhile to investigate the fallout pattern of Ce^{144} in some detail and we have recently undertaken the measurements of the Ce^{144} concentrations in individual samples of rain.

A new radiochemical procedure for cerium, which has recently been developed in this laboratory (22), was used for the determination of Ce^{144} in rain water. The new method depends entirely on the oxidation-reduction and liquid-liquid extraction cycle, and was originally intended for the fission products from the U^{238} spontaneous fission. Values of $7.0 \pm 1.4\%$ were secured by this method for the yields of Ce^{143} and Ce^{144}, respectively, in good agreement with the values obtained by Russell for the yields of Pr^{143} and Ce^{144} from the spontaneous fission of U^{238} (23).

Yields of cerium and strontium isotopes from fast neutron-induced fission of uranium were determined by irradiating a sample of depleted uranium oxide (99.989% U^{238} and 0.011% U^{235}) with $14.5 + 0.4$ Mev neutrons produced by the T(d,n) He^4 reactions in the University of Arkansas 400 KV Cockcroft-Walton positive ion accelerator (24)(25) and the following results were obtained: Ce^{144}, $5.2 \pm 0.4\%$; Sr^{90}, $3.4 \pm 0.3\%$. These results are in agreement with the values of fission yields for fast neutron-induced fission of U^{238} reported by Katcoff (26); Ce^{144}, 4.9%; Sr^{90}, 3.2%.

Although our value for the Ce^{144} yield is considerably higher than the value of $2.68 \pm 0.16\%$ reported by Cuninghame (27), and hence the experiments may have to be repeated, it is of some interest to use our data to calculate the Ce^{144}/Sr^{90} production ratio in the instantaneous fission of U^{238} caused by fast neutrons;

$$\frac{5.2}{3.4} \times \frac{28 \times 365}{285} = 54.8 \text{ (dpm/dpm)}$$

The monthly average Ce^{144} concentrations in rain were computed from the formula

$$\bar{C} = \Sigma F / \Sigma R,$$

where ΣF is the total amount of Ce^{144} (in $\mu\mu c/m^2$) transported by rain during a one-month period and ΣR is the total rainfall (in mm) during the same period.

The existence of a pronounced spring peak in the Ce^{144} fallout rate is obvious in Fig. 3. Considering the decay of Ce^{144} the 1961

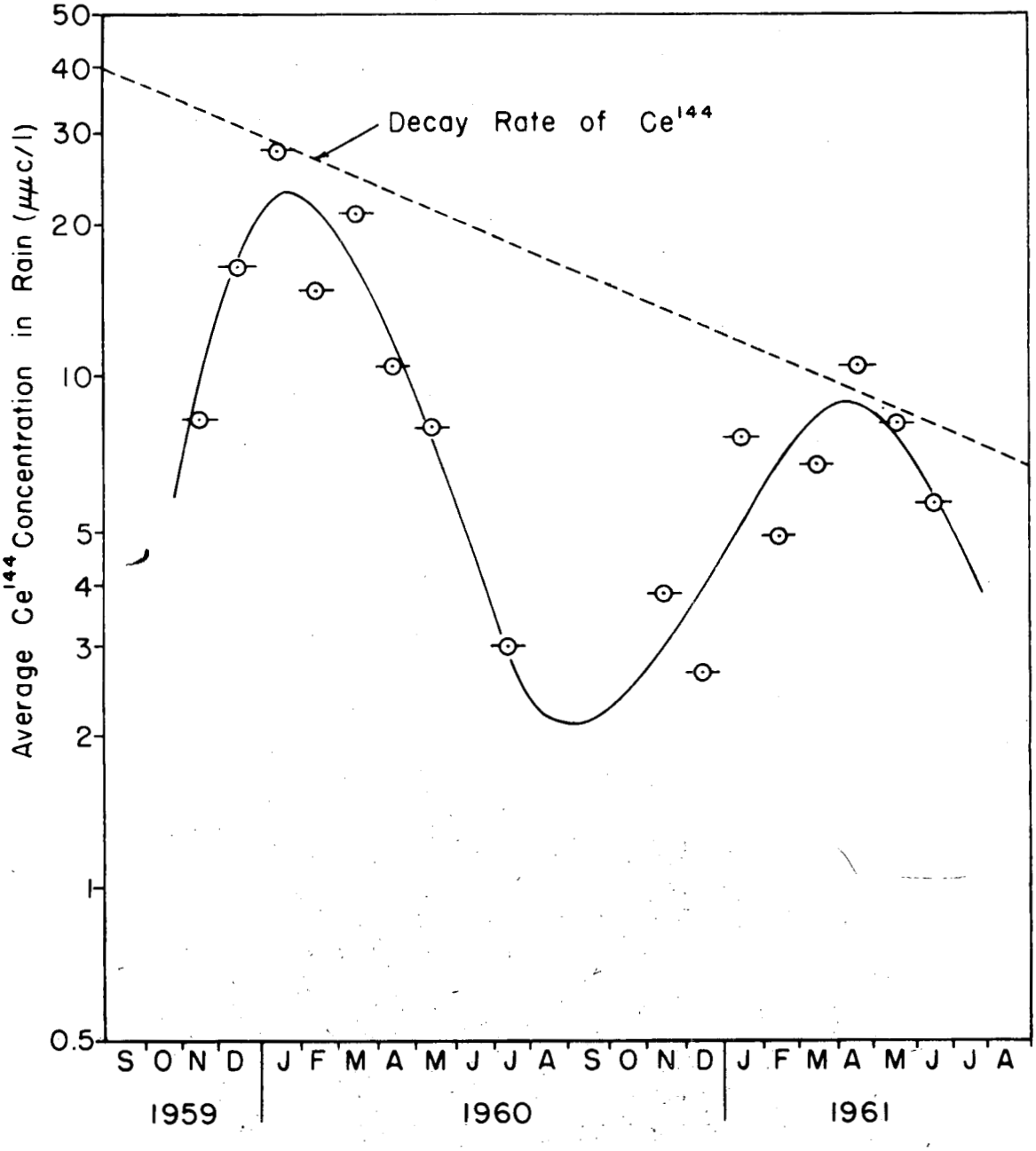

Figure 3. Seasonal Variation of the Ce^{144} Concentration in Rain at Fayetteville, Arkansas

spring peak was just as high as the 1960 peak. Thus, it looks as if the depletion of the Ce^{144} inventory by the fallout did not take place. A possible explanation for this may be that new debris may have been entering the lower stratosphere during this period at a rate similar to that of removal of Ce^{144} by the fallout process.

Fig. 4 shows the seasonal variation of the average monthly Ce^{144}/Sr^{90} ratio follows a cyclic pattern with a minimum in the spring and a maximum in the fall. It thus appears as if we are dealing with two stratospheric air masses; one containing Ce^{144} -rich and the other Ce^{144}-depleted debris. The cause of the spring minimum of the Ce^{144}/Sr^{90} ratio may be explained according to the Brewer-Dobson model (9)(10), at least qualitatively, as due to the presence of Ce^{144}-depleted debris at a very high altitude. As a cold air mass produced in the high stratosphere in the early spring slowly descends to lower levels to cause the spring peak of fallout, the Ce^{144}-depleted debris may show up in the lower stratosphere since the bulk of debris from the fall 1958 Soviet test series must have been largely removed from the lower stratosphere during the latter half of the nuclear test suspension period.

References

1. Kuroda, P.K. On the stratospheric Sr^{90} fallout. Argonne National Laboratory, U.S. AEC report ANL-5920, October 1958. pp. 40.

2. Reynolds, J.H. Determination of the age of the elements. Phys. Rev. Letters 4:8(1960).

3. Kuroda, P.K. Nuclear fission in the early history of the earth. Nature 187:36(1960).

4. Kuroda, P.K. The time interval between nucleosynthesis and formation of the earth. Geochimica et Cosmochimica Acta 24:40 (1961).

5. Kuroda, P.K. On the chronology of the solar system formation. (Submitted to Geochimica et Cosmochimica Acta, 1961).

6. Kuroda, P.K. On the nuclear physical stability of the uranium minerals. J. Chem. Phys. 25: 781(1956).

7. Kuroda, P.K. On the infinite multiplication constant and the age of the uranium minerals. J. Chem. Phys. 25:1295(1956).

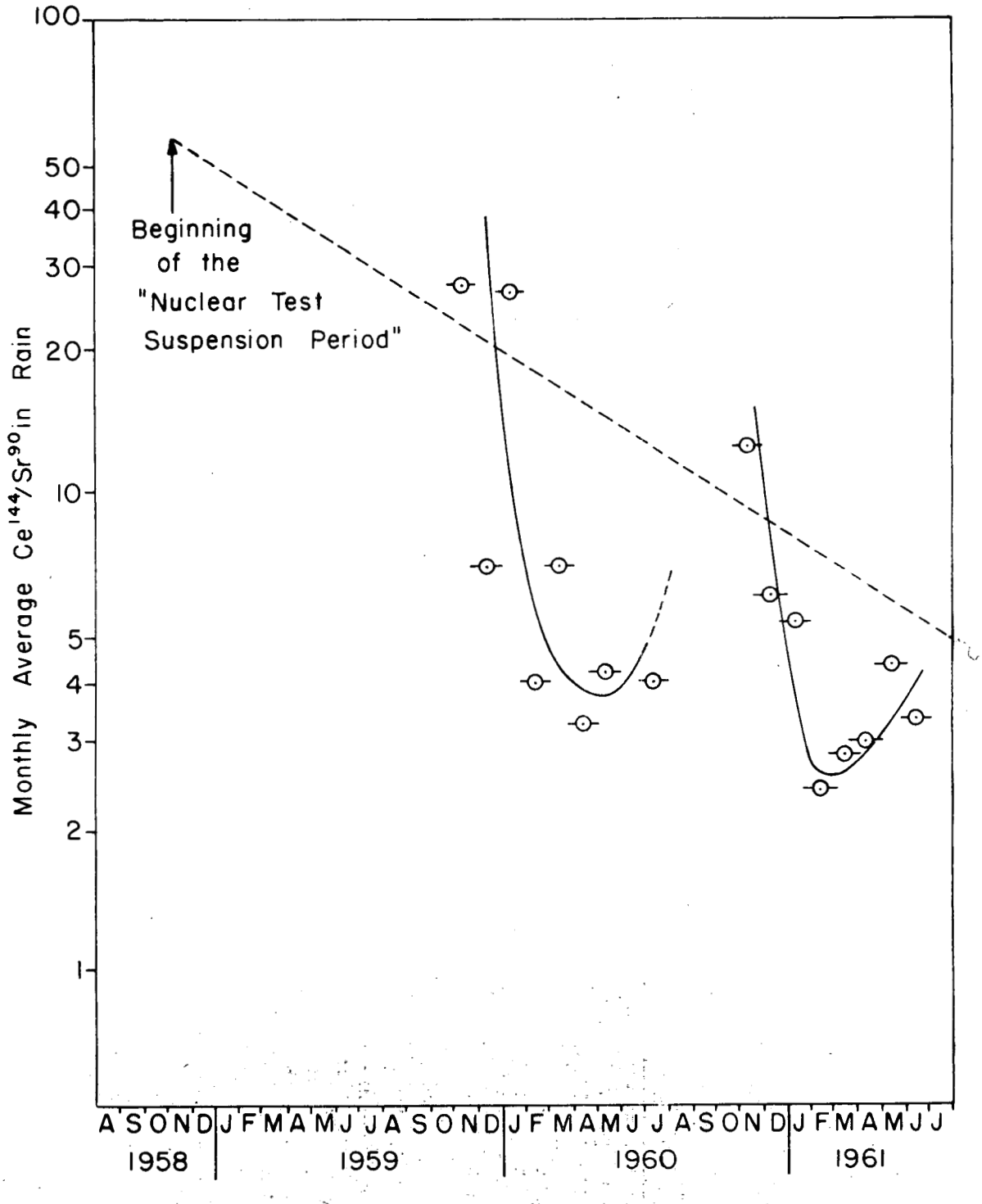

Figure 4. Variation of the Ce^{144}/Sr^{90} Ratio in Rain at Fayetteville, Arkansas. Dotted line I shows the calculated change of the Ce^{144}/Sr^{90} ratio in the stratosphere with time, which must be observed if an imaginary fresh debris with the initial Ce^{144}/Sr^{90} ratio = 54.8 was injected into the stratosphere in the fall of 1958, under the assumptions that (a) the stratosphere is uniformly mixed and (b) it was free of older debris.

8. Kenna, B.T., and P.K. Kuroda. The ratio of induced fission vs. spontaneous fission in pitchblende and natural occurrence of radiochlorine. J. Inorg. Nucl. Chem. 16:1(1960).

9. Brewer, A.W. Evidence for a world circulation provided by the measurements of helium and water-vapor distribution in the stratosphere. Quart. J. Roy. Meteorol. Soc. 75: 351(1949).

10. Dobson, G.M.B. Origin and distribution of the polyatomic molecules in the atmosphere. Proc. Roy. Soc. London A 236:187(1956).

11. Kuroda, P.K., H.L. Hodges, and L.M. Fry. Spring peak of strontium-90 fallout. Science 132: 742(1960).

12. Kuroda, P.K., H.L. Hodges, and H.E. Moore. Fallout from nuclear detonations of February and April 1960. Science 133:1130(1961).

13. Libby, W.F. Radioactive strontium fallout. Proc. Natl. Acad. Sci. U.S. 42:365(1956).

14. Machta, L., and R.J. List. Stratospheric strontium-90 measurements. J. Geophys. Res. 64:1267(1959).

15. Kulp, J.L., A.R. Schulert, and E.J. Hodges. Strontium-90 in man III. Science 129:1249(1959).

16. Storebø, P.B. The exchange of air between stratosphere and troposphere. Norwegian Defense Research Establishment, Intern Rapport FFIF-IR 376, Lillestrom, 1959.

17. Feely, H.W., Strontium-90 content of the stratosphere. Science 131:645(1960).

18. Martell, E.A. Atmospheric aspects of strontium-90 fallout. Science 129:1197(1959).

19. Martell, E.A., and P.J. Drevinsky. Atmospheric transport of artificial radioactivity. Science 132:1523(1960).

20. Libby, W.F. Radioactive fallout particularly from the Russian October series. Proc. Natl. Acad. Sci. U.S. 45:959(1959).

21. Kuroda, P.K., L.M. Fry, H.L. Hodges, and H.E. Moore. Stratospheric residence time of strontium-90. Science(in press 1961).

22. Kuroda, P.K., and M.P. Menon. Determination of trace quantities of fission products in non-irradiated natural and depleted uranium salts. Nuclear Sci. Engrg. 10:70(1961).

23. Russell, I.J. PhD Dissertation, University of Chicago, 1956.

24. Broom, K.M., Jr. 14.5 MEV neutron-induced fission of U^{238}. M.S. Dissertation, University of Arkansas, 1961. pp.44.

25. Broom, K.M., Jr., and P.K. Kuroda. 14.5 MEV neutron-induced fission of uranium-238. Submitted to Phys. Rev. (1961).

26. Katcoff, S. Fission product yields from U, Th and Pu. Nucleonics 16:78(1959).

27. Cunninghame, J.G. The mass-yield curve from fission of natural uranium by 14 Mev neutrons. J. Inorg. Nucl. Chem. 5:1(1957).

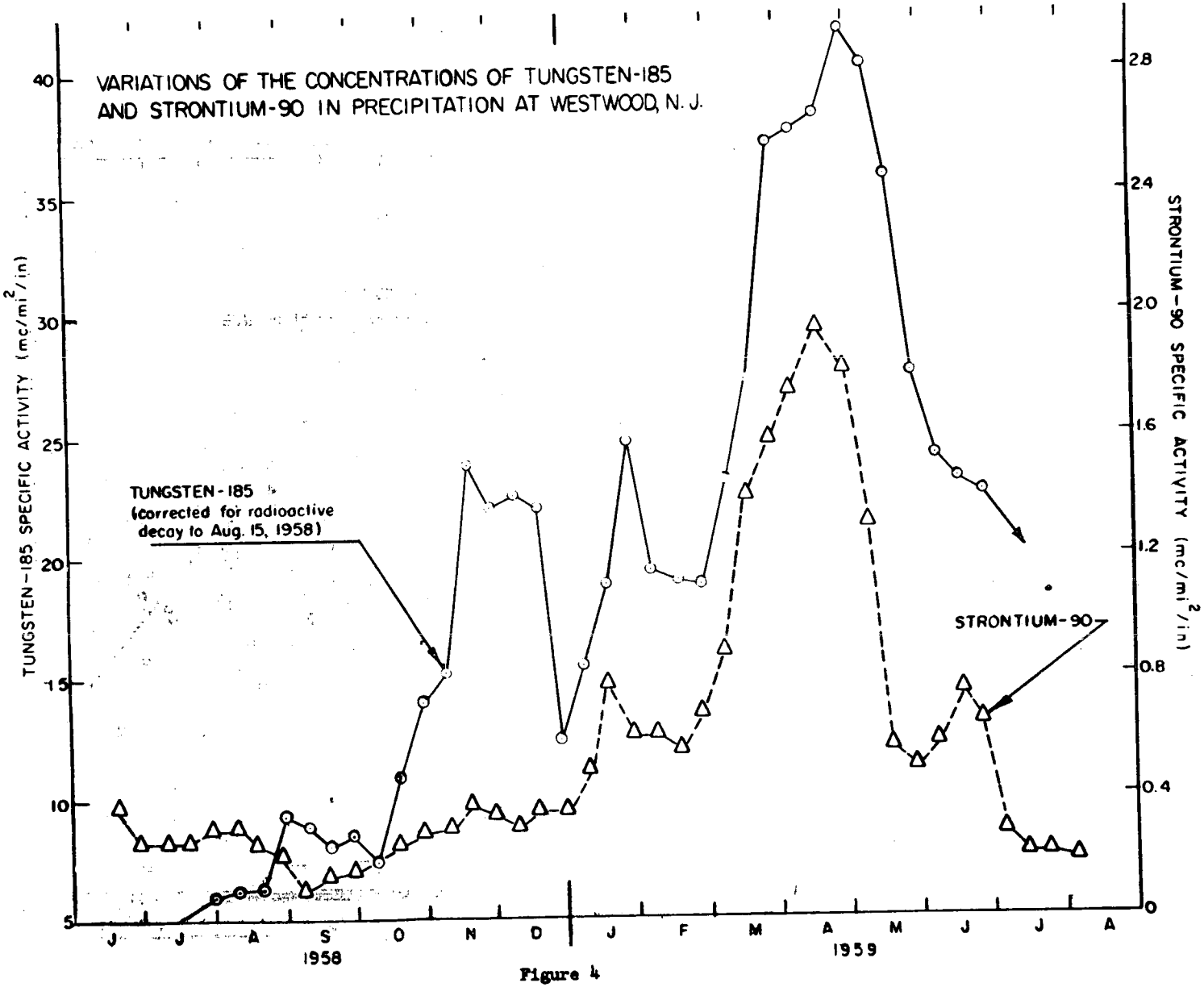
VARIATIONS OF THE CONCENTRATIONS OF TUNGSTEN-185
AND STRONTIUM-90 IN PRECIPITATION AT WESTWOOD, N. J.
TUNGSTEN-185 SPECIFIC ACTIVITY (mc/mi²/in)
STRONTIUM-90 SPECIFIC ACTIVITY (mc/mi²/in)
TUNGSTEN-185
(corrected for radioactive
decay to Aug. 15, 1958)
STRONTIUM-90
40
35
30
25
20
15
10
5
2.8
2.4
2.0
1.6
1.2
0.8
0.4
0
J J A S O N D J F M A M J J A
1958
1959

Figure 4

CESIUM^{137} LEVELS IN UNITED STATES POWDERED MILK AND IN THE POPULATION*

E.C. Anderson, G.M. Ward,** J.Z. Holland,*** and W.H. Langham
Los Alamos Scientific Laboratory
University of California
Los Alamos, New Mexico

Introduction

Cs^{137} is a long-lived radionuclide formed in about 6% abudance in fast neutron fission of Pu^{239}, U^{235}, and U^{238} (1). It probably is secondary only to Sr^{90} as a potentially hazardous material in world-wide fallout from nuclear weapon tests. In event of nuclear war, local and tropospheric fallout of relatively short-and intermediate-lived radionuclides (e.g., I^{131}) may be limiting primarily over either Sr^{90} or Cs^{137}. The long radiological half-life of Cs^{137} affords a long integration time in the soil, and its chemical similarity to K (a required constituent of plants and animals) results in rapid entry into the biosphere. Since it emits both beta and gamma rays, it is potentially both an internal and an external radiation source. Its concentration in muscle results in radiation to the gonads, and its cumulation in the soil increases the general radiation background level. The accumulation of Cs^{137} on the earth's surface and in man, therefore, results in both a potential somatic and a genetic hazard to the general population. Since 1956, the Los Alamos Scientific Laboratory (LASL) has made periodic measurements of the Cs^{137} levels in the United States population and in area sam-

*Work performed under the auspices of the U.S. Atomic Energy Commission.
**On leave from the Animal Science Department, Colorado State University, Fort Collins.
*** Permanent address, Division of Biology and Medicine U.S. Atomic Energy Commission, Washington, D.C.

plings of the powdered milk supply. Reports of the primary data (2-7) and occasional preliminary interpretive articles (8-20) have been published from time to time. The present report is a final summary of the project. The milk measurements have been discontinued as of the time of resumption of nuclear weapon tests by the U.S.S.R. on September 1, 1961, because re-injection of fresh Cs^{137} will obscure the long-term trends of Cs^{137} in the cycle from production to foods and to man, which were of principal interest. A few measurements of people from the New Mexico area will continue to be made to determine rate and extent of increase of Cs^{137} body levels as a result of recent U.S.S.R. tests.

Methods

Sampling of United States Powdered Milk. Beginning in 1956, 50- to 100-lb. samples of powdered milk from major production areas in the U.S. were collected at weekly intervals and assayed for Cs^{137} and naturally-occurring K^{40}. During 1958-1959, the number of weekly sampling sites totaled 55, covering all major powdered milk producing areas of the U.S. and Canada. Since samples were obtained through normal channels from commercial milk-drying plants (which utilize only surplus milk), it was not possible to obtain samples from some States in which milk production does not exceed local requirements. Thus, the mountain and high plains areas (Nevada, Montana, Wyoming, Colorado, Nebraska, and Kansas) were not represented, and sampling points were few and intermittent in the Southeast. On July 1, 1960, the sampling network was curtailed by dropping the Canadian stations and cutting back the U.S. sampling to the 16 most widely distributed and dependable stations. In the fall and winter of 1960-1961, each of the 16 plants retained in the sampling network was visited to obtain detailed information on factors that may have bearing on Cs^{137} levels of milk produced in these specific areas. Dairying practices were evaluated with particular attention to number of cows, size of production area, production level, length of pasture season, type of pasture, type of hay, and amount of silage fed. Soil types and soil acidity were also investigated as well as rainfall patterns and milkshed uniformity. Information was gathered from discussions with plant managers and fieldmen, county agriculture agents, State university staff, and from some farm visits. In addition to detailed information for the 16 selected locations, general information was gathered for all areas that had supplied milk to the network. Some locations were visited and, for others, information was gathered by correspondence or discussion with knowledgeable people.

Sampling of the United States Population. Samplings of the general U.S. population were drawn from visitors to the Los Alamos Scientific

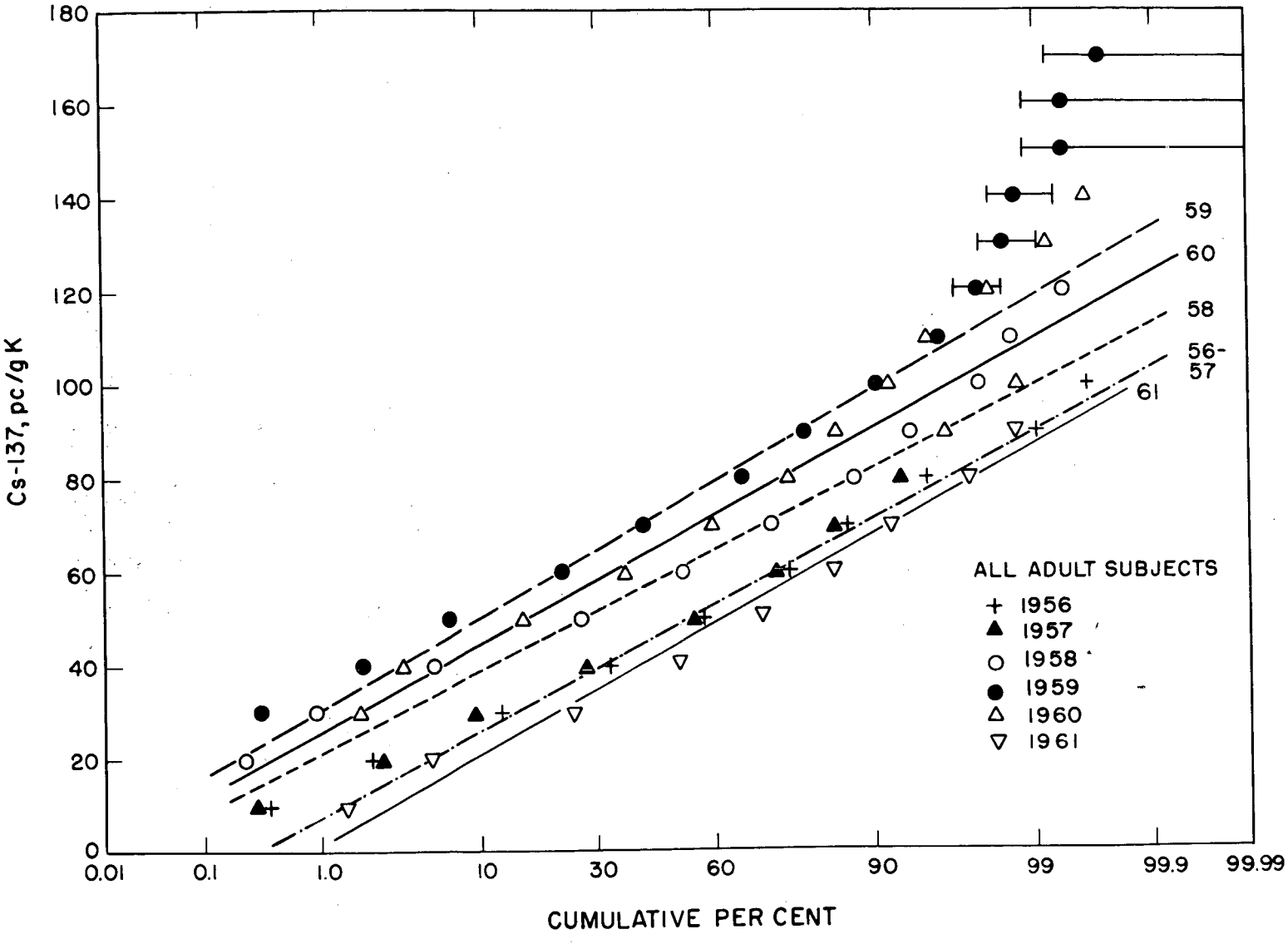

Figure 10. Normal frequency distribution plot of Cs^{137} levels in adult United States residents.

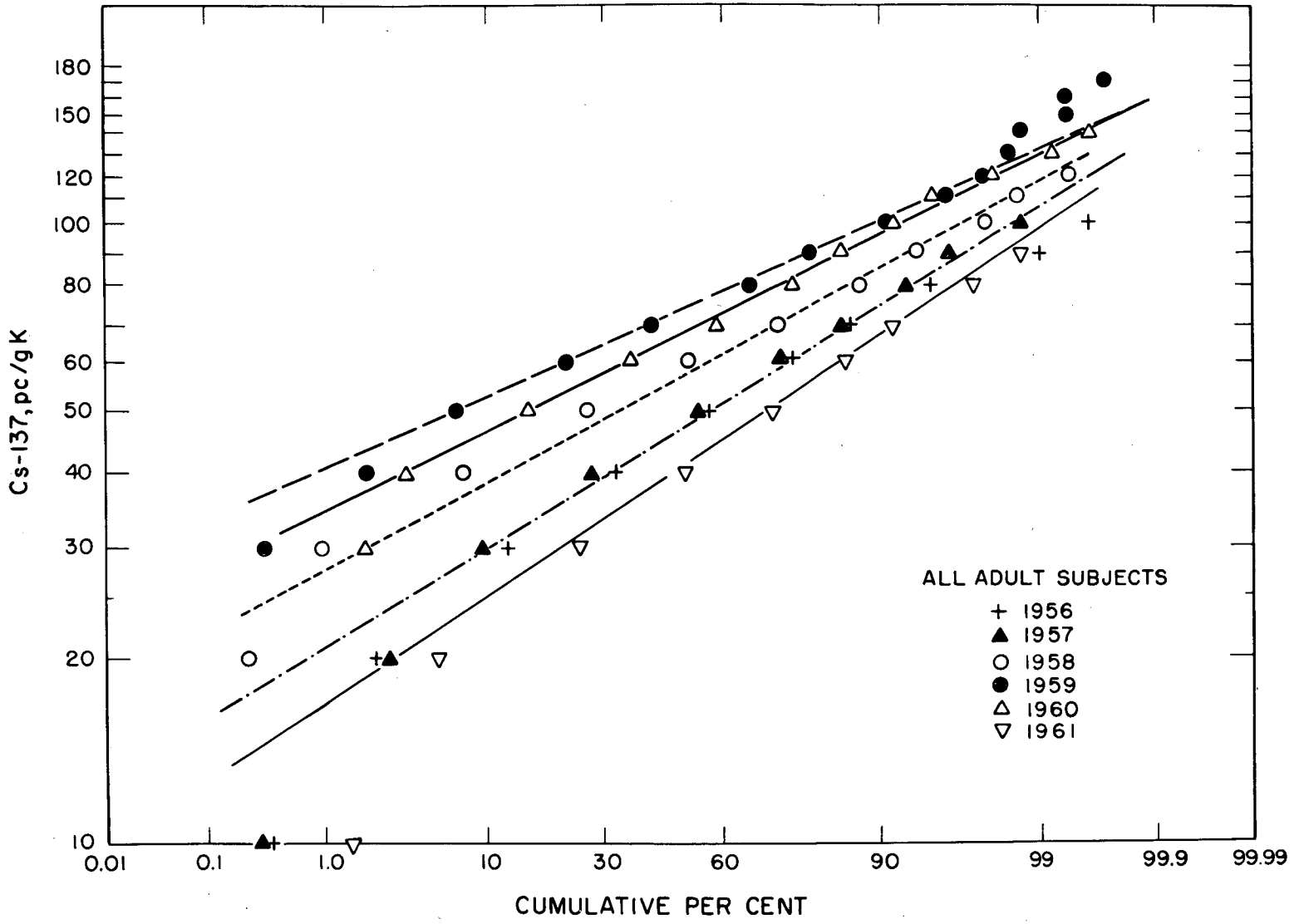

Figure 11. Log-normal frequency distribution plot of Cs^{137} levels in United States residents.

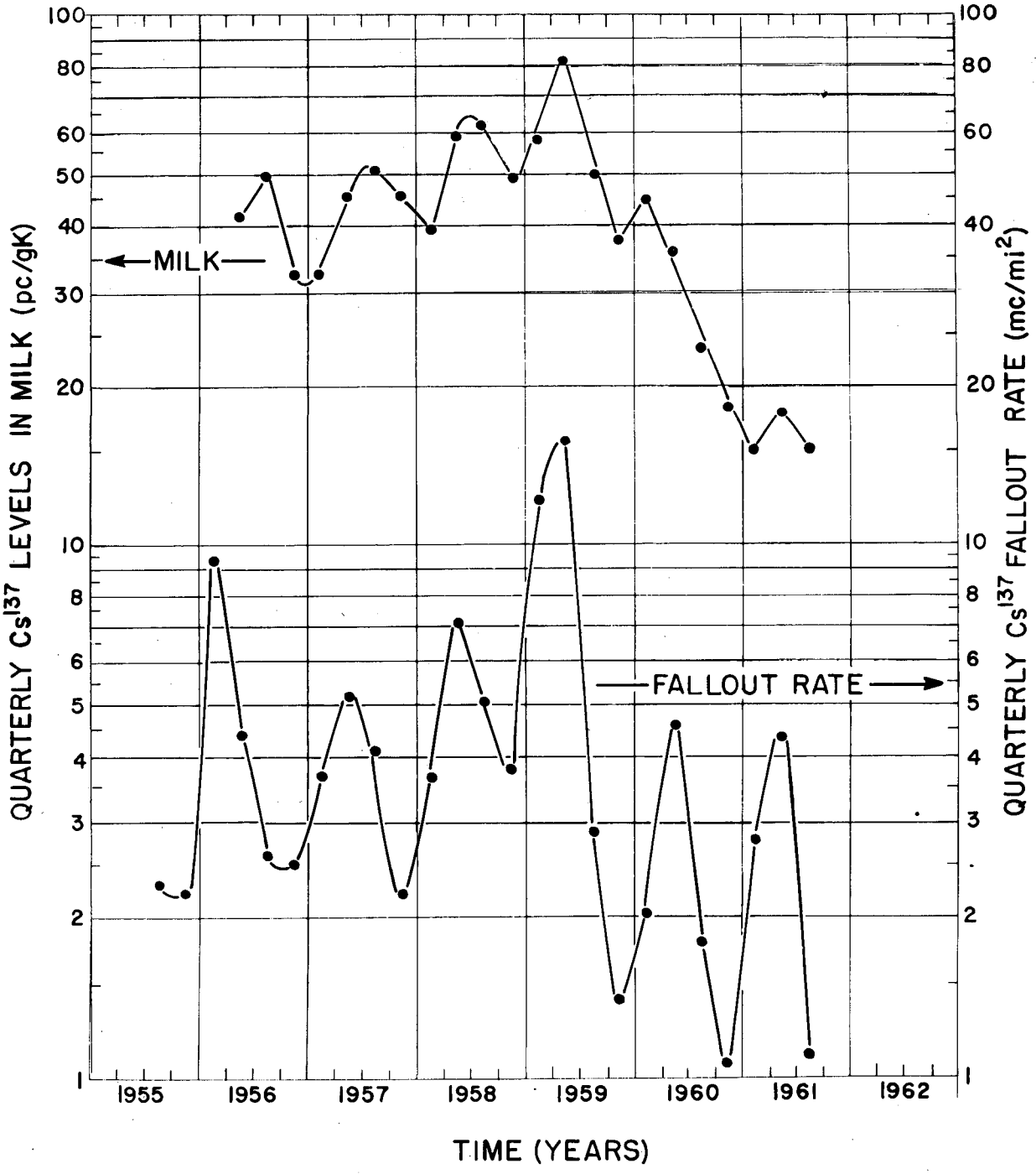

Figure 12. Relationship between quarterly average fallout rate and population-weighted quarterly average Cs^{137} levels in milk.

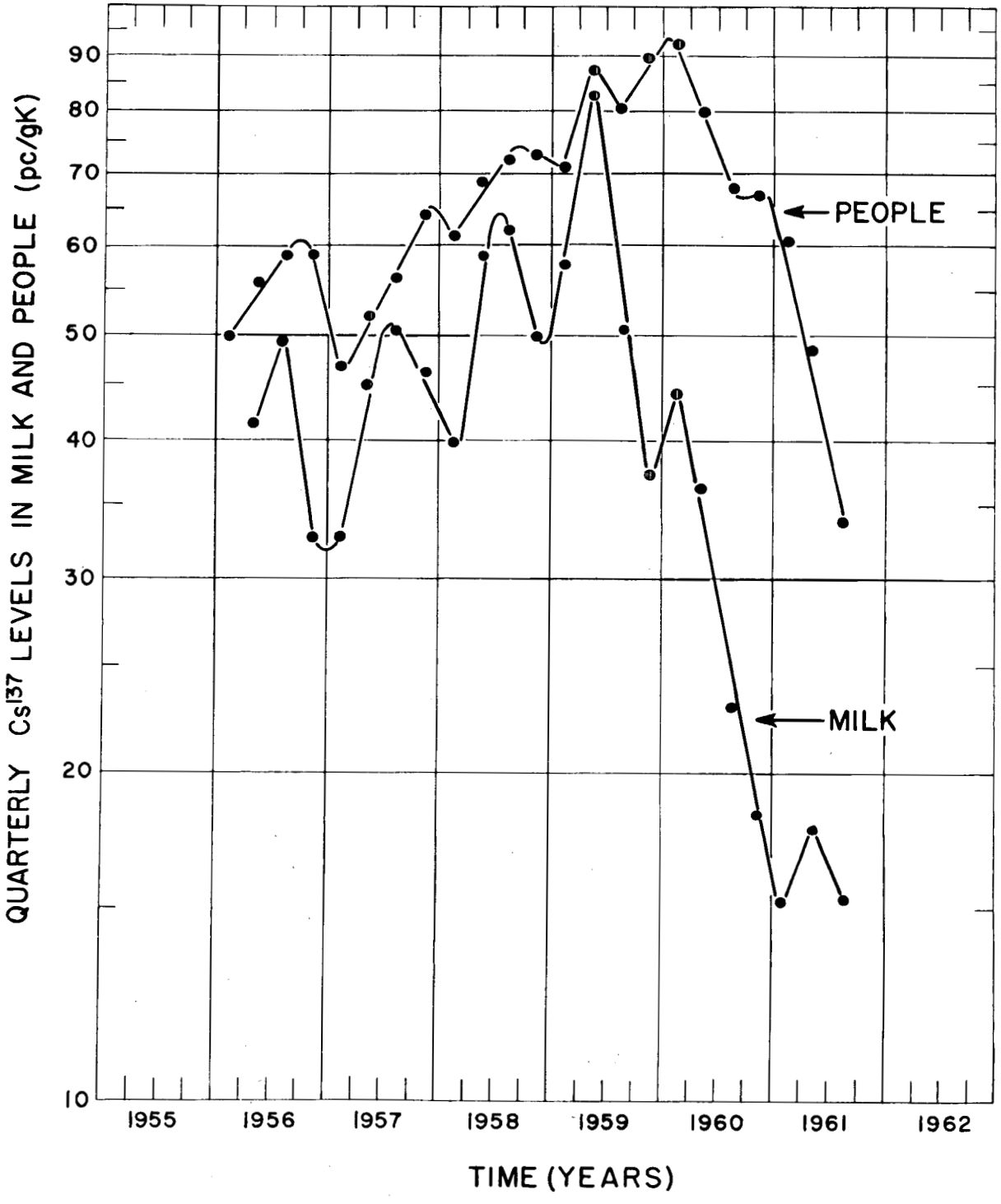

Figure 13. Relationship between population-weighted quarterly average Cs^{137} levels in the United States population and in milk.

TABLE 7. RELATIVE CONTRIBUTION OF MILK TO YEARLY AVERAGE CESIUM^{137} LEVELS IN PEOPLE AND THE AVERAGE CONCENTRATION OF CESIUM^{137} IN THE BALANCE OF THE DIET

Year	Milk Concentration (pc/g K)	Concentration in People (pc/g K)	Calc. Conc. in Rest of Diet* (pc/g K)	Contribution of Cs^{137} Milk to Body Cs** (per cent)
1956	41.0	56.0	27.6	49.8
1957	43.7	54.6	24.4	54.4
1958	53.0	68.7	32.1	52.4
1959	57.1	82.2	42.5	47.2
1960	30.6	71.5	49.7	29.1
1961	16.0	47.9	36.3	22.8
Average	40.2	63.5	35.4	42.6

*Concentration in milk x 1.7 x 0.4 = milk contribution to people. Concentration in people minus milk contribution = contribution of balance of diet. Contribution by balance of diet ÷ 1.7 x 0.6 = concentration in balance of diet.

**Milk contribution x 100 ÷ concentration in people = per cent contribution by milk.